RESPIRATORY HEAT AND MOISTURE LOSS IN HEALTH, ASTHMA AND CHRONIC OBSTRUCTIVE PULMONARY DISEASE (COPD)

by

John McCafferty

A thesis submitted in partial fulfilment of the requirements for the degree of

MD

University of Edinburgh

2005

Daniela,

Muchas gracias por todo. Esto es para ti.

TAJ

DECLARATION

I hereby declare that the work presented in this thesis including the design and construction of the measurement system for Respiratory heat and moisture loss and associated breath targeting software was carried out by myself at the Western General Hospital, Edinburgh and the Dept. Mechanical Engineering, Heriot-Watt University, Edinburgh, except where due acknowledgement is made, and has not been submitted for any other degree.

.John McCafferty (candidate)

.....J Alastair Innes (supervisor)

ABSTRACT

It was hypothesized that Respiratory heat and moisture loss (RHML) would be altered in patients with Asthma and Chronic obstructive pulmonary disease (COPD) due to the effects of airway inflammation and re-modeling. By creating a novel device incorporating humidity, temperature and flow sensors, RHML was measured in 25 normal controls, 33 asthmatics and 17 patients with COPD. In normal subjects RHML was found to be dependent on breathing pattern as defined by tidal volume and minute ventilation whereas no association was found between RHML and body surface area or forced expiratory volume in one second (FEV1). At matched breathing patterns asthmatics whether in exacerbation or stable showed a small but significant increase in RHML compared to controls (exacerbation asthmatics -93.2 $\pm$ 0.8 (SD), p=0.003, stable asthma - 89.3 $\pm$ 7.4, p=0.025 and controls 85 $\pm$ 4.3 Joules/L). No significant difference was found in RHML between the asthmatics with an exacerbation and those with stable disease. COPD patients showed no significant difference in RHML (stable group- 83 $\pm$ 4.8, p=0.23 and exacerbation group - 81 $\pm$ 5.8 Joules/L, p=0.06) compared to controls or between exacerbation and stable groups. Evaporative heat loss was the major heat transfer modality (up to 3-times the dry convective heat loss). It can be concluded that asthma is associated with a measurable increase in heat and moisture loss in breath and that this may reflect the inflammatory and vascular changes known to occur in the asthmatic airway. Further longitudinal studies are required to assess whether the technique developed in this study can provide a practical means to measure inflammation in asthma.

TABLE OF CONTENTS

LIST OF FIGURES

LIST OF TABLES

Nomenclature

A	airway cross-sectional area
BSA	body surface area (m^2)
c_p	specific heat capacity at constant pressure (kJ/kgK)
k	Thermal conductivity (kJ/kgK)
h	enthalpy (kJ/kg)
h_{fg}	Heat of vaporization (kJ/kg)
M	Metabolic rate (watts)
m	mass flowrate (kg/s)
Pa	ambient water vapour pressure (mmHg)
n_i	molar amount of substance (kmol)
P	is the airway perimeter
Q	Total heat flow (Watts)
q	heat flow (Watts)
T	Temperature (^oC)
T_e	Exhaled breath temperature (^oC)
T_i	Inspired air temperature (^oC)
v	Gas velocity (m/s)

V	Volumetric flowrate (l/s)
Vco_2	rates of co_2 production
Vo_2	rate of o_2 production
w	Absolute humidity (mg/kg)
ρ	Density (kg/m^3)

DEFINITIONS

Term	Definition	Units
Absolute humidity	or moisture content is the ratio of the mass of water vapour to the mass of dry air for any given volume.	g per kg dry air
Relative humidity	is the ratio of the actual partial pressure of the vapour to the partial pressure of the vapour when the air is saturated with water, at the same temperature.	%
Enthalpy	describes the 'useable' energy (dry and latent) in air	kJ/kg

ACKNOWLEDGMENTS

Dr Alastair Innes first raised the question of whether exhaled air temperature would correlate with airway inflammation in diseases such as cystic fibrosis and asthma. We sought to explore this question further, following successful funding application, by embarking on a 2-year research program. Throughout this process Alastair was a source of encouragement, advice and patient direction. I am very grateful to him for his help and supervision over this time.

I also acknowledge with gratitude the contributions of Dr Peter Kew and Mr Andrew Haston, (Dept Mechanical Engineering, Heriot-Watt University, Edinburgh, UK) for their contribution to technical aspects of this study including the design and fabrication of the cooler/dehumidifier, and its associated power supply and electronic circuitry related to humidity sensors and thermocouples.

This work was made possible by funding from *Chest, Heart and Stroke Scotland* who gave support in the form of a 2-year research Fellowship. I am particularly grateful to them since it was given at such an early, conceptual stage in the project.

Thanks are also due to the *Wellcome Trust Clinical Research Facility, Edinburgh* for assistance throughout the study in providing clinical and laboratory space as well as IT support and expertise.

INTRODUCTION

The earliest thoughts on heat transfer in relation to human physiology can be traced back to the ancient Greek physiologists and Doctors of the 5th century BC. At this time nature was seen to be made up of the primary and opposing fundamental quantities of hot and cold; wet and dry. These forces were thought to be in competition so that if any one dominated then disease would ensue. *Aristotle* and later *Hippocrates* shared this view and proposed that the heart was the site of a 'central fire', which produced 'vital heat'. This fire was cooled by the overlying lungs, which drew in the 'pneuma' or inhaled air and conveyed this to the heart via the pulmonary vessels thus providing a balance between hot and cold [1]. This early concept, although flawed, represents the first view of a circulatory heat source to the lungs and the exchange of heat with the respired air. *Galen* in the 2nd century described a blood supply from the aorta to the lungs, however many centuries passed before the pulmonary and bronchial circulations were correctly described [2]. It was not until the 16th century that the concept of temperature measurement emerged with the development of *Galileo's* thermoscope [3] and later *Sanctorius* [3] applied the use of a thermometer to the measurement of temperature in man. Following this, in the mid 18th century the idea of thermo-regulation in man was described by *Blayden* [3]. In the late 19th century the nature of the heat sources in the human body *viz a viz* the metabolism of carbohydrate, fat and protein and mechanical work was elucidated. Following on from this into the 20th century a more quantitative analysis on heat transfer in tissues emerged. The landmark work of *Pennes* [4] and the 'bioheat equation' formed the basis for much of the bioheat transfer analysis over the second half of the 20th century. With regard to the study of heat transfer in the human

airway, *Magendie* [5] in 1829 was the first to propose the concept of air being heated and humidified on its path through the respiratory tract. *Goodale* [6] in 1896 measured exhaled air temperatures below body temperature, which led to our current understanding of the respiratory tract recovering heat from expired air. The early part of the 20th century saw further quantitative measurements of respiratory heat loss (*Burch 1945* [7]) and the factors affecting breath temperatures (*Webb* [8], *McCutchan* [36]). Over the last 20 to 30 years much has been done to advance our understanding of the mechanisms of thermally induced asthma. *McFadden* [9] performed detailed bronchoscopic temperature measurements in humans, which together with several mathematical models of respiratory heat exchange [10-18] have provided useful data regarding intra-airway heat and water flux. The work of *Baile* [57-59], *Solway* [19-20] and more recently *Serikov* [21-23] has advanced our understanding of the bronchial and pulmonary circulations and their relation to airway heat exchange.

The aim of this work was to examine the effect of airways disease on the heat and moisture transfer characteristics in the respiratory tract. Chronic obstructive pulmonary disease (COPD) and asthma are caused by inflammation within the airways. Inflammation was classically described by *Celsus* in the 1st century AD to comprise rubor, *calor*, dolor and tumour. It is this 'calor' or heat that represents a final common pathway in inflammation and derives from local vasodilatation resulting from the release of inflammatory mediators such as cytokines, histamine, leukotrienes and nitric oxide among others. The principal hypothesis of the present work is that increased blood flow in inflamed airway mucosa will be detectable as increased heat flux into the lumen when potential confounding influences are carefully controlled

As demonstrated in Chapters 1 and 2 although much has been discovered through invasive measurements and mathematical models of intra-airways heat transfer, there is still a striking lack of data from measurements on patients with asthma, chronic obstructive pulmonary disease (COPD); conditions associated with both acute and chronic inflammatory changes in the airways. A novel means of easily measuring the heat and moisture loss in breath was devised (Chapter 3) and applied firstly to the study of healthy subjects. This allowed definition of the normal range and estimation of the effects of breathing pattern, inhaled air condition and body surface area (chapter 4). Measurements were then made on subjects with asthma and COPD to test the hypothesis that this property would be altered in these conditions (chapter 5).

CHAPTER 1

PRINCIPLES OF HEAT AND MOISTURE EXCHANGE IN THE HUMAN AIRWAY

1.1 Anatomy of the Respiratory tract

The respiratory tract conveys air from the environment to deep within the lung in order for gas exchange to take place. The upper respiratory tract comprises the nasal cavities, para-nasal sinuses, oral cavity, pharynx and larynx that are continuous with the lower respiratory tract consisting of trachea and bronchial tree. The nasal cavity is surrounded by air-filled paranasal sinuses, which communicate with the cavity itself. The pharynx and larynx convey air from oral and nasal cavities to the trachea, which is a tube-like structure on average about 12 cm long and of 18mm internal diameter [24] composed of a fibrous membrane and shaped cartilaginous rings. It bifurcates at the carina into left and right main bronchi, and they in turn divide into lobar branches supplying upper and lower lobes of the left and right lung plus an additional middle lobe on the right. The bronchi further divide by dichotomy down to the terminal bronchioles with an internal diameter of less than 1mm. Approximately 200 mls of air is contained in the conducting airways to this point, in contact with a total surface area of approximately 0.6 m^2. Each terminal bronchiole opens into the respiratory lobule or acinus consisting of alveolar ducts, alveolar sacs and alveoli. These structures collectively form the lung parenchyma, which occupies 90% of the volume of the whole lung, the remaining 10% being non-parenchymal structures such as the conductive airways, blood vessels, septae and pleura.

95% of the parenchymal volume is alveolar air contained within an estimated 300 million alveoli providing a total surface area of approximately 140 m^2 for gas exchange.

The nasal cavity, trachea, bronchi and bronchioles are lined by ciliated mucosa. Sub-mucosal glands and mucosal goblet cells secrete a visco-elastic gel that forms the mucous layer forming the air-wall interface. The cilia are tiny projections bathed in low viscosity fluid that beat at a rate of 17-25 Hz in synchrony with the cilia of neighbouring cells. The cilia therefore propel the mucous blanket in the direction of the pharynx so that particles trapped in the mucous can be cleared. The mucous consists of long glycoproteins which form the framework of the gel together with other inorganic ion species. Gel hydration is controlled by membrane transport of ions and water in a Donan type equilibrium process [25].

The bronchial circulation nourishes the airway epithelium and glands. In the majority of humans two bronchial arteries supply each lung taking their origin from the aorta directly or the upper intercostal arteries. Rarely they may derive from the internal mammary or coronary arterial system. The bronchial arteries give branches to mediastinal structures such as the oesophagus, hilar lymph nodes and the vagus nerve. They enter through the hila and divide on reaching the main segmental bronchi and thereafter follow the branches of the bronchial tree (see Figure 1.1). Normally 2 to 3 branches are given to each bronchus following down as far as the terminal bronchioles. These branches anastomose with each other forming a peribronchial plexus. In addition small arterioles derived from this supply penetrate the muscular layer to form a submucosal plexus (Figure 1.2).

The bronchial capillary network merges with the pulmonary capillary network beyond the level of the pulmonary lobule. The degree of anastomosis between the two circulations is

thought to increase with increasing numbers of bronchi towards the lung periphery. The intra-pulmonary venous drainage of the bronchial circulation is mainly via the pulmonary circulation. The right and left pulmonary arteries are divisions of the pulmonary trunk below the arch of the aorta, which divide and accompany segmental and sub-segmental bronchi, lying mostly dorsolaterally to them. They terminate in dense capillary networks in the walls of the alveolar sacs and alveoli. Pulmonary veins (2 per lung) drain the capillary networks. Smaller venous branches traverse the lung independent of the arteries.

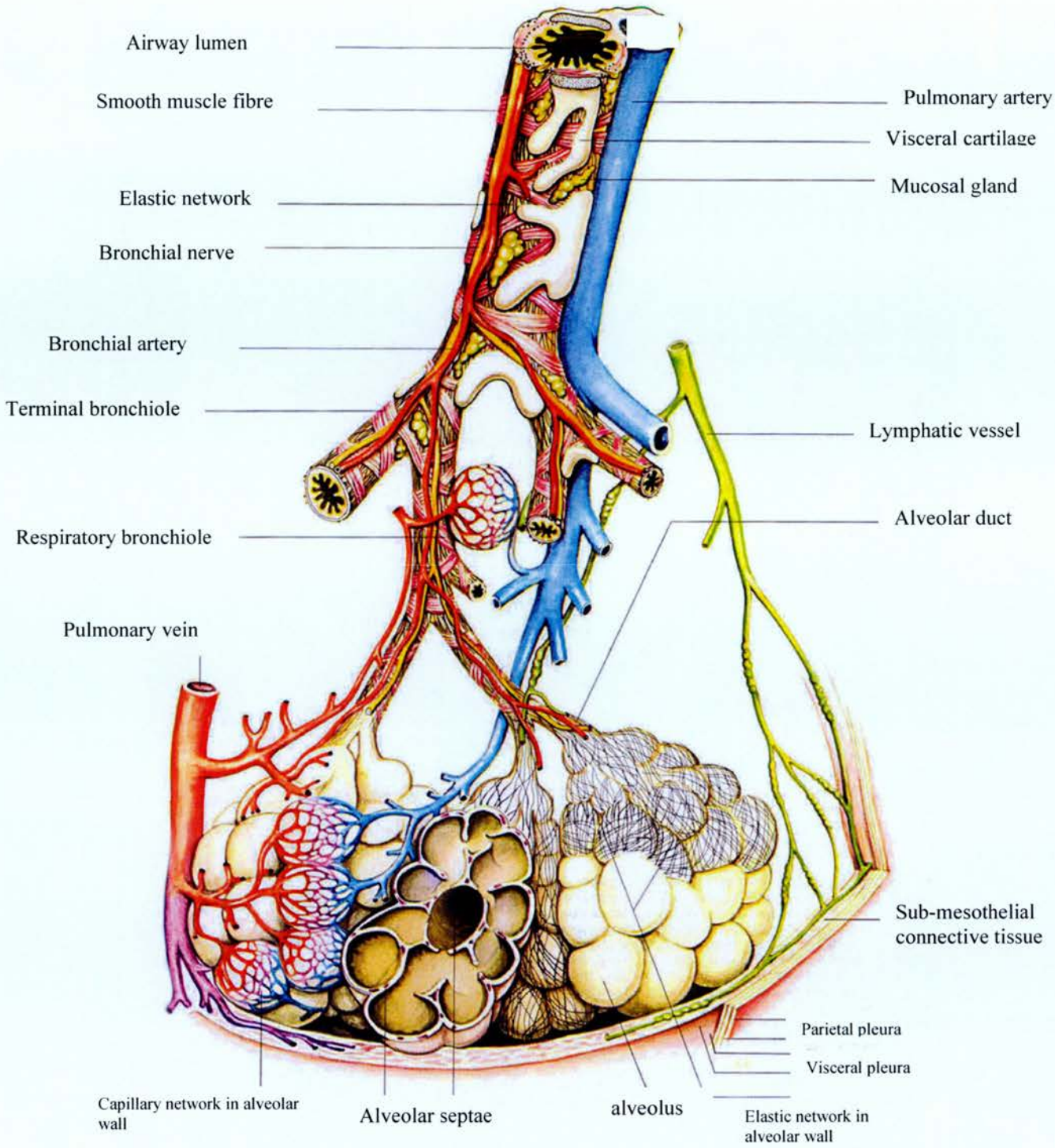

Figure 1.1. Schematic illustration (not to scale) of the anatomy of the airways showing relation of bronchial and pulmonary arterial systems [26]. The bronchial arteries divide on reaching the main segmental bronchi and thereafter follow the branches of the bronchial tree. The right and left pulmonary arteries are divisions of the pulmonary trunk below the arch of the aorta which divide and accompany segmental and sub-segmental bronchi, lying mostly dorsolaterally to them. They terminate in dense capillary networks in the walls of the alveolar sacs and alveoli.

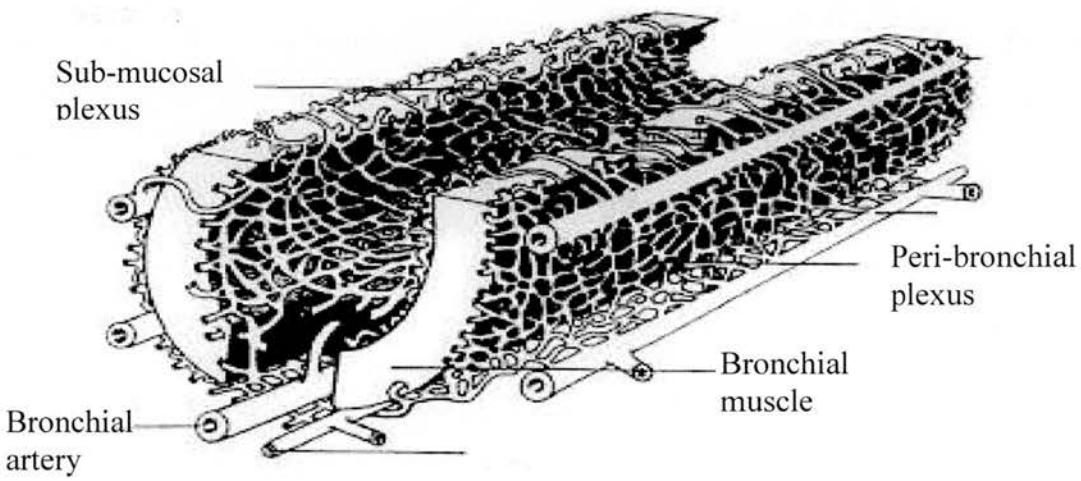

Figure 1.2. Illustration of the ultra-structure of the respiratory bronchiole showing arrangement of bronchial artery supply and peribronchial and sub-mucosal plexus. Normally 2 to 3 branches of the bronchial artery are given to each bronchus following down as far as the terminal bronchioles. These branches anastomose with each other forming a peribronchial plexus. In addition, small arterioles derived from this supply penetrate the muscular layer to form a sub-mucosal plexus.

1.2 Air-conditioning and heat recovery within the airway

The respiratory tract and the skin represent the body's interface with its environment. Across this interface the internal energy generated is ultimately dissipated. The skin loses heat by conduction, convection, radiation and evaporation of sweat, which combined forms about 90% of total body heat loss at rest. The remaining 10% is lost via the respiratory tract. Despite its large surface area and blood supply, a number of features of the respiratory tract serve to minimize the loss of moisture and heat. The enclosed airways prevent radiative loss. The branching system of bronchi and bronchioles results in an increasing surface area to volume ratio as air moves deeper into the lung thereby increasing the efficiency of heat transfer during inspiration and minimizing losses on expiration. The cooling of the mucosa during inspiration allows heat recovery from the air by condensation as it passes over the same surface on expiration. As well as exchanging metabolic heat the respiratory tract serves a crucial air conditioning function. It is able to warm and saturate inspired air so that at an alveolar level, air is fully saturated with water vapour and attains core temperature. This ensures the integrity of the alveolar membrane and its optimum function in gas exchange. Remarkably, this is achieved under extremes of climatic conditions. *McFadden* [9] mapped the human airway by measuring the intraluminal temperatures to sub-segmental level from bronchoscopically placed temperature sensors. As shown in figure 1.3, even under extreme sub-zero temperatures ($-18^{\circ}C$) inspired air is warmed to $32^{\circ}C$ by the time it reaches the carina.

Heat exchange within the airways comprises inspiratory and expiratory phases. Inspired air is warmed and humidified to $37^{\circ}C$ and 100% relative humidity [27,28]. Heat is

transferred to the inspired air by means of convection and evaporation of water from the mucosal surface. As water evaporates to humidify the inspired air its latent heat is transferred and the mucosa is cooled. During quiet breathing this process is mostly achieved by the airway proximal to the trachea [9]. However with colder or dryer ambient conditions or at higher minute ventilation the airway is further thermally stressed and the point at which the inspirate is fully conditioned moves deeper within the bronchial tree [9] (see figure 1.3). This is sometimes referred to as the isothermal saturation boundary (ISB). This boundary is dynamic and will vary with inspiration and expiration as well as with ambient conditions of temperature, moisture content and breathing pattern. Studies have shown that under extreme conditions of cold dry air at high minute ventilation, airways down to 1mm diameter actively participate in heat and water exchange [9].

During expiration, air at 37°C and fully saturated will cool and its water vapour condense on the mucosa downstream of the ISB enabling recovery of some of its latent heat and water content. The air will then exit at a certain temperature (T_e) below deep airway temperature. T_e has been shown to be directly proportional to the inspired temperature (T_i) and inspired moisture content (w_i). Numerous studies have proposed predictive equations relating T_e as a function of T_i and w_i based on experimental data. For example, taking the equation of *Varene et al* [47], for T_i between 10 to 30°C and relative humidity of inspired air of 50%, $T_e = 26 + 0.25T_i$. This equation would yield an expired air temperature of 31.5°C (for $T_i = 22$°C).

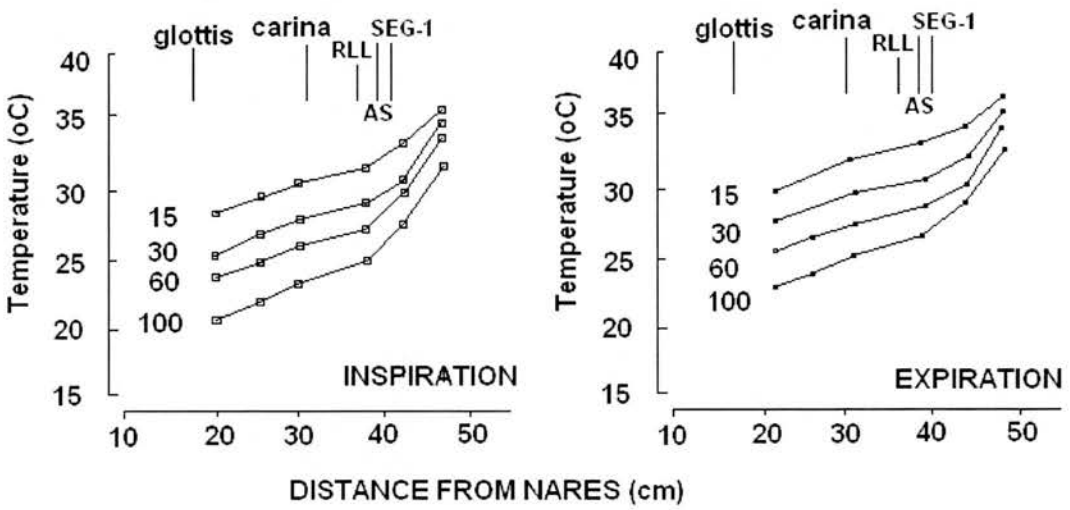

Figure 1.3. Invasive measurements of temperature during inspiration and expiration within the airways of subjects breathing frigid air (-18°C) at minute ventilations of 15, 30, 60 and 100 l/min. McFadden et al[9]. Even under extreme sub-zero temperatures inspired air is warmed to 32°C by the time it reaches the carina.

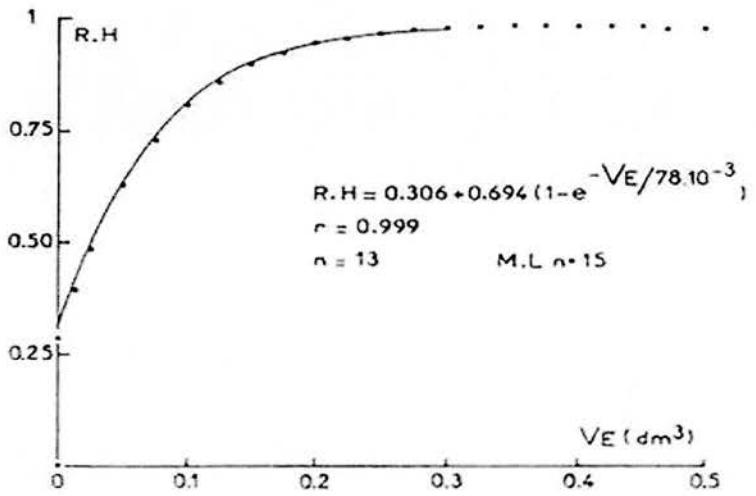

Figure 1.4. Water content of expirate as a function of volume as measured using mass spectrometry (*Ferrus* [48]). The expirate is initially unsaturated and then rises to full saturation exponentially with expiratory volume in a similar way to temperature profiles. The degree of unsaturation is slight and limited to the first part of the expiratory cycle so that for the purpose of energy exchange analysis expired air can be assumed to be fully saturated at T_e.

There is disagreement in the literature regarding the moisture content of expired air. Some authors assume expired air to be fully saturated [29-31] whilst others have found it to be unsaturated [32-35]. *Ferrus et al.* [48] looked at instantaneous variations in relative humidity of expired air using rapid response thermometry and mass spectrometry. They demonstrated (figure 1.4) that the expirate is initially unsaturated and then rises to full saturation exponentially with expiratory volume in a similar way to temperature profiles. They conclude that the degree of unsaturation is slight and limited to the first part of the expiratory cycle and imply that for the purpose of energy exchange analysis expired air can be assumed to be saturated at T_e. *Ferrus et al* [48] also found that the absolute humidity of the expired air was independent of minute ventilation but was a direct function of tidal volume and an inverse function of respiratory rate. The authors propose a bi-compartmental model of expiration whereby the first compartment comprises an unsaturated, cooler 'dead space', which on expiration mixes with the larger warmer saturated compartment. It would follow that at lower tidal volumes (and higher respiratory rates) the unsaturated 'dead space' would form a proportionally greater contribution to the expirate. The converse would be true for higher tidal volumes with lower respiratory rates.

1.3 Mathematical Models of heat-exchange in the airways

A number of mathematical models have been developed in the study of respiratory heat exchange for a variety of reasons. Firstly, the heat balance and predictive equations have evolved from the study of human body energetics and thermal comfort. They seek to

quantify heat loss from the respiratory tract under various environmental conditions and conditions of exercise. Secondly, more complex models have been developed to examine the heat and moisture transfer processes within the airways. The invasive nature of measurement in humans prevents detailed measurements of local heat and moisture fluxes deep within the respiratory tract. These models have proved useful in estimating the intra-airways effects of cold air hyperventilation and explaining the mechanisms of exercise induced asthma. Finally, the lumped heat capacity model considers the coupled process of airway heat exchange and pulmonary blood flow to propose a non-invasive index of cardiac output and lung thermal volume [21].

1.3.1 Overall Heat Balance Equation

At a fundamental level, heat exchange from the respiratory tract can be thought of as a closed process at steady state where air enters with a temperature and moisture content (T_i and w_i) and exits with the altered condition T_e and w_i following the process of evaporation and condensation within the airway. The total heat exchanged with the environment can then be described according to the equation;

Total heat exchange (q) = [Change in dry air sensible heat] + [Change in water sensible heat] + [Heat required to evaporate water]

$$q = q_c + q_e = \underbrace{mc_{pa}(T_e - T_i)}_{\text{Dry Convective component}} + \underbrace{mc_{pw}(w_e - w_i)(T_e - T_i) + m(w_e - w_i)h_{fg}}_{\text{'evaporative' component}} \qquad (1.1)$$

Where, q = total (convective + latent) heat flow from the airway, c_{pa}= heat capacity of air, m = mass flow rate of air, c_{pw} =latent heat capacity of water, h_{fg} = latent heat of evaporation of water, (T_e-T_i) = temperature difference between inspired and exhaled air, (w_e-w_i) = difference in moisture content between inspired and exhaled air.

This assumes a closed system where inspiratory and expiratory ventilations are equal and the difference in water vapour concentrations between inspired and expired gases to be due only to condensation and evaporation processes. If a respiratory quotient of 0.85 is assumed, and the difference in CO_2 content between inspired and exhaled air is of the order 4%. This would imply a net volume change of (1-0.85)×4/100= 0.6%. The magnitude of this error is therefore considered small. In addition the density and specific heat capacity of inspired and expired gases are assumed constant. If the boundary of this closed system is extended to the gas exchange portion of the lung, the heat flux due to gas exchange must be included in the above equation. The evolution of CO_2 from blood to alveoli is endothermic and the combination of O_2 with blood is exothermic. The heat balance equation would then become;

$$q = q_c + q_e + q_{co_2} + q_{o_2}$$

where;

$$q_{co_2} = \frac{Vco_2}{22.3} h_{co_2} \quad \text{and} \quad q_{c_2} = \frac{Vo_2}{22.4} h_{o_2}$$

22.3 and 22.4 are the molar volumes of co_2 and o_2 respectively (l), hco_2 and ho_2 are the heats of reaction in kcal/mol,Vco_2 and Vo_2 are rates of co_2 and o_2 production (l/min).

1.3.2 Predictive Equations

Based on experimental data, predictive equations have been derived by a number of authors in an attempt to quantify overall respiratory heat and moisture loss under various ambient conditions and exercise. These are useful in the area of human body energetics and heat balance. *McCutchan and Taylor* [36] established a relationship between the condition of inspired and expired air of the form $T_e = f(T_i, w_i)$ or $w_e = f(T_i, w_i)$. Substituting this in equation (1.1) above gives $q = f(T_i, w_i)$. They proposed the following predictive equation (adapted to SI units) based on their data.

$$q = m\,(0.799\,T_i + 1884\,w_i - 98.3) \qquad (1.2)$$

m = mass flowrate kg/s

T_i = inspired temperature (°C)

w_i = humidity ratio (kg moisture per kg dry air)

Therefore for a subject breathing with a minute ventilation (Ve) of 15l/min, air at 7°C with absolute humidity 5.8 g/kg dry air. Now,

$$m = \rho Ve = 1.25 \times \frac{15}{60} \times 10^{-3} = 3.125 \times 10^{-4} \text{ kg/s}$$

Then from equation 1.2;

$$q = 3.125 \times 10^{-4} \times (0.799 \times 7 + 1884 \times 0.0058 - 98.3) = 25.5 \text{ watts}$$

Thus for a range of ambient conditions and ventilation rates the overall respiratory heat loss can be predicted. *Fanger* [37] used the equations of *McCutchan and Taylor* [36] and

combined them with a relation between ventilatory exchange and oxygen uptake to obtain the following equation.

$$q = 0.00023\ M\ (44 - p_a) \qquad (1.3)$$

Where M = metabolic rate (watts) and p_a is the ambient water vapour pressure (mmHg). A similar model is proposed by *Welch* [38].

1.3.3 Local temperature, moisture, heat and water flux models

Quasi steady-state model

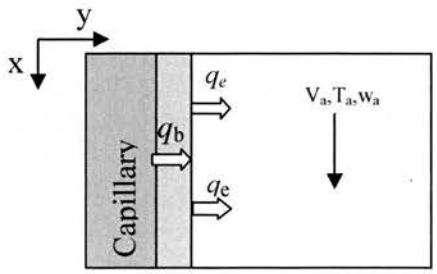

Hanna and Sherer [11] propose a model based on the idealised airway shown;

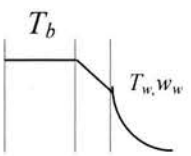

Steady-state heat balance at mucous-air interface at distance x along airway;

$$q_b = q_c + q_e$$

where q_b is the heat conducted through the airway wall, q_c is the heat convected from the mucosal surface and q_e is the heat due to evaporation of water at the surface. These quantities can be expressed in terms of their respective temperature and moisture gradients thus;

$$q_b = \frac{k(x)}{\Delta y}\left[T_b(x) - T_w(x)\right]$$

$$q_c = h(x)\left[T_w(x) - T_a(x)\right]$$

$$q_e = k_m(x)(w_w - w_a)h_{fg}$$

where *k(x)* is the thermal conductivity of the idealised airway wall, *h(x)* is a surface-air convective heat transfer coefficient and k_m *(x)* is the local water vapour mass transfer coefficient and h_{fg} is the latent heat of vaporization of water.

Therefore,

$$\frac{k(x)}{\Delta y}\left[T_b - T_w(x)\right] = h(x)\left[T_w(x) - T_a(x)\right] + k_m(x)(w_w - w_a)h_{fg}$$

A mass balance on an airway element yields,

$$v(x)\frac{dw_a}{dx} = \frac{P(x)}{A(x)}\left[k_m(w_w - w_a)\right] \tag{1.4}$$

where *v(x)* is the local mean air-stream velocity, P(x) is the airway perimeter and *A(x)* is the airway cross-sectional area.

Similarly an energy balance on the element gives,

$$v(x)\frac{dT_a}{dx} = \frac{P(x)(T_w(x) - T_a(x))}{\rho c_{av} A(x)}\left[h(x) + mc_{pw}\right] \tag{1.5}$$

where c_{pw} and c_{pa} = specific heat capacity of water and air respectively (KJ/kgK)

assuming the breath to be fully saturated at the airway wall and assuming a temperature range of 15°C about body temperature, then from the *Clausius-Clapeyron* equation, the water vapour content and temperature at the mucous-air interface are related by;

$$w_w = 22.4 \exp\left[\frac{-4.97 \times 10^3}{T_w}\right] \tag{1.6}$$

We thus have a system of 4 coupled, non-linear differential and algebraic equations which can be solved numerically to yield temperature and moisture profile as a function of distance (x) through the respiratory tract. Solution requires estimation of the transfer coefficients h(x), k(x) and $k_m(x)$. *Hannah and Shearer* [11] used the experimentally derived values of *h(x)* from cast models. Mass transfer coefficients, $k_m(x)$, were derived from the heat transfer coefficients assuming a complete analogy between heat and mass transfer. The blood temperature distribution along the airways was taken to follow a linearly increasing value from expired air temperature at the portal to a plateau body temperature at the bronchial periphery. Geometrical variables were taken from the detailed measurements of *Weibel* [24]. Intra-airways temperature and moisture profiles generated from this model showed good agreement with the invasive measurements of *McFadden* [9].

Non-steady state Model

Daviskas, Gonda and Anderson [14] developed a time-dependent model of heat and moisture transport in the airways. They emphasise the importance of residence time of air as a dominant factor for heat transfer. The mean air residence time (t) is therefore defined as;

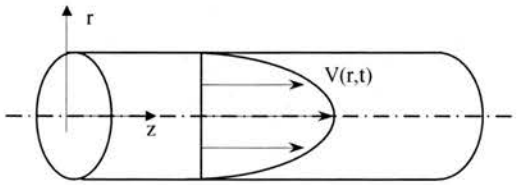

t = mass of air / mean mass flowrate rate in airway (s)

An energy and mass balance for air flowing through a tube (as shown above) gives a second order partial differential equation relating temperature or water vapour concentration (X) as a function of time and position (radius r, angle θ and distance z) as follows;

$$\frac{\partial X}{\partial t} + v\frac{\partial X}{\partial z} = D\left[\frac{1}{r}\frac{\partial X}{\partial r} + \frac{\partial^2 X}{\partial r^2} + \frac{1}{r^2}\frac{\partial^2 X}{\partial \theta^2} + \frac{\partial^2 X}{\partial z^2}\right]$$

If heat and water vapour transport in the radial direction only is considered and diffusion is angle independent this reduces to

$$\frac{\partial X}{\partial t} = D\left(\frac{1}{r}\frac{\partial X}{\partial r} + \frac{\partial^2 X}{\partial r^2}\right)$$

X(r,t) is temperature (°C) or water vapour concentration (mg/l) and D is either the thermal diffusivity of air (D_a) or the water vapour diffusivity in air (D_w). This second order differential equation has an analytical solution of the form;

$$X(r,t) = X_w - \frac{4(X_w - X_o)}{R_w^{\,2}} \sum_{n=1}^{\infty} \frac{e^{-D\lambda_n^{\,2} t}}{\lambda_n^{\,2}}$$

which relates the mean airway condition, X, as a function of residence time (t), radius (r), airway wall condition (X_w), the constant λ and the thermal or water vapour diffusivity, D. *Daviskas et al.* [14] took wall temperature to be related to inspired temperature, T_m, air flowrate V and distance along the airway, L according to the equation

$$T_w = T_m + (37 - T_m)\left[1 - e^{-(0.00564Ve + 0.276)L/V}\right]$$

The water vapour concentration at the airway wall (C_w) was calculated according to the airway temperature (T_w) and assuming 99.5% saturation.

The diffusivity, D is analogous to the convective heat and mass transfer coefficients in the steady-state model of *Hanna* [11]. They are related to local geometry and flow conditions

and derived from empirical relationships. The model was evaluated numerically allowing prediction of intra-airways temperature and moisture profiles as shown in Figure 1.5.

Further models with increasing degrees of complexity have been developed by other authors [13-18]. At resting levels of ventilation during inspiration the main regions of air conditioning are the nasal cavity, naso and oropharynx, larynx and the upper trachea.

These models tell us that the point at which the air is fully conditioned shifts at least six or seven generations depending on ventilation, and inspired conditions. For example, data from invasive measurements and mathematical models [46] would suggest that at minute ventilations of 15l/min and inspirate temperatures of 7°C, airways down to the 9th generation take part actively in heat and moisture exchange, with the lower airway (trachea to distal bronchi) contributing at least 50% of the total respiratory heat and moisture loss under these conditions. A decrease in inspired air temperature and water content at fixed minute ventilation produces a proportionately larger increase in heat loss from the extra-thoracic airways relative to intra-thoracic whereas an increase in minute ventilation at fixed inspired conditions produces the opposite pattern. Mathematical models would also suggest that an increase in simulated bronchial blood flow when coupled to an increase in mucosal thickness would produce a pronounced increase in airway temperatures. For example, *Tsai et al.* [18] looked at modeling the effects of changes in the mucosal and sub-mucosal layer. If the thickness of this layer was increased from 0.2mm to 0.9mm this would produce a 0.7°C increase in airway temperature. If this effect is combined with an increase in mucosal blood flow to maximal values (as might be seen in asthma) this could lead to an estimated increase of 1.7 °C in exhaled temperature.

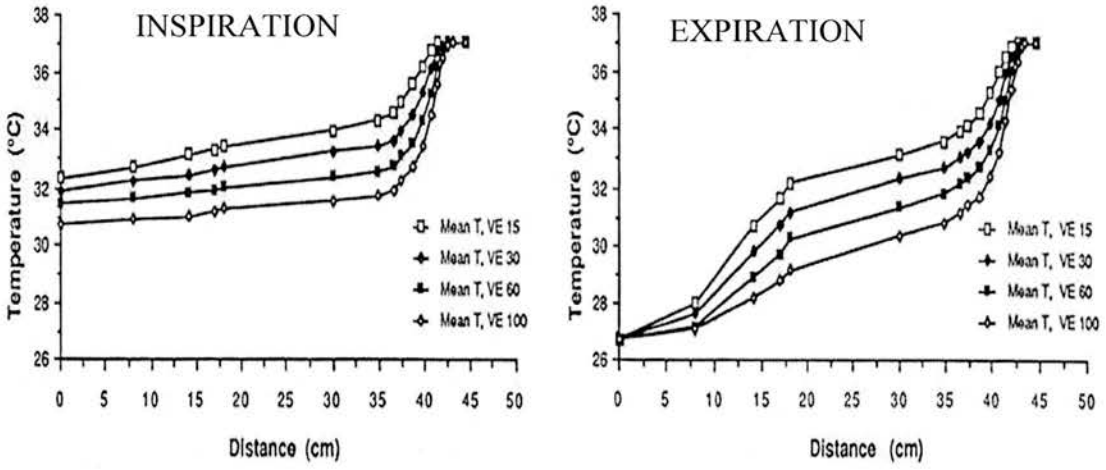

Figure 1.5. Theoretical predictions of intra-airway temperatures during inspiration and expiration from the model of *Tsu et al* [17]. Temperatures are calculated assuming inspired air at 26.7 °C, rh=50%. Values are calculated for minute ventilations (V_E) of 15, 30, 50 and 100l/min as shown.

1.3.4 Lumped heat capacity model

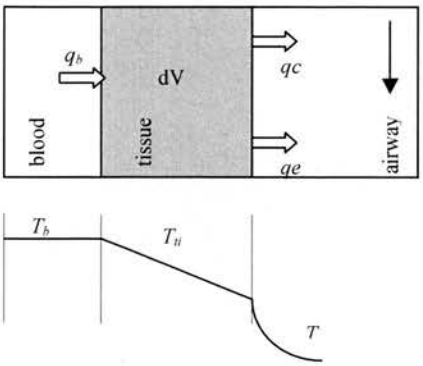

The Heat capacity model of *Serikov* [21] is not concerned with intra-airway temperature and moisture profiles but rather seeks to relate pulmonary blood flow and lung 'heat capacity' to airway thermal loading. Such a model proposes the use of airway temperatures as a non-invasive index of cardiac output and lung heat capacity or 'thermal volume'. Consider an element of airway tissue of volume dV as shown below which is subject to a cooling load applied by a step decrease in respired air temperature and humidity.

The change in tissue temperature is related to the balance of heat fluxes according to the equation;

$$dV\rho_w c_{pw}\frac{dT_{ti}}{dt} = \int(q_b - (q_c + q_e))dS \tag{1.7}$$

where; q_b = heat flux to the lung tissue from the pulmonary blood flow.

$q_e + q_c$ = ventilatory heat flux (convective + evaporative components).

S = surface area, T_{ti} = tissue temperature, q_b is defined according to the bioheat equation;

$$q_b = k_T \rho_w c_{pw} (T_b - T_{ti}) \cdot V_p \tag{1.8}$$

where k_T = tissue thermal conductivity, T_b = mean capillary blood temperature, V_p = pulmonary blood flow

The ventilatory heat flux (q_e+q_c) is given by;

$$q_e + q_c = V_e \left[\rho_G c_{pa} (T_{GO} - T) + (T_{GO} c_{pw} w_o - T c_{pw} w) + (w_O - w) h_{fg} \right] \tag{1.9}$$

Serikov et al [21] relate mean integrated temperature (T_{ti}) to expired air temperature (T) using a coefficient of proportionality K_R,

$$T_{ti} = K_R T$$

Where, $K_R = T_b / T_0$, T_b = body temperature and T_0 = temperature of expired air at the beginning of ventilatory loading. Substituting this in equations (1.8) and (1.9) yields a first order differential equation relating the change in expired air temperature with time under conditions of ventilatory cooling load

$$\frac{dT}{dt} + AT + B = 0 \tag{1.10}$$

where the constants A and B are given by

$$A = \frac{1}{V}\left[\frac{V_p K_T}{\rho_w c_{pw}} + V_E \mathrm{X}_2\right] \quad \text{and} \quad B = \frac{-1}{V}\left[\frac{V_p T_b K_T}{\rho_w c_{pw}} + V_e T_{G0} \mathrm{X}_1 + V_e \mathrm{X}_3\right] \tag{1.11}$$

$$X_1 = \frac{\rho_a c_{pa}}{\rho_w c_{pw}}\ , \quad X_2 = X_1 + \frac{0.0018 hfg}{\rho_w c_{pw}}, \quad X3 = \frac{0.02 hfg}{\rho_w c_{pw}}$$

The solution to equation (1.10) is given by

$$T(t) = \left(1 + \frac{B}{AT_o}\right) T_0 e^{-At} - \frac{B}{A} \tag{1.12}$$

which can be represented graphically (Figure 1.8). The measurement of the time constant, A, in the temperature decay curve will allow evaluation of pulmonary blood flow (and hence cardiac output) and thermal volume from equations (1.8) and (1.12).

1.3.5 In-vivo measurements of contribution of bronchial and pulmonary circulations to respiratory heat exchange.

Serikov [22] made airway temperature measurements in human subjects on cardiopulmonary bypass; a situation effectively representing selective bronchial artery lung perfusion. Following the application of a cooling load, by switching subjects from breathing warm to cold dry air, the temperature decay was observed. With bronchial perfusion alone (cardiopulmonary bypass) the time constant for temperature decay increased from 35s (prior to c-p bypass) to 56s and the peak expired temperature decreased by 1.4°C. This

evidence supports the idea that bronchial perfusion alone is not sufficient to supply the heat transferred to the airway under moderate cooling loads and that the pulmonary circulation forms the major contribution.

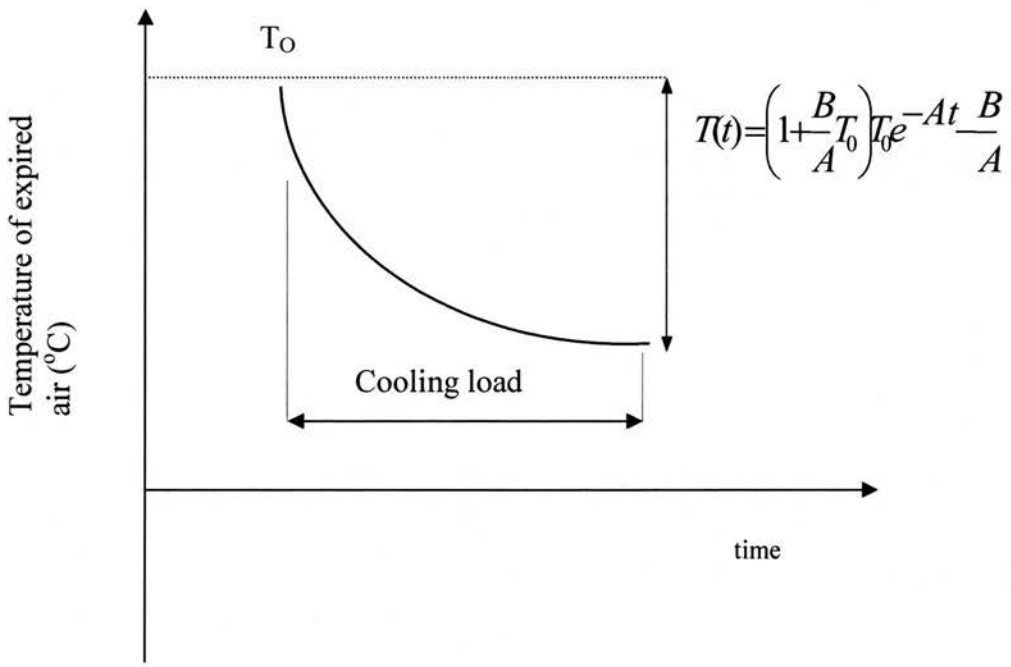

Figure 1.8. Idealised curve of maximal expired air temperature against time under cooling load provided by step change to ventilation with frigid air.

CHAPTER 2

THE MEASUREMENT OF AIRWAYS HEAT AND MOISTURE LOSS

2.1 Quantifying Respiratory heat and moisture loss

A number of studies have been conducted over the 20th century aimed at measuring the heat loss from the human respiratory tract. The earliest and largest study was conducted by *Burch* [7]. Essentially all studies since this have employed similar measurement methods. Figure 2.1 shows the technique of *Ferrus* [48]. A heat balance is performed according to equation (1.1). By measuring inspired and expired temperature and water content together with mass/volumetric flowrate the total heat flux from the respiratory tract can be calculated under conditions of steady state. Temperature measurements were made using thermometers, thermistors or thermocouples, flowrate by pneumotachometer or total body plethysmography. Water content in expired air was measured in all studies by the 'freeze-out' method of condensing the breath water vapour by passing it through tubes immersed in a frozen media. The condensate was then weighed and expressed as a fraction of flow volume. Inlet conditions were in some cases controlled by means of environmental chambers or the use of dry compressed gas mixtures. The results of these studies are summarised in Table 2.1. Parameters have been expressed in SI units to allow comparison.

Burch [7] in the largest of the studies employed a 'freeze-out' technique (aluminium coils immersed in flask of solid CO_2) to measure the moisture content of inspired and expired air. Thermocouples recorded inspired and expired air temperatures. Low-pressure

positive displacement gasometers measured volume flowrate. The heat loss, comprising sensible and latent components could thus be calculated from the steady-state heat balance equation (1.1). Subjects were monitored under 'room conditions'. No strict control of ambient conditions was made. The dominance of the evaporative (q_e) over the convective heat loss (q_c) modality is clearly seen from the results. Under ambient conditions of 20-21°C and rh 50-60% an average of 166.8-mg/min water loss representing 6.7 W of evaporative heat versus 1.6 W of convective exchange was found. *McCutchan* [36] employed a similar technique to *Burch* [7] but provided stricter control over inspired conditions by means of an environmental chamber. This study measured the effects of normal and high temperatures at a range of moisture contents on the respiratory heat exchange. Results were in good agreement with those of *Burch* [7]; the slightly dryer inspirate accounting for the higher moisture and heat loss. With reference to Table (2.1), the studies of *Ferrus and Varene* [48] *Caldwell* [49], and *Cain* [50] further demonstrate the importance of the evaporative heat loss component to overall respiratory heat exchange. This component can account for between 70 to 95% of the overall heat exchange depending on the inspired conditions. Decreasing the moisture content of the inspirate will increase this component as will increasing the minute volume according to these studies. From these data it can be estimated that on average, in a temperate climate, the heat loss from the human airway is between 10-15 W with 70-80 % of this being due to the evaporation of water from the airway leading to a daily water loss of around 350 mls.

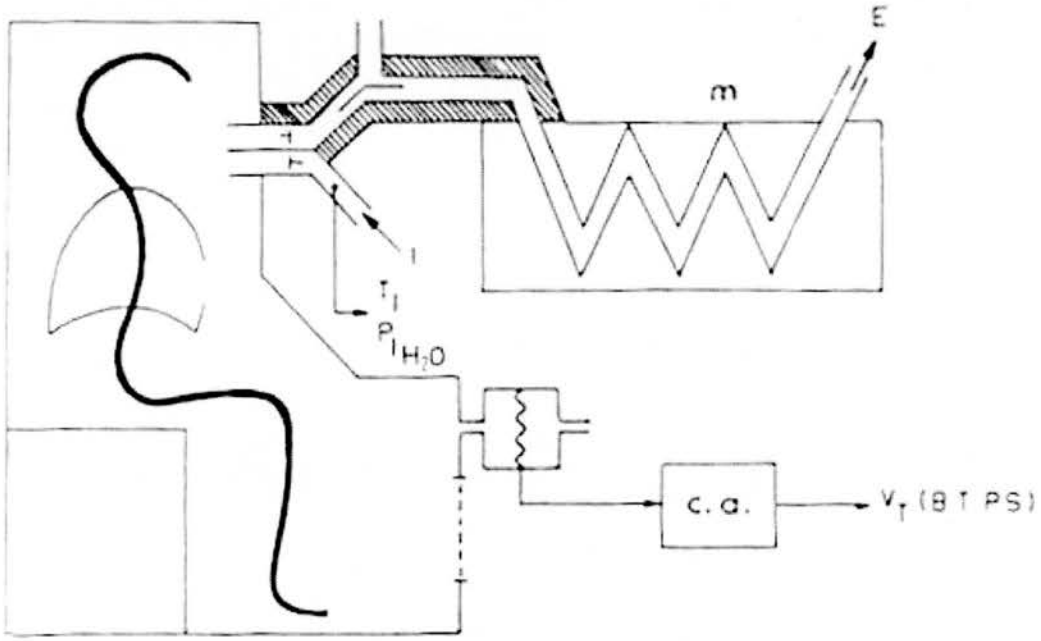

Figure 2.1. Schematic of the apparatus for the measurement of RHML by Ferrus et al. [48]. By measuring inspired and expired temperature and water content together with mass/volumetric flowrate the total heat flux from the respiratory tract can be calculated under conditions of steady state. Temperature measurements were made using thermometers, thermistors or thermocouples, flowrate by pneumotachometer or total body plethysmography. Water content in expired air was measured in all studies by the 'freeze-out' method of condensing the breath water vapour by passing it through tubes immersed in a frozen media. Inspired air water content was measured by means of a wet bulb thermometer.

STUDY	Design No.of subjects	Inspired Conditions Ti (^{o}C)/ rh(%)/ventilation	Water loss (µl/min)	Respiratory Heat Loss (Watts) q_e	q_c	q_T
Burch 1945 [7]	56	20-21/ 50-60 /6.9	166	6.7	1.6	8.3
McCutchan 1950 [36]	5	21-24 / 20-40 / 7.5	227	8.5	2.6	11.1
Caldwell 1969 [49]	5	25-27 / 0/ 9.85	282	11.9	0.9	12.8
Ferrus and Varene 1986 [48]	5	24.8 / 0/ 6.74	179	7.0	0.5	7.5
Cain 1990 [50]	5	0 / 0/ 8.7	440	26.7	1.2	28.0

Table 2.1. Comparison of measurements of respiratory heat and moisture loss (RHML). Lower inspired temperature and humidity is associated with higher measured heat and moisture loss. At similar inspired air temperatures but with dryer inspired conditions there is a greater evaporative heat loss compared to convective heat loss.

2.2 Factors affecting Respiratory Heat Loss

Considering Figure 2.2 it can be seen that both external and internal factors will alter the quantity of heat lost via the respiratory tract. The metabolic heat generated within the lung tissue (Q_g) is thought to amount to approximately < 5% of the total heat lost and is normally neglected in heat balance calculations. Total heat loss will vary between individuals depending on size. Most studies therefore express the heat loss according to total body surface area as calculated from height and weight.

2.2.1 Inspired air conditions.

As with heat loss from the skin, the temperature and relative humidity of the external environment will affect the rate of heat and moisture loss. Lower inspired air temperatures and moisture contents place an increased thermal burden on the airway whereby more heat and moisture will be transferred under these conditions. Table 1 illustrates this point. *Burch* [7] was unable to measure any significant effect of lowering inspired air temperature and humidity perhaps due to the lack of controllability and only very slight degree of change in these parameters (15°C, rh 60%) for comparison. However under conditions of hot, dry inspirate (50°C, rh 18%) an increased evaporative loss was measured. This was found to be smaller if at the same temperature more moisture was present (50°C, rh 49%).

The study of *Cain* [50] shows that dry inspired air at 0°C results in an excess of two-fold increase in respiratory heat loss over dry warmer air (*Caldwell* [49]) and an approximate 3-fold increase over warmer wetter air (*Burch* [7]). The proportion of 'evaporative' heat loss over convective is even higher under the more extreme conditions. *McCutchan* [36] found

that in subjects at rest, respiratory heat loss correlated strongly with inlet temperature and humidity. They proposed the following predictive equation (adapted to SI units) based on their data.

$$Q = m\,(0.799\,T_i + 1884\,w_i - 98.3)\ (W)$$

m = mass flowrate kg/s

T_i = inspired temperature (^{o}C)

This demonstrates that a set of conditions exist where heat can be gained by the respiratory tract. Interestingly, even with air temperatures equal to core temperature, if the air is dry enough there can still be a net heat loss from the respiratory tract due to the dominance of evaporative cooling over convective warming.

.

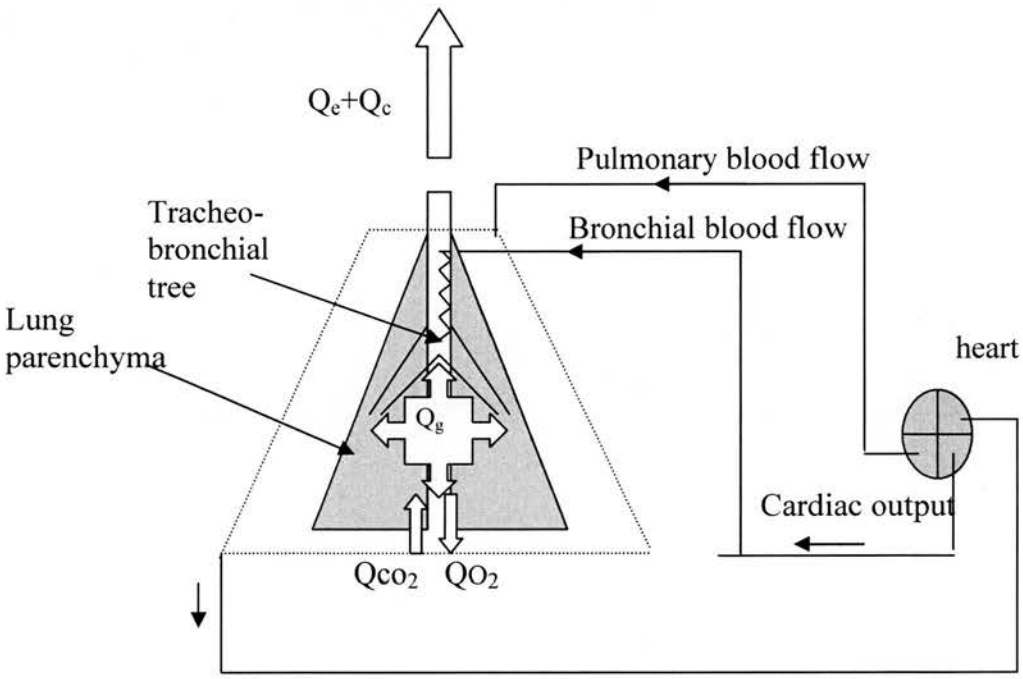

Figure 2.2: Schematic diagram showing respiratory heat flux components and heat delivery via bronchial and pulmonary circulations. Heat is generated through cellular metabolism (Q_g) in lung tissue which is thought to amount to <5% of the total. Heat is also transferred through gas exchange - the evolution of CO_2 from blood to alveoli is endothermic (Qco_2) and the combination of O_2 with blood is exothermic (QO_2).

2.2.2. Ventilatory Pattern

Minute ventilation has been shown to correlate with respiratory heat loss. In the study of *Burch* [7], minute volume varied for the group of 56 subjects, with a mean 3.8 $l/m^2/min$ and a range 2.8 to 5.3 $l/m^2/min$. A high degree of correlation was found for the group between minute volume and respiratory water loss. In smaller groups of subjects *Burch* [7] looked at the effect of breathing pattern and various ambient conditions on respiratory water loss. Although not quantified, slow deep breathing was associated with more water loss per litre respired than rapid shallow breathing. *Ferrus et al.* [48] did quantify the water loss in relation to breathing pattern and found the water loss (per litre respired) not to vary with changes in minute ventilation but to increase with increasing tidal volume patterns.

2.2.3 Exercise

Exercise involves a number of physiological changes that will increase respiratory heat loss. Exercise results in an increase in the heat generated by the body through increased muscle work and metabolic rate. The raised cardiac output delivers increased blood flow to the lungs via the bronchial and pulmonary circulations. Minute ventilation will be raised to meet the requirement of increased O_2 uptake and CO_2 excretion.

Cain et al. [50] measured respiratory heat loss at various ambient conditions and work rates. They found that at $0^{o}C$, raising the metabolic rate (through exercise) four-fold resulted in an increase in respiratory heat loss from 28 W to 82 W. Interestingly, some studies show exercise work rates do not affect expired air temperature or water content [33-36]. However, others found expired air temperature and water content to decline with increasing work

rates. A strong correlation is found between respiratory heat loss and minute ventilation when exercising. *Mitchell et al.* [52] measured respiratory water loss at various work loads. They found a strong correlation between water loss and oxygen uptake (Vo_2), which was in good agreement with the empirical equation proposed by *Fanger* [37] up to 70% VO_2 max. *Tabka et al.* [53] investigated the time course of respiratory heat exchange during exercise and rest conditions. They found that when breathing warm dry ambient air at rest or during exercise there was a fall in the water content of the expired air over the first 15 minutes of testing followed by a recovery period where moisture loss was found to return to original rates. The authors related this to dehydration of the bronchial mucosa followed by an adaptive response restoring hydration; the mechanism of which is unclear. This phenomenon may explain the disagreement cited above regarding the exhaled air condition during exercise.

2.2.4 Core temperature

It has long been established that an increased or increasing body temperature is associated with increased minute ventilation. *Barltrop* [54] found an increase of 3.8 l/min for a 2°C rise in core temperature. The increase in minute volume is mainly due to an increase in tidal volume rather than respiratory rate. It was *Walker* [55] who first proposed that pyrexial patients would have a warmer bronchial mucosa with the result that expired air temperatures and water loss would be elevated. *Hanson* [56] addressed this point in his study where subjects' core temperatures were raised by immersion in hot water baths. Dressing the subjects in a vapour immersion suit with a controllable air inlet allowed core temperature to be set at a steady level. Various ambient conditions were set by means of a climatic chamber. A clear increase in respiratory heat loss was found at increasing core

temperatures. This was found to be mainly due to the effect of increased minute volume accompanying increased core temperature. Exhaled air temperature was not found to be affected by changes in core temperature.

2.2.5 Pulmonary and bronchial blood flow

Heat is delivered to the airways via the bronchial and pulmonary circulations. The anatomy was described earlier – the bronchial circulation with its sub-mucosal and peri-bronchial plexuses being in more intimate contact with the airway compared to the pulmonary circulation down to airways of 1mm diameter. The bronchial arterial system however has a low flowrate, carrying less than 1% of the cardiac output at systemic pressure whereas the pulmonary circulation carries the entire cardiac output at lower pressure. The relative contribution of each circulation to respiratory heat exchange was studied by *Baile et al* [58]. In this study anaesthetised and ventilated dogs were used. Respiratory heat loss was evaluated by measuring inlet and outlet conditions and ventilation rate and applying the heat balance equation (1.1). The tracheo-bronchial heat transfer (Q_b) was calculated by measuring bronchial blood flow (BBF) using a radio-isotope microsphere technique, measuring blood and tracheal temperatures (T_b, T_t) and applying the equation;

$$Q_b = BBF\ c_p\ (T_b - T_t)$$

where c_p is the specific heat capacity of blood. Their results showed that under conditions of hyperventilation with cold air, respiratory heat loss amounted to around 42 Watts under conditions of steady state. A 60% increase in tracheo-bronchial blood flow was measured over baseline corresponding to a tracheo-bronchial heat transfer (Q_b) of 10 Watts. This

would imply an additional heat source (pulmonary circulation) was supplying the remainder of heat (32 Watts) to the airway.

Solway et al [19,20] reached a similar conclusion in a study comparing the effects of temporary occlusion of a single lower lobe artery or interrupting the bronchial arterial supply on airway temperatures. Dogs mechanically hyperventilated with cold air had their left lower lobe pulmonary artery occluded by balloon catheter. This produced an ipsilateral fall in airstream temperatures. The contralateral airstream temperatures remained unchanged. On release of the occlusion temperatures were restored. Under similar conditions the bronchial circulation was occluded using vascular clamps, which had no effect on airstream temperatures. The authors interpret this to indicate that the pulmonary circulation is the dominant source of heat over the bronchial circulation to the respiratory tract. This evidence would certainly suggest that the pulmonary circulation has an effect on airway temperature at this level of the respiratory tract in dogs. However no measurements were made of airway humidity or moisture transport in this study. Moisture transport is known to form the major portion of respiratory heat exchange. It is therefore debateable whether this evidence can be extrapolated to the human lung in health or disease.

More recently *Serikov et al.* [22] provides further support for the lesser contribution of the bronchial circulation as a heat source for the airways under moderate cooling loads. They further extend their investigations to explore the functional implication of this and conclude that the major role of the bronchial circulation is in water transport to the bronchial mucosa. By selectively perfusing the bronchial and pulmonary circulations of isolated dog lungs and making simultaneous airway temperature measurements they were

able to show that for a fixed pulmonary arterial flow, increasing the bronchial flow to a value exceeding the upper limit of the normal range resulted in no significant increase in airway temperature compared to that with pulmonary perfusion alone. They also looked at airway temperature measurements in human subjects on cardiopulmonary bypass; a situation effectively representing selective bronchial artery lung perfusion. As described earlier they use a lumped heat capacity model to relate the rate of temperature decay and drop in exhaled air temperature to tissue perfusion and thermal volume (see previous section). Following the application of a cooling load, by switching subjects from breathing warm to cold dry air, the temperature decay was observed. With bronchial perfusion alone (cardiopulmonary bypass) the time constant for temperature decay increased from 35s (prior to c-p bypass) to 56s and the peak expired temperature decreased by 1.4^{o}C. This evidence supports the animal study showing that bronchial perfusion alone is not sufficient to supply the heat transferred to the airway under moderate cooling loads. By measuring the rate of equilibration of tritiated water (THO) between the circulations and the lung parenchyma and respired air they found the time constant for equilibration between pulmonary perfusate alone and lung parenchyma was four times greater than that between combined bronchial and pulmonary perfusate. This would imply that the increased rate of filtration of water from the high-pressure bronchial circulation promotes water exchange in the lung interstitium. In addition, a higher ratio of tracer gas to perfusate was found indicating that bronchial vessels were contributing significantly more to mucosal hydration.

2.3 The effect of airways disease on respiratory heat and moisture loss

It was *Walker* [55] in 1961 who pointed out that the ability of the respiratory tract to condition inspired air and to conserve heat and water during expiration rests mainly on the integrity of the airway mucosa and its normal water content and that airway disease is bound to interfere with this function. At that time there was a paucity of data from measurements on patients with respiratory disease. Since that time a large body of data has emerged mainly exploring the mechanisms of exercise induced asthma. However there is still little known about the thermal and moisture transfer characteristics found in conditions such as asthma, COPD and Bronchiectasis.

Thermally induced asthma

Exercise induced asthma is the term used to describe the occurrence of airflow obstruction following exercise or hyperventilation. It should perhaps more correctly be termed thermally induced asthma as it has been demonstrated that both exercise and voluntary hyperventilation produce the same effect in individuals with this tendency [61]. A substantial body of evidence supports increased airway heat flux and mucosal cooling triggered by increased minute ventilation as important initiators in airway narrowing [62-66]. Two main theories concerning the mechanism of airway narrowing exist; namely, the osmotic or airway drying hypothesis [67,68] and the thermal hypothesis [70]. The osmotic hypothesis supports the idea that mucosal drying results in a hyperosmolar surface lining fluid, which leads to intracellular water flux and cell shrinkage. This is said to stimulate the release of inflammatory mediators and thereby cause smooth muscle contraction. The thermal hypothesis would propose that airway cooling followed by rapid rewarming stimulates a vasoconstrictive followed by a reactive hyperaemic response in the bronchial

microcirculation. Some studies implicate nitric oxide [70] and IL-8 [71] and even interactions with surfactant function [72] in the mechanism of thermally induced airway inflammation. This in turn would lead to airway wall oedema and airway narrowing. Some would support a unified hypothesis given that it is difficult to separate the processes of cooling and drying as detailed earlier in this review.

Asthma, COPD and Cystic Fibrosis

It is now known that subjects with even mild stable asthma have increased vascularity in their airways [73-75]. This would suggest that there would be increased respiratory heat and moisture loss in this group compared to a control group. Furthermore, the degree of inflammation should correlate with the level of heat and moisture loss. At present there are no published data on this question. Similarly, marked hyperaemia of the mucosa is seen at bronchoscopy in the airways of patients with COPD during acute exacerbations. Some studies have sought to measure the bronchial blood flow in patients with chronic bronchitis and emphysema [76-80]. The results are inconclusive partly due to technical difficulties in measuring bronchial blood flow accurately and in part due to the co-existence of both the inflammatory bronchitic process together with the destructive emphysematous process (which would cause a reduced bronchial flow in the area of lung affected). *Caldwell* [49] in a small study measured the heat and moisture loss in a group of patients with COPD versus controls and found a marginally increased heat loss in the COPD group when expressed as a fraction of total heat production. The patient numbers were small, there was no distinction between disease types (bronchitic or emphysematous) and no assessment made of disease severity. Bronchiectasis is another airway disease process that might be expected to alter the heat and moisture exchange process. It is well described that there is marked proliferation of the bronchial vasculature

in this patient group [81]. This may provide the increased water requirements needed for the large volume sputum production seen in this condition. A small study by *Primiano et al.* [82] looked at breath temperature and moisture contents at the airway opening in 4 patients with stable Cystic Fibrosis. They failed to show any difference in exhaled temperature or moisture content between subjects breathing air at 22°C ± 2°C. Inlet conditions were not strictly controlled in this study and were set at a value whereby the isothermal saturation boundary (ISB) would be proximal to the trachea. The part of the bronchial tree of most interest would not be engaged in significant heat or moisture transfer due to the low thermal burden therefore it would be unlikely that differences in breath temperatures and moisture content would occur between the CF and control groups. Few studies have looked at measuring aspects of heat and moisture exchange in airways disease. Recent studies have looked at the nasal mucosa and found an impaired ability of patients with allergic rhinitis to humidify inspired air [83]. In asthmatic patients, studies have reported a faster rise in exhaled breath temperature [84] and higher exhaled plateau temperatures [85] compared to controls whereas in COPD the converse was found [86] suggesting altered heat loss patterns in these airway diseases. However, these studies did not attempt to quantify evaporative heat loss. Breath temperatures alone, do not take into account heat loss due to water transport processes, which form the major part of the total airway heat exchange [36,48,49,50].

CHAPTER 3

A NEW TECHNIQUE TO MEASURE RESPIRATORY HEAT AND MOISTURE LOSS

3.1 Introduction

As was described in the previous chapter there have been a number of studies carried out over the last hundred years or so aimed at quantifying the net heat lost from the human respiratory tract. Respiratory heat loss comprises convective and evaporative components; the former requires knowledge of the temperature difference between the inspired and exhaled air whereas the latter requires measurement of the net moisture lost in breath. Accurate and quick response thermocouples and thermistors have been around for some time and allow reliable measurement of breath temperatures. However it has only been relatively recently that small electronic humidity sensors have been made available offering a means to accurately measure breath moisture content without having to employ the cumbersome wet bulb thermometer or the fairly elaborate 'freeze-out and weigh' equipment previously used – techniques which do not lend themselves easily to larger clinical studies. Previous studies have demonstrated the site of airway heat and moisture exchange and that inspired air condition and ventilation are important

determinants of this. The aim of the new technique outlined here was to draw on the advances in electronic moisture sensors, provide a controllable inspired air condition and breathing pattern and thus allow a more precise and convenient measurement of respiratory heat and moisture loss in a large number of human subjects including those with airways disease.

3.2 Equipment design

3.2.1 Rationale for equipment design

The data of McFadden et al. [9] suggests that unless subjects breathe cooled inspirate and at elevated minute ventilation, the bulk of heat and moisture transfer will take place in the upper airway (above the glottis). Data from invasive measurements and mathematical models [46,47] would suggest that at minute ventilations of 15l/min and inspirate temperatures of 7°C, airways down to the 9th generation take part actively in heat and moisture exchange, with the lower airway (trachea to distal bronchi) contributing at least 50% of the total respiratory heat and moisture loss under these conditions. Alterations in RHML brought about by pathological changes in the lower airways should therefore have significant impact on the total RHML measured.

In the present study therefore the degree of thermal loading (i.e. V_e =15l/min. T_i=7°C) was chosen in order to engage enough of the bronchial tree in heat and moisture exchange to reflect differences in the lower airways. That said, it is well recognized that the thermal loading associated with isocapnic hyperventilation can induce changes in airway resistance and indeed bronchial blood flow in subjects with exercise induced asthma [46]

and even in normal subjects [109] and that a test such as the one described here could potentially alter the very parameter it seeks to measure. However, the level of thermal loading used in this test was low (~20W) representing approximately 10% of values found by most studies to induce changes in FEV_1 in asthmatics and equivalent to those found not to induce a measurable increase in bronchial blood flow in normals [109]. It is therefore unlikely that the ventilatory pattern and inspired air condition used here would have a significant effect on inducing changes in airway resistance and airway circulation.

3.2.2. Compact air-conditioning unit

The new device was designed (shown in Figure 3.1) to comprise a purpose-built air-conditioning module delivering air at up to 1500ml/s with a controllable temperature (3 to 40°C) and moisture content (5 to 40g/kg dry air). The cooler/de-humidifier was constructed using Peltier heat pumps fitted to flat plates in contact with cooling fin plates as shown. Fans attached to the inlet of the finned section generated the air-flow which could pass directly to the outlet of the cooler or could be directed via a circuit containing a reheater and humidifier thereby allowing control of the temperature and moisture content of the inspired air.

3.2.3. Breathing circuit

Subjects breathed through a 2-way valve (Hans-Rudolf). Inspired air was supplied in a flow-past configuration from the air-conditioning unit at a flowrate exceeding the peak inspiratory flowrate. Dead-space (valve plus mouthpiece and filter) was 30ml and was further minimized by the placement of a divider separating inhaled and exhaled air-streams. To ensure eucapnia the exhaled CO_2 was measured continuously and then CO_2 was added to the inspiratory limb of the circuit during the course of a typical 6 minute test.

3.2.4. Instrumentation

Exhaled water content is difficult to measure, because if air is allowed to cool in the equipment, moisture is lost by condensation. To overcome this problem, exhaled breath (Figure 3.1) first passed a temperature sensor close to the mouth (measuring exhaled temperature) then down a 15cm heated tube at the end of which humidity and temperature were measured. These distal measurements yielded breath water content, and allowed back-calculation of exhaled humidity at the mouth. The small valve dead-space volume, the presence of a divider within this dead space and the use of the heated tube section ensured negligible loss of moisture through condensation in the circuit.

Temperature sensors were K-type thermocouples (chromel-alumel bead type), with a 90% response time of 50ms. All sensors were calibrated whilst connected to their signal amplifier and data acquisition channel against a mercury standard in a water bath between 0 to 40 ^{o}C. Humidity sensors were of thermoset polymer capacitance construction (*model HIH-3602-A, Honeywell, USA*) supplied factory calibrated giving relative humidity with an accuracy of ±2% and an estimated 95% response time of 5s. Expiratory air flow was measured using an ultrasonic phase-shift flow meter (*model FR-413, BRDL, Birmingham, UK*), which was calibrated for volume (litres ATPS) using standard volume syringes (*vitalograph, UK*). The sensor's 100% response time was 12ms; linearity was <2% and the residual error due to temperature variation <1% in the temperature range 0-40^{o}C.

Thermocouple and humidity sensor output were amplified and sampled at 100Hz and captured on a 16-channel computerized data acquisition system (*model 1401, CED, Cambridge, UK, software*: *spike 2, CED, Cambridge, UK*) to allow real time signal display and storage of data to disk.

3.2.5. Ventilation pattern targeting.

In order to compare measurements between subjects, specific ventilatory patterns were imposed by feeding the expiratory flow signal into a PC with purpose built breath-targeting software, which generated a visual and auditory target for expiratory flow-rate and respiratory rate respectively. Inspiratory to expiratory ratio was set at unity. Eucapnia was maintained at the higher minute ventilations by measuring end-tidal CO_2 and adding CO_2 to the inspirate.

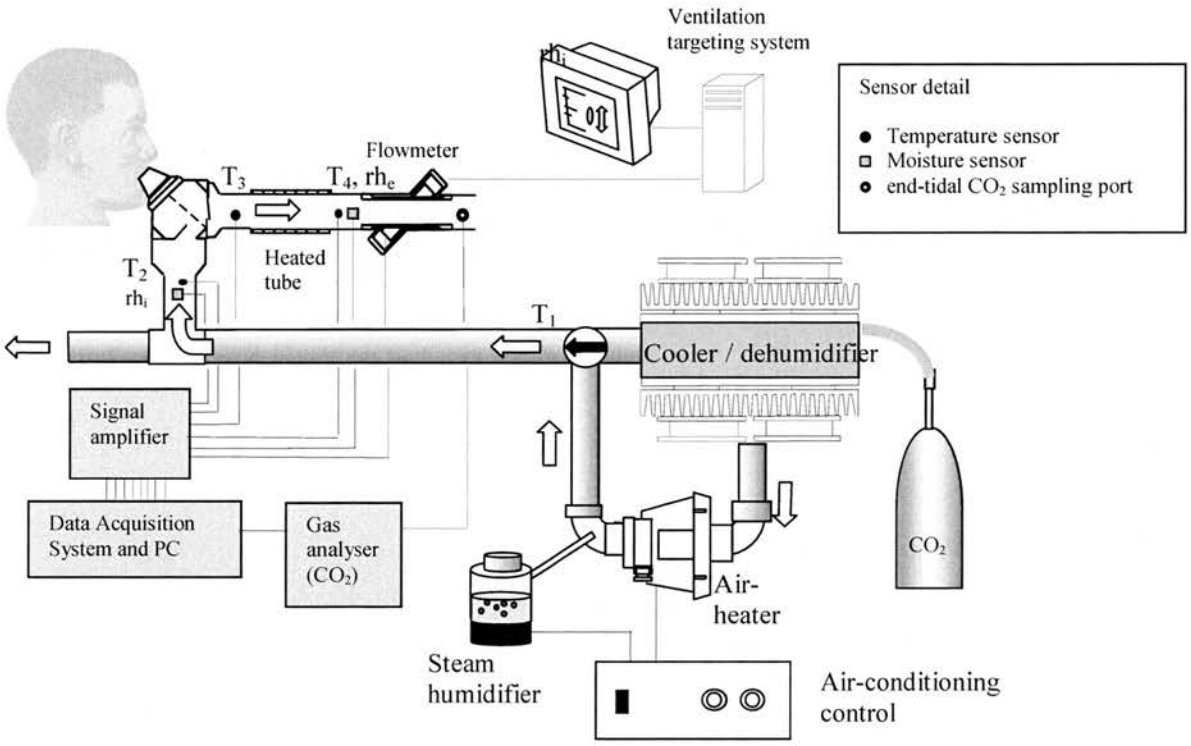

Figure 3.1. Schematic of apparatus and instrumentation for the measurement of respiratory heat and moisture loss (RHML). Subjects breathe through a non-rebreathing 2-way valve at a pattern set by the ventilation targeting system which generates an audiovisual feedback signal setting ventilation rate and expiratory flow respectively. An air-conditioning unit controls the temperature and moisture content of the respired air. Temperature and moisture sensors are located as shown. At higher minute ventilations eucapnia is maintained by monitoring exhaled CO_2 and adding CO_2 to the circuit as required.

Figure 3.2. Photograph showing apparatus for the measurement of respiratory heat and moisture loss (RHML). The device was designed to be trolley-mounted and portable but the data acquisition and display equipment could easily be miniaturised for clinical application .

Figure 3.3. Photograph showing the author seated at apparatus for the measurement of respiratory heat and moisture loss (RHML). The subjects follow an audio-visual target for ventilation on a PC monitor.

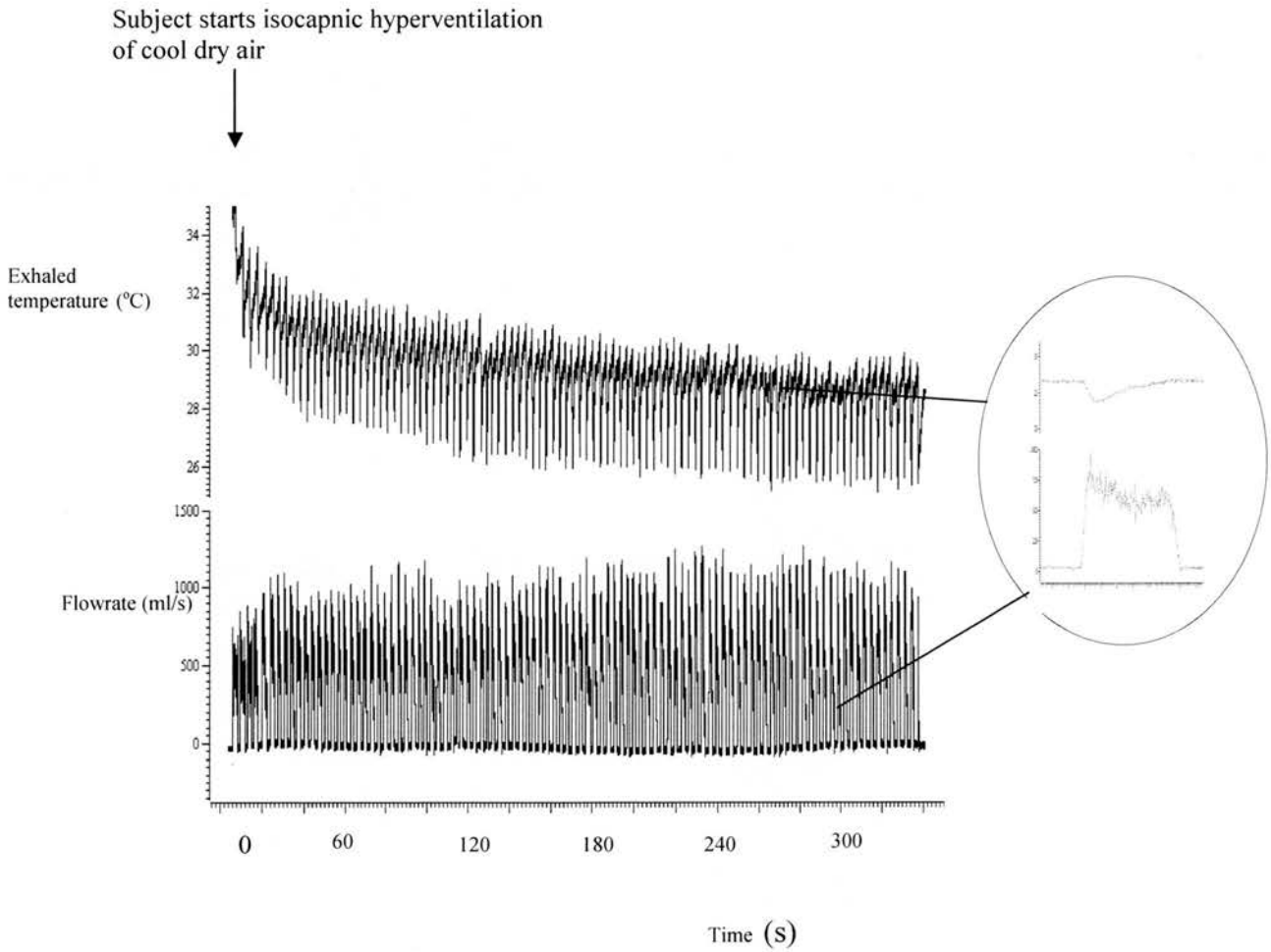

Figure 3.4. Expiratory temperature and flow-rate signals showing time to steady-state following imposition of a cooling load associated with isocapnic hyperventilation of cold air. The inset shows an single breath expiratory temperature and flow signal - the flow signal approximating to the square wave target.

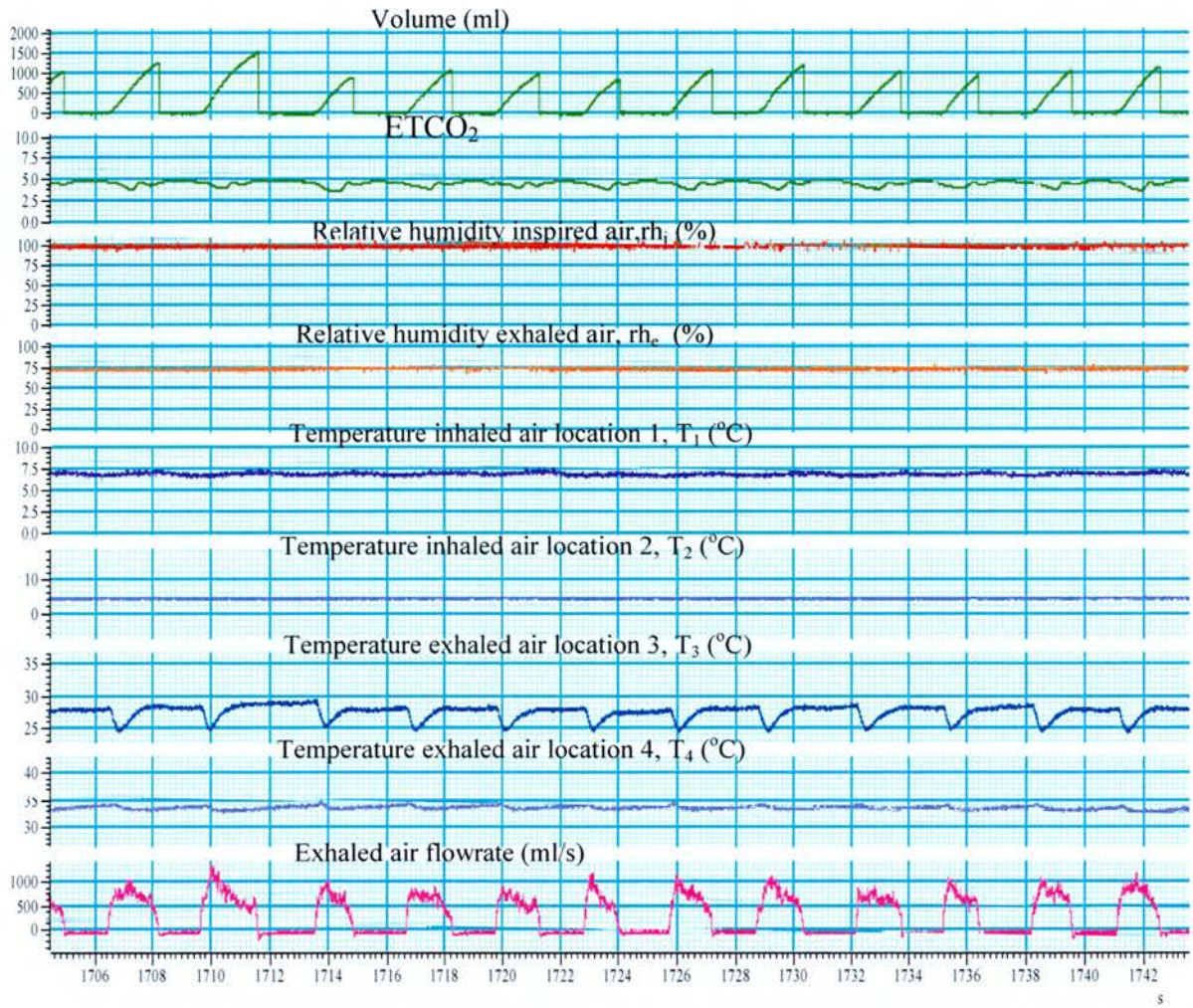

Figure 3.5. Thermocouple and humidity sensor output was conditioned by purpose built multichannel amplifiers. All signals were sampled at 100Hz and captured on a 16-channel computerized data acquisition system (*model 1401, CED, Cambridge, UK*), which interfaced with software (*spike 2, CED, Cambridge, UK*) to allow real time signal display and storage of data to disk.

3.3 Analysis

3.3.1. The thermodynamics of the respiratory cycle

Atmospheric air, and indeed breath, as well as comprising the main constituent gases nitrogen, oxygen and carbon dioxide also contain water that exists as a superheated vapour. Water in this state can be treated as a gas. A mixture of such gases can be regarded as a single substance provided the constituents do not react chemically with each other. The thermodynamic properties of moist air can be determined experimentally, just as for single substances, and tabulated or represented graphically. When considering a mixture of gases the Gibbs-Dalton law states [89];

> *The pressure and internal energy of a mixture of gases are respectively equal to the sums of the pressures and internal energies of the individual constituents when each occupies a volume equal to that of the mixture at the temperature of the mixture.*

Thus,

$$P_a = P_{O2} + P_{CO2} + P_{N2} + P_{H2O}$$

where, P_a =air pressure, $P_{subscript}$ = partial pressure of constituent gas.

The pressure that each gas component exerts is called its partial pressure. Pressure, volume and temperature can be related according to the perfect gas equation;

$$P_i V = n_i R T$$

where P_i = partial pressure of constituent, n_i= molar amount of substance (kmol), R = universal gas constant, T = temperature.

The *perfect gas equation* therefore defines the thermodynamic state of both air and its constituents individually.

The term **water vapour pressure** represents the partial pressure of water vapour in air and will be proportional to the absolute amount of vaporised water and the temperature of the air. **Specific humidity** (or moisture content) is the ratio of the mass of water vapour to the mass of dry air for any given volume. **Relative humidity** is the ratio of the actual partial pressure of the vapour to the partial pressure of the vapour when the air is saturated with water, at the same temperature. **Enthalpy** is a useful term that describes the 'useable' energy (dry and latent) in air. The enthalpy of moist air is given by

$$H = h_a + wh_s,$$

Where H = total enthalpy, h_a = enthalpy of dry air (dependent on temperature and pressure), w = specific humidity, h_s = enthalpy of water vapour.

The term wh depends on both the temperature and pressure of the air. If air pressure is fixed, w and temperature can be regarded as the only independent variables that define the thermodynamic state of the moist air. A **psychrometric chart** can thus be constructed for air at atmospheric pressure plotting specific humidity versus temperature with constant enthalpy lines overlaid. This allows easy visualisation of the thermodynamic state of air water mixtures and calculation of heat transfer. Consider the respiratory cycle shown in Figure 3.5; Air at the typical indoor ambient condition of 22°C and relative humidity 40% contains approximately 5mg per litre dry air of water. Inspiration raises the tidal air to

37°C, fully saturated. The airway mucosa therefore provides around 35mg of water per litre dry air inspired. On expiration around 15mg of water condenses on the airway returning around 30% of the mucosal water resulting in a net loss of approximately 20mg of water per litre respired.

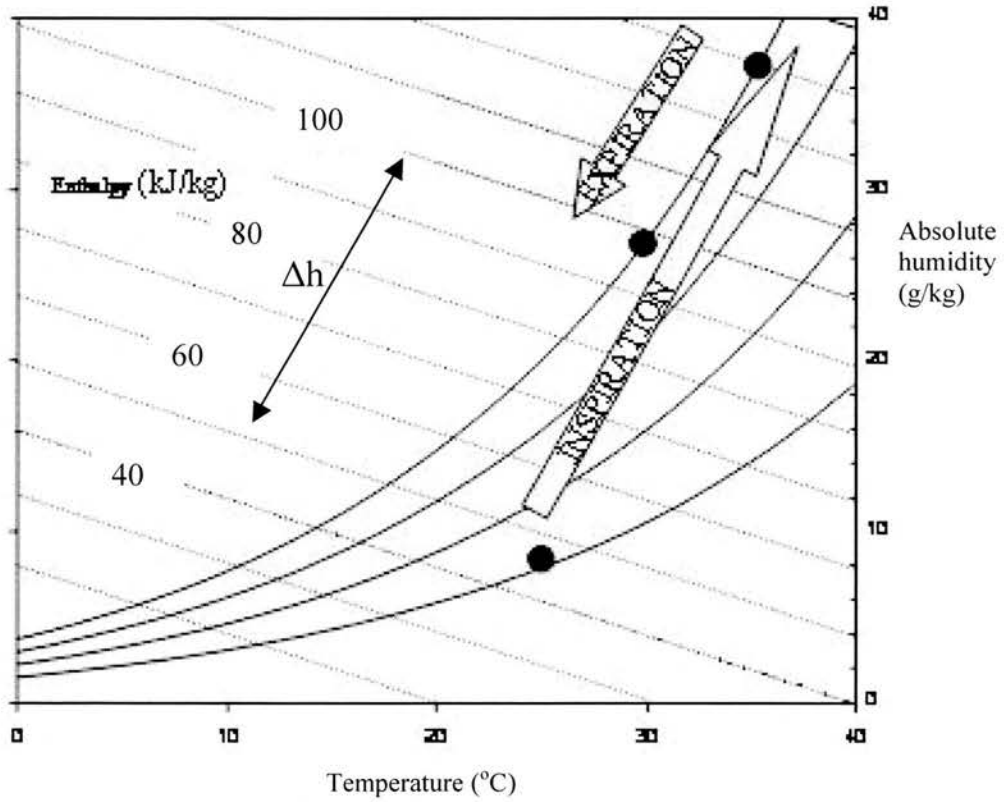

Figure 3.6. The thermodynamics of the respiratory cycle. A 'psychrometric chart' plots absolute humidity versus temperature for air at atmospheric pressure with the curves of constant relative humidity overlaid. Enthalpy (h), which is a measure of the 'useable energy', associated with both air temperature and moisture content are included. During inspiration, of room air its temperature and moisture content is raised to core temperature, as heat and moisture are lost from the respiratory mucosa. During expiration, air from the deep airways is cooled and some of its water condenses resulting in a partial recovery of some of the heat and moisture lost on inspiration but nevertheless a net loss of heat and moisture (Δh).

If this system is assumed to be at steady-state and closed whereby inspiratory and expiratory ventilations are equal (see section 1.3.1) and the difference in water vapour concentrations between inspired and expired gases to be due only to condensation and evaporation processes alone then the respiratory heat loss (Q_l) can be expressed as;

$$Q_l = \rho V (h_e - h_i) \qquad 3.2$$

where ρ=air density (kg/m^3·ATPS), V=flow rate (m^3/s ATPS), h_e, h_i = enthalpy (kJ/kg) of exhaled and inhaled air respectively (derived from temperature and humidity sensor measurements referred to the psychrometric properties of air at atmospheric pressure [90].

The convective heat loss (Q_c) is calculated from;

$$Q_c = \rho V c_p (T_e - T_i) \qquad 3.3$$

The specific heat capacity of air at constant pressure (c_p) was taken as 1.008 kJ/kgK (an average between values for inspired air and alveolar gas). T_e and T_i are the mean temperatures of the exhaled and inhaled air respectively.

3.3.2. Calculating respiratory heat and moisture loss (RHML)

To calculate the respiratory heat and moisture loss it is necessary first to calculate the energy content (enthalpy, h) of the expirate and inspirate as described above. Exhaled temperature varies slightly within breaths due to pulsatile flow and the effects of anatomical and equipment dead space (Figure 5.2). To calculate the exhaled enthalpy, temperature is first averaged for the duration of expiration and this value, together with

the exhaled humidity, is used to derive exhaled enthalpy using a psychrometric chart [90]. Inspirate enthalpy is derived from inspirate temperature and humidity using the same chart. Total respiratory heat and moisture loss (RHML) was then calculated as the product of minute volume × air density × difference between inspirate and expirate enthalpy (equation 3.2 above). Total RHML comprises heat used to raise dry air temperature (convective) and heat used to evaporate moisture (evaporative). The convective component (Qc) was calculated from the product; minute volume × air density specific heat capacity of air × difference between inspired and expired temperature (equation 3.3 above).

The evaporative component (Q_e) was then calculated as;

$$Q_e = RHML - Qc$$

Because RHML depends on minute ventilation, and because (despite targeting) not all subjects will achieve identical ventilation, respiratory heat loss can also be expressed as the energy loss (Joules) per litre ATPS ventilation, Q' thus;

$$Q' = \frac{Q}{V} \times 10^3 .....Joules / litre$$

Worked example

Figure 3.7 shows the signals obtained from measurements taken from a subject following a ventilation pattern with target minute ventilation, Vm =15l/min and tidal volume, Vt

=1500 ml. A 6 minute sampling period is chosen to allow equilibration of signals to steady–state (Fig 3.7(a)). The final 3 respiratory cycles were chosen for analysis (Fig 3.7(b)).

Referring to Fig 3.7 (c), for each of the 3 respiratory cycles, the mean exhaled breath temperature is calculated as;

$$T_e = \frac{\int_0 T dt}{\int_0 dt}$$

This mean value is evaluated by the data analysis software as;

$T_e = 28.5\ ^oC$ at location 1 and $T_e = 35.5\ ^oC$ at location 2.

The measured relative humidity of the exhaled air at location 4 (distal end of heated tube) is;

$rh_e = 71.5\%$

From the thermodynamic properties of moist air at atmospheric pressure (psychrometric chart [90]) the absolute humidity of the exhaled for $rh_2 = 71.5\%$ and $T_4 = 35.5^oC$ is;

$W_2 = 26.4\ g/kg\ dry\ air$

Since no mass is lost between location 3 and 4 this is also the absolute humidity of the exhaled air at location 3 (mouthpiece). From the psychrometric chart for moist air at atmospheric pressure the enthalpy of the exhaled air at location 3 (h_e) is found to be:

h_e=96.0 kJ/kg

The mean temperature and relative humidity of the inhaled air in this example were;

T_2=6.5°C and rh_i=95%

This yields the absolute humidity and enthalpy of the inspired air to be;

w_1=5.6 g/kg dry air and h_i=20.6 kJ/kg

The enthalpy difference between the inhaled and exhaled air (Δh) is therefore given by;

$$\Delta h = 96 - 20.6 = 75.4 \text{ kJ/kg}$$

Now the mass flowrate of air is given by;

$$m = \rho V$$

where V= the mean volumetric flowrate during each respiratory cycle and ρ is the density of air at T_4.

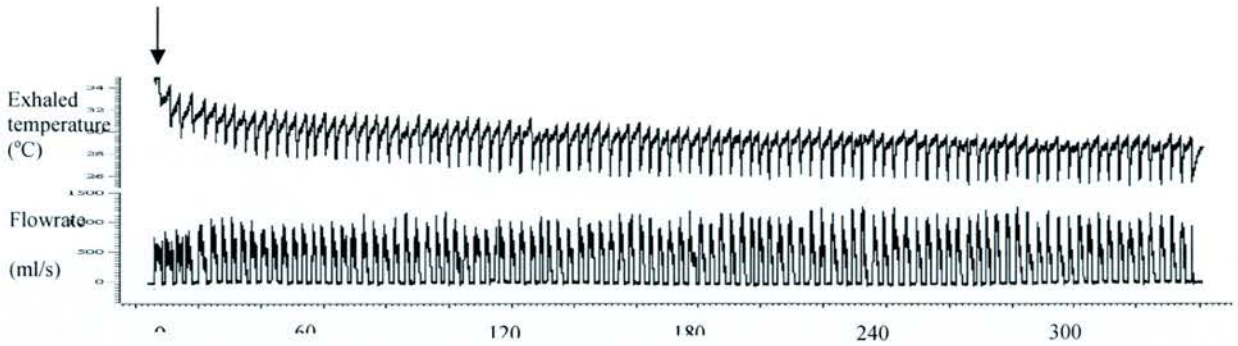

A

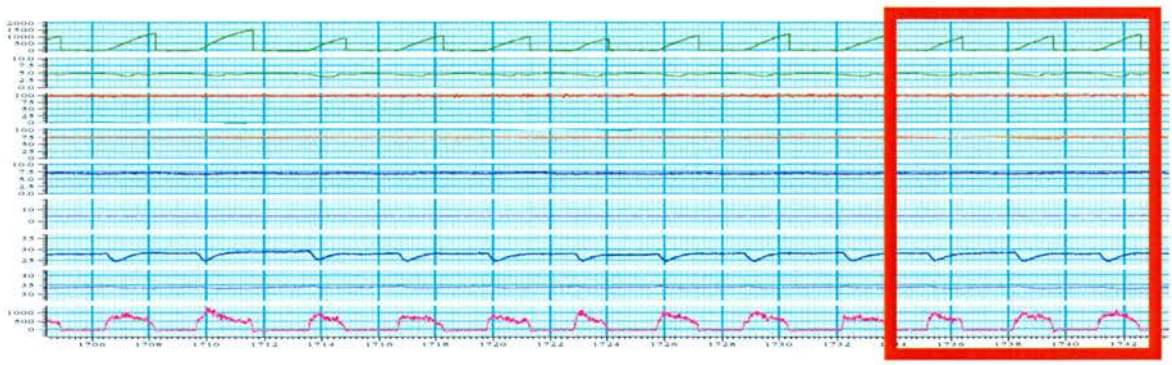

B

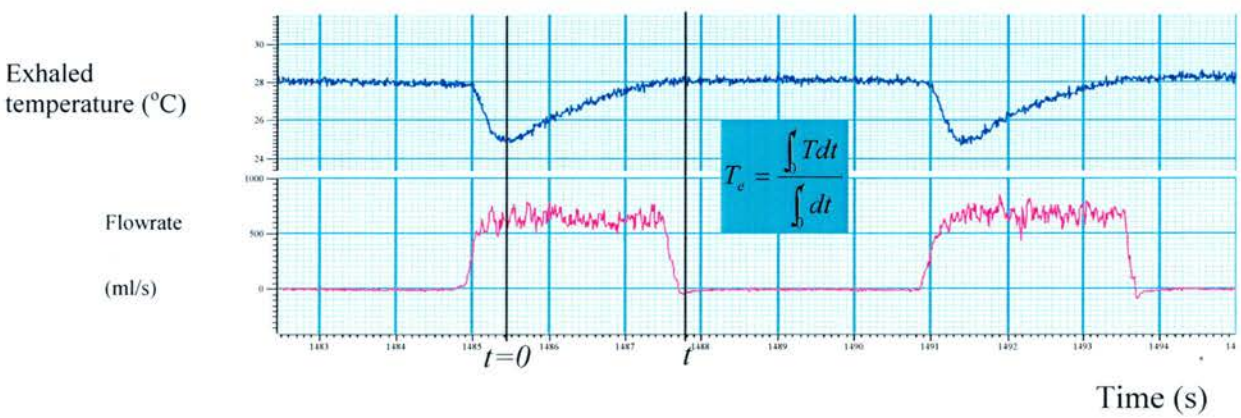

C

Figure 3.7. The evaluation of mean exhaled temperature from pulsatile temperature signals at steady state. (A) Showing time to steady-state, (B) showing breaths analysed and (C) showing calculation of mean exhaled breath temperature.

In this example $V = 349.7$ ml/s and $\rho = 1.097\ kg/m^3$ giving;

$$m = 383.7\ mg/s$$

Finally the total respiratory heat loss (Q) is calculated as;

$$Q = m\,\Delta h = 29.3\ watts$$

The convective heat loss is calculated from equation (3.3) as

$$Q_c = m\,c_p\,(T_3 - T_2) = 8.5\ watts$$

Therefore the evaporative heat loss is;

$$q_e = q - q_c = 20.4\ watts$$

The total rate of moisture loss is given by;

$$W_t = m\,(w_2 - w_1) = 478\ \mu l/min$$

CHAPTER 4

THE MEASUREMENT OF RESPIRATORY HEAT AND MOISTURE LOSS (RHML) IN NORMAL SUBJECTS

4.1 Introduction

Measuring respiratory heat and moisture loss has been studied in the past mainly in the context of human body energetics where it has been found to account for around 10% of total body heat loss. As described in Chapter 2 RHML has been shown to increase with exercise and with lowered inspired temperature and humidity. The process of heat exchange in the airways is complex and dependent on factors such as; temperature and moisture gradients between lumen and airway mucosa, heat and moisture transfer coefficients, flow regime and velocity, gas-wall residence time and airway geometry. These factors are affected by breathing pattern, such as, minute ventilation and tidal volume, body surface area (BSA) and airway resistance. The extent to which these factors influence overall RHML has not yet been quantified. As previously described, invasive measurements have helped to demonstrate the sites of intra-airway heat and moisture flux under varying ventilation and inspired air conditions and mathematical models have offered similar insights into this complex process. However, precise non-invasive measurements of steady state respiratory heat and moisture loss in humans

breathing at controlled ventilatory patterns have not been reported. Therefore the influence of factors such as tidal volume, minute ventilation, and body size has yet to be quantified.

The aim of this study was to employ the technique described in the previous section to measure precisely respiratory heat and moisture loss in normal subjects and to quantify the effects of ventilatory pattern (minute volume and tidal volume), body surface area (BSA) and forced expiratory volume in 1-second (FEV1).

4.2 Methods

Subjects

The Lothian Regional Ethics Committee granted study approval for tests on human subjects. Subjects free from known cardio-respiratory disease were enrolled in the study. To ensure subjects were close to a basal metabolic state they were requested not to have a meal within 2 hours of testing and were rested for at least half an hour in the laboratory prior to measurements.

Measurement protocols

Measurements were made on two groups of subjects according to protocols 1, 2 and 3 shown in Table 4.1. The effect of nasal conditioning was removed by requiring subjects to wear a nose-clip. Height, weight, blood pressure, pulse and aural temperature were recorded. Spirometry was then performed prior to and following respiratory heat and moisture loss measurements.

The effect of minute ventilation on RHML

As described in Chapter 3 subjects were requested to follow a visual target on a computer screen, which set expiratory flowrate and an auditory cue, which set ventilatory rate. To assess the effect of minute ventilation (protocol 1) on RHML, 10 subjects were instructed to follow flowrate targets of 250, 500, and 750ml/s at ventilatory rates of 5, 10, 15 breaths per minute such that with ideal targeting, subjects would achieve a minute ventilation of 7.5, 15 and 22.5l/minute respectively at a tidal volume of 1500ml. Data recordings were made for at least 6 minutes which allowed breath and circuit temperatures to achieve a steady state

The effect of tidal volume on RHML

To assess the effect of tidal volume on RHML (protocol 2) subjects were instructed to maintain a square-wave expiratory signal adhering to a flowrate target of 500ml/s at a ventilatory rate of 10, 15 and 30 breaths per minute such that with ideal targeting, subjects would achieve a tidal volume of 1500, 1000, and 500ml respectively at a minute ventilation of 15 litres/min.

The effect of inspired air temperature

10 subjects were required to breathe at targets of Vt =1500ml and Ve = 15l/min with inspired air conditions of 7.2°C, absolute humidity 5.8 g/kg. This allowed comparison with the subjects in protocol 1 who had matching breathing pattern but inspired air conditions of 21°C and absolute humidity of 6.7 g/kg.

.

Protocol	No. of subjects	Sex (m:f)	Height (cm)	Age (yrs)	FEV1 (litres)	Inspired air temperature (°C)	Ventilatory pattern Minute Ventilation(l)	Tidal volume (ml)
1	10	4:6	167	34	3.9	21	7.5 15 22.5	1500
2	20	13:12	171	37	3.8	7.2	15	500 1000 1500
3	10	4:6	173	37	3.7	7.3	15	1500

Table 4.1. Test subject details and protocols 1, 2 and 3. In protocol 1 subjects breathed at low, intermediate and high minute ventilation for a fixed tidal volume target. Subjects in protocol 1 breathed at low, intermediate and high tidal volume for a fixed minute volume target. In protocol 3 subjects breathed at matching ventilation to the intermediate pattern in protocol 1 but at the lower inhaled temperature.

Analysis.

Statistical analysis was performed using *Sigmastat* and *SigmaPlot 2001 for Windows version 8.0 (SPSS Science Inc, USA).* Linear regression and correlation coefficients were calculated with the same program. One-way analysis of variance (ANOVA) was used to analyse the relationship between ventilation pattern and RHML. This was performed on *Minitab* software.

Body surface area was calculated using the formula of *Mosteller*;

$$BSA = \sqrt{\frac{H.Wt}{3600}}$$

where, BSA=body surface area (m^2), H= height (cm), wt=weight (cm).

4.3 Results

Overall Respiratory heat and moisture loss in normal subjects.

For normal subjects at a ventilatory target of 15L/min breathing air at 21°C, RHML measurements were found to be normally distributed with an overall mean of 21.4 Watts (SD=7.1). Evaporative heat loss was 15.5 (±4.7) Watts and convective 6 (±5.8) Watts. Evaporative loss accounted for 72% of the total RHML.

The effect of minute ventilation on RHML

Higher minute ventilations were associated with increased RHML (Fig4.1). For target minute ventilations of 7.5, 15 and 22.5L subjects achieved 8.9 (±2.4), 16.4 (±5.6), 23.7 (±2.7) L and RHML was measured as 11.6 ± 2.9, 21.4 ±7.1, and 29.5 ±3.0 Watts respectively ($p<0.001$, one-way ANOVA). For the same breathing patterns respiratory water loss was 230 (±57), 417 (±126) and 581 (±58) microlitres per minute ($p<0.001$).

The effect of tidal volume on RHML

The lowest tidal volume target pattern of breathing was associated with significantly lower RHML (Fig 4.2) than the highest tidal pattern (18.8 ±2.4 vs 21.1 ±1.1 W, $p<0.001$). However the difference between the intermediate pattern and the two extreme patterns failed to achieve statistical significance (20.0±1.4 vs 18.8±2.4 and 21.1±1.1 W, $p>0.05$, one-way ANOVA). As described in section since RHML is strongly dependent on

minute ventilation, RHML can be usefully expressed in Joules per litre respired which would translate to low, intermediate and high values of 75.3 ±9.5, 80.2 ±5.7 and 84.2 ±4.4 J/L respectively.

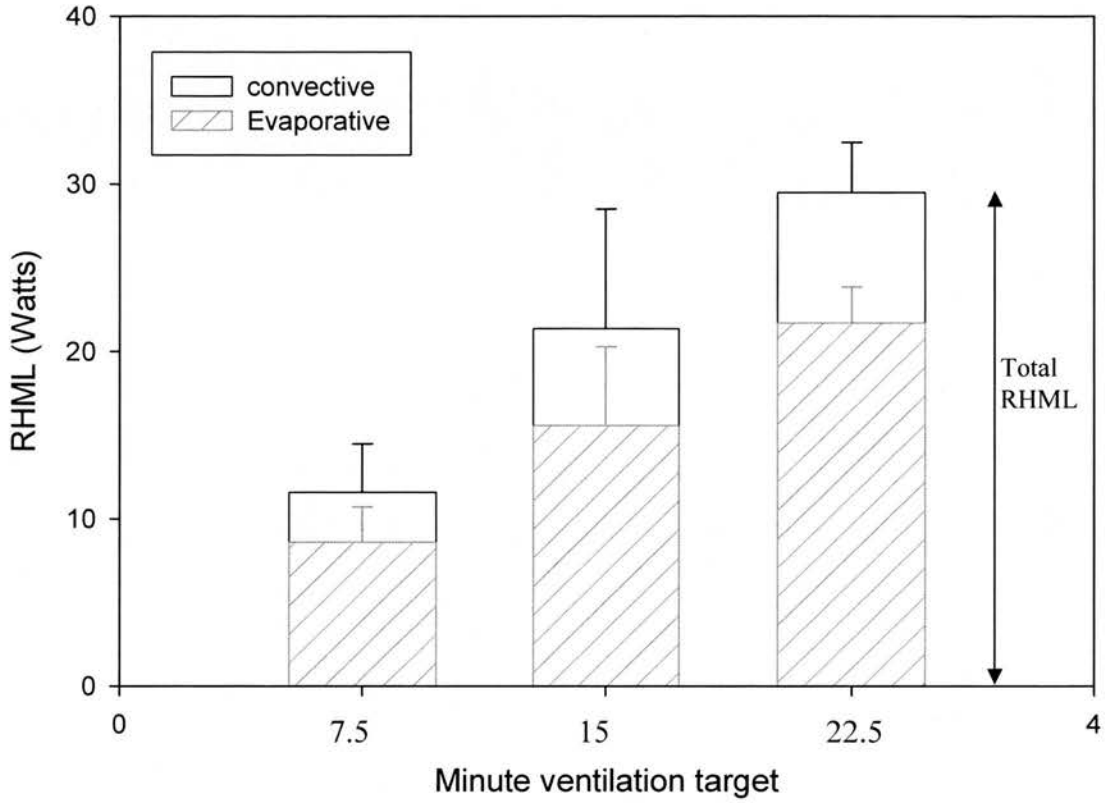

Figure 4.1 Protocol 1 - Measured RHML at low, intermediate and high minute ventilations (Vm). One way ANOVA shows significant increase in RHML with Vm, $p<0.001$. Measurements also show the evaporative component of RHML to be much greater than the convective component. Limits indicate standard deviation.

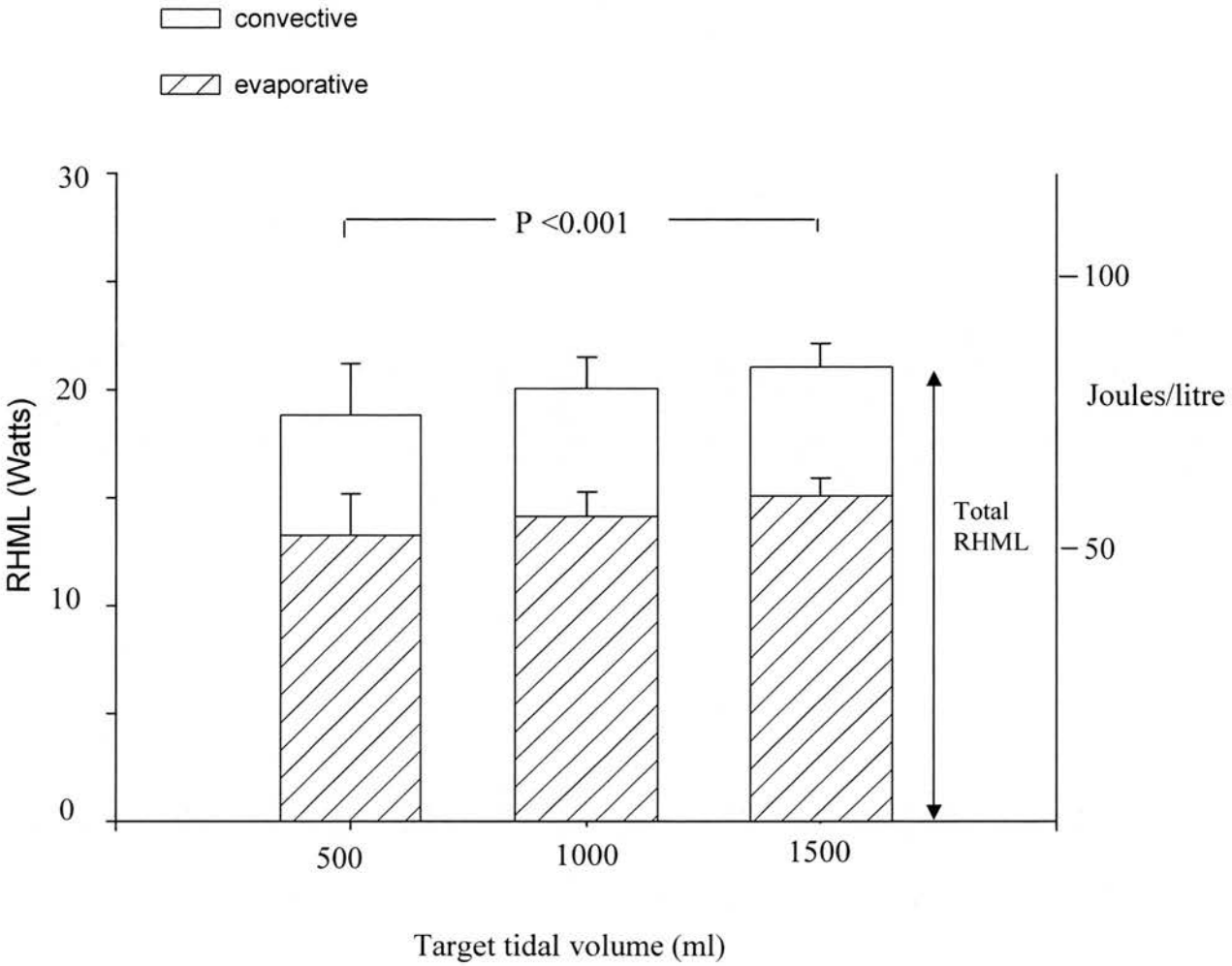

Figure 4.2. Protocol 2 - Measured RHML in Watts at low, intermediate and high tidal volume patterns for a fixed minute volume target of 15l/min. The lowest tidal volume target pattern of breathing was associated with significantly lower RHML (Fig 4.2) than the highest tidal pattern (18.8 ±2.4 vs 21.1 ±1.1 W, $p<0.001$). However the difference between the intermediate pattern and the two extreme patterns failed to achieve statistical significance (20.0±1.4 vs 18.8±2.4 and 21.1±1.1 W, $p>0.05$, one-way ANOVA).

The effect of inspired air temperature.

For subjects breathing at equivalent tidal and minute volume patterns the effect of breathing cooler air was found to yield increased RHML (Fig 4.3). Comparing protocol 1 and 3 – matching ventilation patterns were achieved (Vt =1.65 and Vt = 1.7L respectively)). The cooler inspired conditions produced a total RHML of 24.3±3.8 watts versus 21.4 watts ($p<0.01$) for the warmer more moist air. Evaporative heat loss was 17.4 vs 15.5 watts and convective loss 6.9 vs 5.7 watts.

The effect of Body surface area (BSA) on RHML

For the group of 20 controls in protocol 2 the BSA was normally distributed about a mean of 1.9 m^2 (SD=0.21). No significant correlation was found between body surface area and RHML (Fig.4.4, $R^2= 0.0036$)

The relation between FEV1 and RHML

For the group of 20 controls in protocol 2 FEV1 was normally distributed about a mean of 3.6 litres (SD=0.85). There was no significant dependence found between RHML and FEV1 (Fig 4.4, $R^2=0.014$).

Exhaled air condition

For subjects breathing the warmer more moist air the exhaled air was found to be 100% saturated with a mean temperature of 31.0°C and the absolute humidity of the exhaled breath was 29.2 g/kg dry air. Under the cooler conditions the exhalate was just into the supersaturated region of the psychrometric chart with a mean exhaled temperature of 27.7°C and absolute humidity of 25.8 g/kg dry air. Water recovery under the warmer

conditions is calculated as 34% of the total water added during inspiration. This compares to 43% under the cooler inhaled conditions.

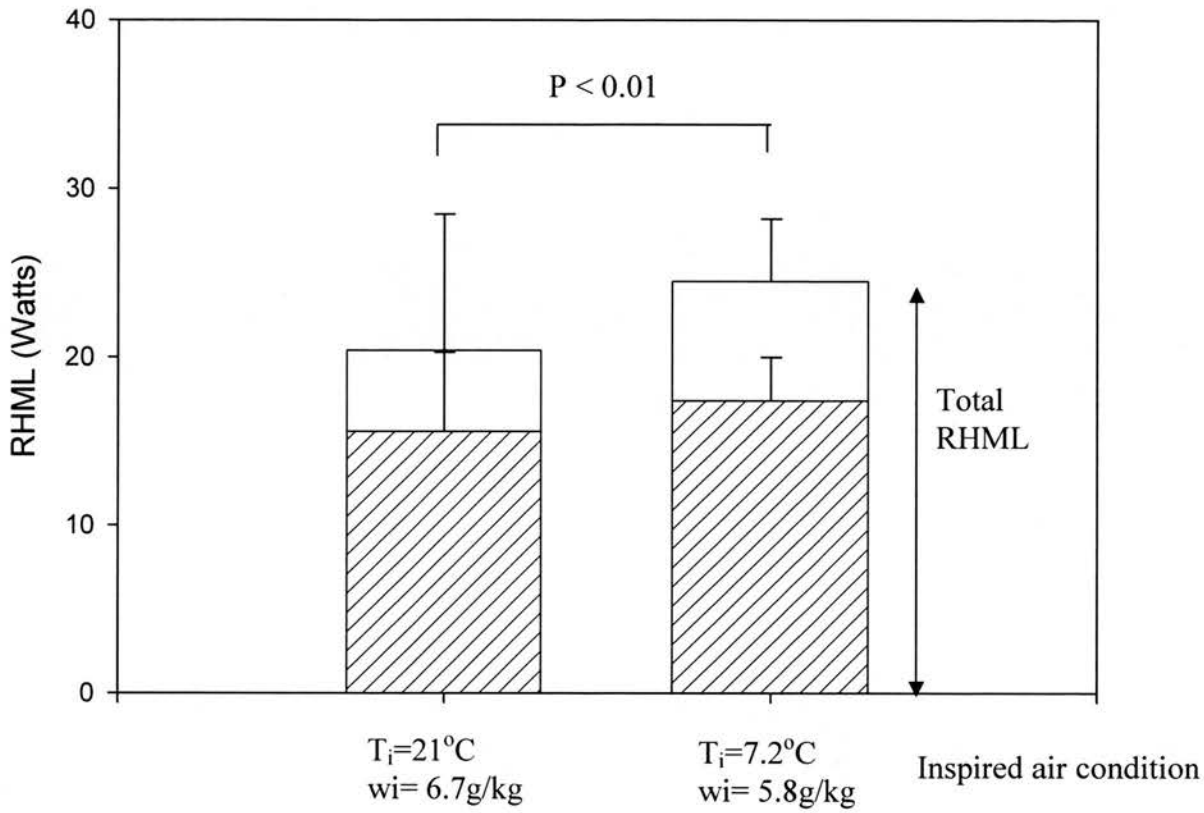

Figure 4.3. Protocol 3 – The effect of inhaled air temperature on respiratory heat and moisture loss. Subjects breathing colder air at equivalent ventilatory patterns lost more heat than those breathing the warmer air.

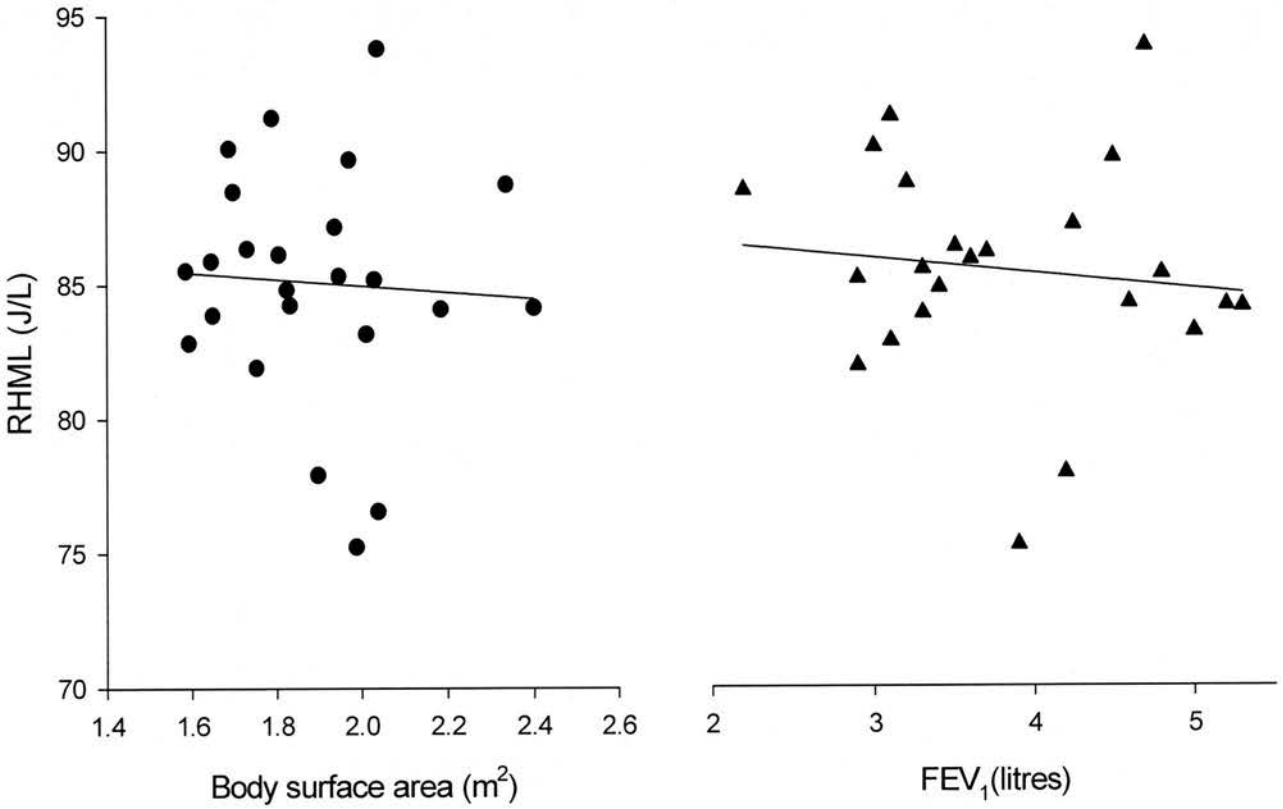

Figure 4.3. Relationship of FEV1 and BSA to RHML. No significant correlation was found implying the residence time effects of physical size and airway calibre on RHML are negligible compared to ventilation pattern and inspired air temperature and humidity.

4.4 Discussion

This novel technique proved successful in being easily applied to multiple measurements of respiratory heat and moisture loss (RHML) in human subjects by controlling and measuring ventilatory pattern and inspired and exhaled air condition. The real time measurement of air temperatures and moisture content allowed accurate measurements at steady state.

Mean exhaled air condition with subjects breathing room air (21°C) was 100% saturation at 31 °C. This is good agreement with the predictive models [29] and comparable with other published measurements [31,32]. Under the cooler dryer inspirate conditions the exhalate was found to be supersaturated. This was also found in the studies of *Livingstone et al.* [34] although not reported in other studies [35, 36]. The type of mouthpiece or facemask and the position of the thermocouple in relation to the mouth are important in this regard. The temperature was measured just distal to the 3-way valve rather than within the mouth. If the inhaled air is cold enough the effect of this mixing will be to push the exhalate just into the supersaturated region of the psychrometric chart for a short time until it is warmed within the heated-tube section. This is commonly seen as people breathe on a cold winter's day where the exhaled breath is visible as a supersaturated vapor.

Although more net heat and moisture is lost under the cooler conditions, proportionally more heat is recovered on expiration, which illustrates the ability of the human respiratory tract to regulate losses. This adaptation is more effective in other mammals where conservation of respiratory water loss is more important. For example, the kangaroo rat, a desert animal that does not drink but relies on the water in plant material has been found

to conserve its respiratory heat and water losses. It has been shown that it is able to recover around 54% of the water that was added to humidify air on inspiration [42]. Similarly the camel is estimated to recover around 70% of the potential respiratory loss [42]. Interestingly it is thought to achieve this by virtue of its large nasal turbinate surface area estimated at around $1000cm^2$ (compared to $12cm^2$ for humans), which allows more efficient water recovery on exhalation.

Measurements made in this study give the overall mean RHML at resting ventilations in normal human subjects to be 11.3 watts, 72% of which is lost through evaporation of moisture from the respiratory tract and 28% from convective cooling. Using the data on overall human body heat balance, heat loss from the respiratory tract represents around 10% of total human body heat loss. 10% of metabolic heat is therefore dissipated through respiration under typical indoor conditions. The mean evaporative water loss was found to be 230 µl/min which would translate to a daily respiratory water loss of around 330ml. These values are in good agreement with other studies (Table 4.2), which employed the more elaborate 'freeze–out' techniques; in particular between the present study and studies 1 and 2. Results from the other studies generally give higher values probably due to the cooler dryer inspired conditions used. They also show that at the lower inspired humidities the evaporative component forms a greater proportion of RHML over the dry convective component.

The technique devised in this study was found to be sufficiently sensitive to detect differences in RHML with ventilatory pattern. The effect of minute ventilation (Vm) on RHML was quantified whereby respiratory heat and moisture loss was found to rise with Vm. Low tidal volume breathing was associated with lower RHML per litre than high

tidal volume breathing for the same minute volume target. This implies that shallow breathing liberates less heat and moisture from the mucosa than slow deep breathing for the same minute ventilation. At low tidal volumes the breathing valve dead-space and that volume of inspired air in contact with areas of the oral cavity not participating in heat and moisture exchange form a larger proportion of the tidal breath resulting in less heat exchange per litre of respired gas. These results suggest that the optimum ventilatory pattern to allow direct comparisons of RHML between subjects would be a tidal volume of approximately 1500ml at a minute ventilation of 15 litres per minute. No correlation was found between BSA and RHML implying the residence time effects of physical size and airway caliber are negligible compared to the dominant effects of ventilation pattern and inspired air temperature and humidity on RHML.

In this study, for the purpose of comparison, the inspiratory to expiratory (IE) ratio was set at 1:1 with subjects also being required to reproduce a square-wave expiratory waveform. It is recognised that ventilatory pattern is not solely defined by minute

.

STUDY	Design No.of subjects	Inspired Conditions Ti (°C)/ rh(%)/ventilation	Waterloss (µl/min)	Respiratory Heat Loss (Watts) q_e	 q_c	 q_T
1.Burch 1945 [7]	56	20-21/ 50-60 / 6.9	166	6.7	1.6	8.3
2.McCutchan 1950 [36]	5	21-24 / 20-40 / 7.5	227	8.5	2.6	11.1
3.Caldwell 1969 [51]	5	25-27 / 0 / 9.8	282	11.9	0.9	12.8
4.Ferrus and Varene 1986 [48]	5	24.8 / 0 / 6.7	179	7.0	0.5	7.5
5.Cain 1990 [51]	5	0 / 0 / 8.7	440	26.7	1.2	28.0
6.McCafferty 2005	20	21 / 40 / 8.9	230	8.6	2.9	11.5

Table 4.2. Comparison of study results with those of previous studies. RHML increases with lower inspired temperature and humidity. At lower inspired humidities the evaporative component forms a greater proportion of RHML over the dry convective component. Good agreement is found between the present study and studies 1 and 2.

ventilation and tidal volume values but that factors such as IE ratio and the shape of the inspiratory/expiratory flow rate signals may also be important in the context of airway heat and water transport. Mathematical models of this complex process [14] would suggest that a low IE ratio pattern would result in a lower expiratory water vapour concentration compared to a high IE pattern for the same tidal volume and minute ventilation. Further studies are required to assess the significance of this effect on measured RHML

This novel technique offers advantages over previous methods of quantifying RHML and was able to quantify the effect of differences in ventilatory pattern and inspired air condition on this parameter. It is likely therefore that this technique would possess sufficient sensitivity to be usefully applied to measurements in patients with airways disease.

CHAPTER 5

RESPIRATORY HEAT AND MOISTURE LOSS IN ASTHMA AND COPD

5.1 INTRODUCTION

As described in Chapter 1, heat is delivered to the airways via the bronchial and pulmonary circulations. The bronchial circulation with its sub-mucosal and peri-bronchial plexuses is in more intimate contact with the airway compared to the pulmonary circulation down to airways of 1mm diameter [26]. The bronchial circulation is also the dominant source of the airway lining fluid, evaporation of which is a major contributor to respiratory heat exchange. The interaction between airway disease and heat and moisture loss has been most extensively studied in exercise-induced asthma [63-70] where the effect of high thermal and hydration burdens has been thought to induce an abnormal airway response associated with vasoconstriction followed by reactive hyperaemia in the bronchial microcirculation. The effect of the spontaneously inflamed airway on respiratory heat and moisture exchange is less clear. It is now known that subjects with asthma have increased vascularity in their airways and increased bronchial blood flow [73], which may cause some degree of dysregulation in mucosal heat and water transport. The effect of chronic obstructive pulmonary disease (COPD) on respiratory heat exchange is less clear as this disease is heterogeneous in its pathophysiology involving on the one hand the emphysematous process of destruction of the pulmonary capillary bed, airway

wall thickening, mucous hypersecretion, and loss of bronchial vascularity and on the other hand the acute effects of inflammatory mediators causing bronchial vasodilatation, mucosal capillary engorgement and leakage. Few studies have looked at measuring aspects of heat and moisture exchange in airways disease. Recent studies looking at the nasal mucosa have found an impaired ability of patients with allergic rhinitis to humidify inspired air [83]. In asthmatic patients, studies have reported a faster rise in exhaled breath temperature [84] compared to controls whereas in COPD the converse was found [85]. In another study exhaled plateau temperature was reported to correlate with exhaled nitric oxide levels in asthmatic children [86], suggesting respiratory heat loss may reflect airway inflammation in asthma. However, these studies did not control inspirate conditions or ventilation nor did they attempt to quantify evaporative heat loss. As demonstrated in the present study, breath temperatures alone do not take into account heat loss due to water transport processes, which form the major part of the total airway heat exchange.

The aim of this study was to investigate the respiratory heat transfer characteristics of patients with asthma and COPD compared to healthy controls with particular emphasis on quantifying both the respiratory heat and moisture loss (RHML) under carefully controlled conditions of inspirate and ventilation.

5.2 METHODS

Subjects

Thirty-three asthmatic patients, 17 patients with COPD and 25 control subjects were studied (Table1). The asthmatic and COPD groups were further subdivided into those with a current exacerbation and those with stable disease and were drawn from hospital

inpatient and outpatient populations respectively. Review of medical records, patient questionnaire and pulmonary function tests confirmed the diagnosis of asthma according to the American Thoracic Society criteria [87] and in the COPD group according to the Global Initiative for Chronic Obstructive Lung Disease criteria [88]. For both asthma and COPD, an exacerbation was defined by hospitalisation as a result of increased symptom severity (dyspnoea, cough, increased sputum production or wheeze) and the requirement for oral corticosteroid therapy. Subjects with heart disease, lung cancer, pulmonary embolus, recent upper respiratory tract infection, coryzal illness, pregnancy or focal chest X-Ray changes were excluded from the study. All subjects who were pyrexial as determined by an aural temperature greater than 37°C were not enrolled in the study.

Group	Number	Age	Sex (M:F)	FEV1 (% pred)	Therapy β_2-agonist	inhaled steroid	oral steroid
Controls	25	37(10)	12:3	107(14)	0	0	0
Asthmatics							
exacerbation	13	44(10)	5:8	66(20)	13	13	13
Stable	20	52(10)	9:11	70(22)	20	20	0
COPD							
exacerbation	7	68(5)	4:3	35(9)	7	0	7
Stable	10	68(7)	5:5	47(17)	10	7	0

Table 5.1: Patient and control group characteristics. All asthmatics met the ATS [88] criteria for the diagnosis of asthma and the COPD group complied with the GOLD[89] criteria. An exacerbation was defined by hospitalisation as a result of increased symptom severity (dyspnoea, cough, increased sputum production or wheeze) and the requirement for oral corticosteroid therapy. Data are given as group mean with standard deviation (SD) in parenthesis.

Test Protocol

Study approval for tests on human subjects was granted by the Lothian Regional Ethics committee. Informed consent was obtained from all patients.

To ensure patients were close to basal metabolic state they were requested not to have a meal within 2 hours of testing and rested for at least half an hour in the laboratory prior to measurements. Height, weight, blood pressure, pulse and aural temperature were recorded. Spirometry was performed before and after respiratory heat and moisture loss measurements. To assess with-subject variation, eighteen normal subjects underwent three repeat measurements of RHML within a 2-week period.

RHML Measurements

To optimise the thermal challenge to the airway (see page 38), subjects breathed conditioned air (7°C) through a 2-way valve as shown in Figure 5.1. The effect of nasal conditioning was removed by requiring subjects to wear a nose-clip. Subjects were requested to follow a visual target on a computer screen, which set expiratory flowrate and an auditory cue, which set respiratory rate. They were instructed to maintain a square-wave expiratory signal adhering to a flowrate target of 500ml/s at a respiratory rate of 10 breaths per minute such that with ideal targeting, subjects would achieve a tidal volume of 1500ml at a minute ventilation of 15 litres/min. Data recordings were made for at least 6 minutes which was the time found to be required to allow breath and circuit temperatures to achieve a steady state (Figure 5.2).

Statistical Analysis.

Statistical analysis was performed using SigmaPlot and SigmaStat software *(SPSS Science Inc, USA).* Un-paired t-tests were used to compare the data and a value of $p<0.05$ was considered significant.

5.3 RESULTS

All subjects in the control and disease groups were apyrexial and no difference was found between groups in the mean core temperature as assessed by mean tympanic temperature (table 5.2). Spirometry performed before and following measurement of RHML showed no significant change in FEV_1 as a result of isocapnic hyperventilation of air at 7°C.

Reproducibility in normal subjects

The repeatability of RHML measurements was analysed using a one-way analysis of variance for repeated measures [93]. For three repeat measurements on 18 normal subjects the within subject standard deviation (measurement error) was 2.1 J/L. Therefore in an individual the difference between a subject's measurement and the true value could be expected to be less than 4.1 J/L for 95% of measurements.

Comparison of normal subjects with asthma and COPD patients (Figure 5.1)

Asthmatics whether the exacerbation or stable group showed significantly increased RHML compared to controls (Figure 5.3); exacerbation group-93.2 J/L (SD=8.0),

p=0.003 (versus controls) stable group - 89.3 (SD=7.4), p=0.025 (versus controls) and controls 85 (SD=4.3) Joules/L. No significant difference was found in RHML between the asthmatics with an exacerbation and those with stable disease. Breath targeting was successful in achieving matching between asthmatics and controls with all groups breathing at 10 breaths per minute (exacerbation group-tidal volume, V_t =1.7L (SD=0.3), stable group – 1.8L (SD=0.4) and controls 1.7L (SD=0.3)).

No significant difference was found in RHML between COPD patients (stable group-83 (SD=4.8), p=0.23 and exacerbation group-81 (SD=5.8), p=0.06 Joules/L) over controls or between exacerbation and stable groups. COPD patients found targeting harder. Mean V_t was lower in COPD groups compared to controls (stable group-1.4L (SD=0.3) and exacerbation group-1.4L (SD=0.2)).

Evaporative heat loss (Figure 5.2) accounted for the major heat transfer modality (up to 3-times the dry convective component) and accounted for the difference seen between controls and asthmatics ($p<0.05$), table 5.3) whereas no significant difference was found in the convective component. This translates to a mean mucosal water loss of 395 µl/minute (controls), 455 µl/minute (asthmatics) and 320 µl/minute (COPD) for a target tidal volume of 1500ml and a minute ventilation of 15 litres/min.

No correlation was found between FEV_1 and RHML for control (R^2=0.0147), asthmatic (R^2=0.0045), or COPD (R^2=0.015) groups.

		Controls	Asthma		COPD	
			Exacerbation	stable	Exacerbation	stable
Aural Temperature (°C)		36.3	36.3	36.3	36.2	36.2
Pre-test FEV1(L)		3.81	1.91	2.03	0.88	1.04
Post-test FEV1(L)		3.8	1.9	2.01	0.91	1.02
Tidal volume (L)		1.7 ±0.3	1.7 ±0.3	1.8 ±0.4	1.4 ±0.2	1.4 ±0.3
Resp rate (bpm)		10	10	10	10	10
Inspired air conditions	Temp (°C)	7.5±1.3	7.3 ±1.0	7.2± 0.9	7.9 ±1.1	7.7 ±1.3
	moisture(mg/L)	6.7 ±0.4	6.0 ±0.7	6.2 ±0.8	6.5± 0.5	6.5± 0.8
Exhaled air condition	Temp (°C)	27.9±1.0	28.7 ±1.0	28.7±1.2	27.9 ±1.1	27.8±1.3
	moisture(mg/L)	30.4±1.2	32.2±1.9	31.3±2.0	29.6±1.3	29.6±1.8
RHML (J/L)		85.0±4.3	93.2±8.0	89.3±7.4	81.0±5.8	83.0±4.8

Table 5.2 Patient and control group data (±SD) showing a groups to be apyrexial and to have comparable mean aural temperatures. The level of isocapnic hyperventilation of cool air used was found not to produce significant changes in FEV1 in controls, asthmatics and patients with COPD.

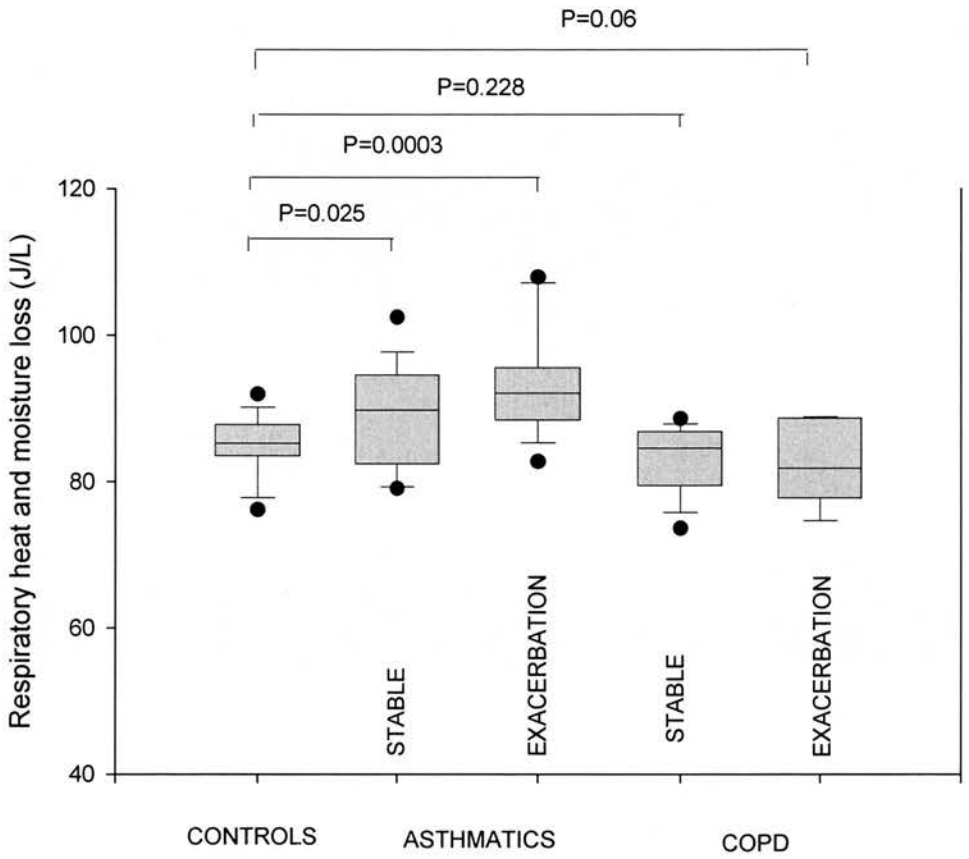

Figure 5.1: Total Respiratory heat and moisture loss (RHML) in Joules per litre ATPS ventilation in patients with Asthma and COPD compared to controls. Values plotted are group means with ± 95% confidence intervals denoted by error bars. P-values represent significance level based on unpaired t-tests between group data. 1 Joule = 0.239 calories.

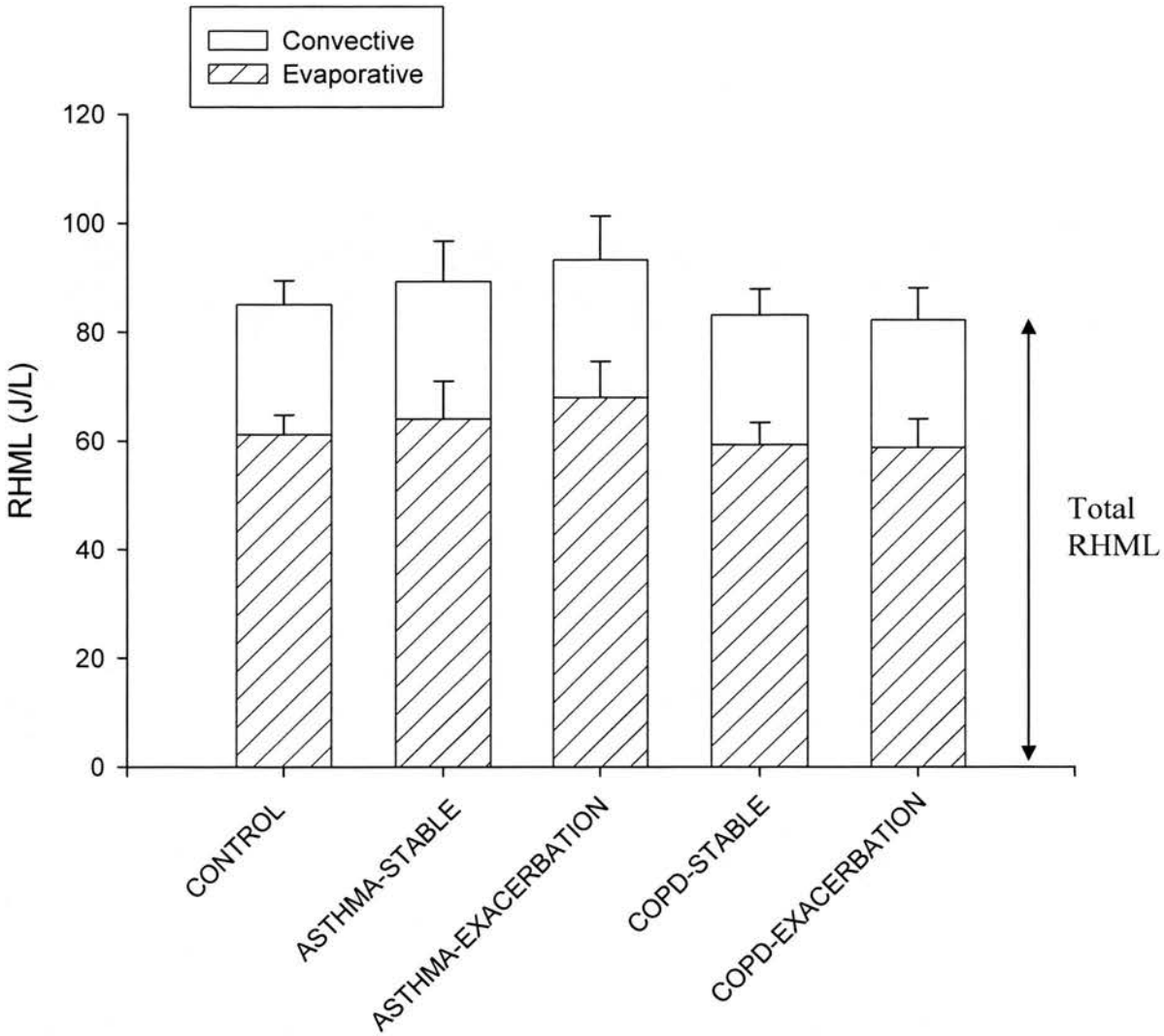

Figure 5.2. Total respiratory heat and moisture loss (RHML) together with convective and evaporative components in controls, patients with asthma and COPD. Heat loss by evaporation from the airway mucosa accounts for the major component. 1 Joule = 0.239 calories.

	Convective (J/L)	Evaporative (J/L)	Total RHML (J/L)
Controls	23.9 ±1.6	61.1 ±3.5	85.0 ±4.3
Asthma-stable	25.3 ±1.3	64.0 ±6.9	89.3 ±7.4
Asthma-exacerbation	25.2 ±1.9	68.0± 6.5	93.2 ±8.0
COPD-stable	23.8 ±1.7	59.3 ±4.1	81.0 ±4.8
COPD-exacerbation	23.5 ±0.98	58.7 ±5.2	83.0 ±5.8

Table 5.3: Comparison of mean (± SD) convective, evaporative and total heat loss (RHML) between control, asthmatic and COPD groups. Significantly more heat is lost in asthmatics compared to controls which derives from the evaporative rather than the convective component ($P<0.01$). No difference was found between controls and those with COPD.

5.4 DISCUSSION

Asthmatics were found to have higher levels of respiratory heat and moisture loss compared to controls. Possible underlying mechanisms include airway inflammation, mucosal vascularity and bronchial blood flow increasing heat flux, increased pulmonary blood flow (cardiac output) or an effect of medication on airway heat transfer in these patient groups.

Although animal studies [20, 57] suggest that in health the pulmonary circulation is the dominant heat source under moderate cooling loads these conclusions are derived from studies on the normal airway. More recently, studies in patients on cardio-pulmonary bypass, again with normal lungs [22] suggest a lesser contribution of the healthy bronchial circulation as a heat source but a greater role in water transport to the bronchial mucosa under moderate cooling loads. In the present studies, we found increased heat and moisture loss in asthmatics, the majority (approx 75%) of which is evaporative heat loss. This may indicate that the bronchial circulation in asthmatics is 'upregulated' and thereby contributes more as a heat and water source to the airway. If these results for moisture transfer are extrapolated over time, asthmatics, in the course of an exacerbation, may be losing in excess of a litre per day of water from the respiratory tract – an important factor to consider in the overall fluid balance of this patient group. This also highlights the importance of quantifying moisture loss when looking at heat exchange within the airway.

The size of the fluid compartment from which airway water is lost can be estimated from the airway dimensional data of Weibel [24]. If it is assumed that airways down to 0.5mm diameter are involved in moisture transport under moderate ventilatory loads and assuming the depth of airway lining fluid to vary from 10 microns down to 2 microns in

the more distal airways then the airway water compartment comprises around 640 µl. The present study found the mean respiratory moisture loss in controls to be 395 µl /min. Together these results highlight the dynamic nature of airway surface liquid with over 60% of the liquid being lost by evaporation and being replaced by the mucosa each minute.

Necessarily, all the asthmatics were receiving inhaled beta-2 agonists, which are known to have vasodilating properties on the bronchial circulation and could theoretically have contributed to the measured increases in RHML. However, drug effects are unlikely to be a major contributor as a similar increase in RHML was found in patients with chronic asthma, who had not received high dose beta-2 agonists in the previous 24 hours (none use home nebulisers), compared to the group with exacerbation, all of whom were receiving high nebulised doses at the time of study. Furthermore, we have attempted to detect a treatment effect by comparing RHML before and after 2.5mg nebulised salbutamol and found no change in two stable asthmatics and four normal subjects.

All asthmatics were on inhaled corticosteroids, which are known to have transient vasoconstrictive effects on the airway [94] and therefore the potential to reduce the heat and moisture loss. Although this may have partially masked the differences found between asthmatics and controls or stable and exacerbation groups this effect is likely to have been small and transient against the inflammatory and vascular mechanism already discussed. Although ideally we would have standardized the dose and timing of inhaled steroids between groups, our intention was to study patients in a real clinical setting where such strict controls are not practical.

We were unable to demonstrate a statistically significant difference in RHML between the stable and asthma exacerbation group. The stable group was drawn from patients, on average older, with moderately severe disease, many with a degree of fixed airflow obstruction associated with chronic inflammation and remodeling. Conclusions regarding differences between patients with acute exacerbations and stable disease would be best achieved in a longitudinal study on the same cohort.

One further possible confounding effect in asthmatic patients is cold-induced bronchoconstriction. The data of McFadden et al. [9] suggest that unless subjects breathe cooled inspirate and at elevated minute ventilation, the bulk of heat and moisture transfer will take place in the upper airway (above the glottis). In the present study the degree of thermal loading (i.e. V_e =15l/min. T_i=7°C) was chosen in order to engage enough of the bronchial tree in heat and moisture exchange to reflect differences in the lower airways. That said, it is well recognised that the thermal loading associated with isocapnic hyperventilation can induce changes in airway resistance and indeed bronchial blood flow in subjects with exercise induced asthma [103] and even in normal subjects [110] and that a test such as the one described here could potentially alter the very parameter it seeks to measure. However, the level of thermal loading used in this test was low (~25W) representing approximately 10% of values found by most studies to induce changes in FEV_1 in asthmatics and equivalent to those found not to induce a measurable increase in bronchial blood flow in normals [103]. FEV_1 was measured before and after each test and no change was seen. It is therefore unlikely that the ventilatory pattern and inspired air condition used here had a significant effect on inducing changes in airway resistance and airway circulation.

In the COPD group we found no significant difference in RHML between patients and controls. COPD is diverse in its pathophysiology; there is acute inflammation associated with the release of mediators such as bradykinin, prostaglandins among others, which can certainly be seen as the hyperaemic airways at bronchoscopy. However, histological and flow studies [76-79] have demonstrated reduced pulmonary and bronchial vascularity in the lungs of patients with COPD as a result of chronic inflammation and remodeling. Destruction of conducting airway surface area by emphysema will also reduce RHML. It is therefore possible that these mechanisms counteract each other resulting in the observed normal respiratory heat and moisture loss. This heterogeneity of phenotype in COPD may also have contributed to the increased variation in RHML measured in this group.

No difference was found in RHML between stable COPD and those with an exacerbation. Numbers were smaller in these groups as patients with advanced airflow obstruction were less able to target their ventilation at the required level. Also those with exacerbations had received nebulised therapy and oral steroids for at least 24 hours prior to testing. These factors may have confounded any differences between these groups. Again, longitudinal measurements in the same patients during the stable and exacerbation phases of disease may be a more sensitive way to examine the association between RHML and airway inflammation

In conclusion, this study has employed a novel technique in the measurement of respiratory heat and moisture loss (RHML) in patients with asthma and COPD and shown the asthmatic group to have increased RHML over controls. This may represent a useful

marker of inflammation in asthma. Further study should be directed at longitudinal measurements in asthmatics in order to evaluate the clinical utility of this technique.

CHAPTER 6

DISCUSSION AND CONCLUSIONS

Our understanding of the process of heat and moisture loss from the respiratory tract has advanced since the early concepts of Hippocrates and Aristotle. It has now been established that the airways have two circulatory systems, namely the bronchial and pulmonary circulations which both contribute to heat and moisture transport. However, the relative contribution of each circulation to respiratory heat exchange has still to be fully quantified and it has still to be firmly established how lung disease processes which are known to alter both pulmonary and bronchial circulations may as a consequence affect local and overall respiratory heat and moisture exchange.

It has also been shown that inspired air is warmed and humidified on its course to the distal airways and alveoli and that exhaled air cools and its water content partially condenses on the proximal airway allowing partial recovery of the heat and moisture lost during inspiration. Invasive measurements [9] have told us something about sites of heat exchange under certain inspired conditions and breathing rates and offered an insight into the possible mechanisms of exercise (or thermally) induced asthma. Mathematical models have shown reasonable correlation with these measurements in normal subjects. However models by their nature make assumptions such as the temperature and moisture gradients between airway mucosa and lumen and flow regimes deep within the lung and are limited in their ability to build in the large number of pathological changes known to affect the airway such as changes in airway caliber, wall thickness, mucous hypersecretion,

pulmonary capillary and mucosal blood flow. Notwithstanding the limitations of such models, simulation of the conditions thought to occur in airway inflammation, such as changes in mucosal wall thickness and mucosal blood flow, would suggest that there would be measurable changes in the resultant airway heat exchange. For example, the data of McFadden et al. [9] and others would suggest that at minute ventilations of 15l/min and inspirate temperatures of 7°C, airways down to the 9th generation take part actively in heat and moisture exchange, with the lower airway (trachea to distal bronchi) contributing at least 50% of the total respiratory heat and moisture loss under these conditions. Alterations in RHML brought about by pathological changes in the lower airways should therefore have significant impact on the total RHML.

There have been few studies looking at the measurement of respiratory heat and moisture loss in subjects with airways disease. The techniques used in the past (mainly in the study of normal subjects) were cumbersome and as a result limited the size of studies and made them difficult to apply to groups of patients. Invasive measurements by their nature were not suitable for patients often with fairly advanced lung disease. With this in mind the present study covered new ground by designing a compact device capable of making real time measurements of RHML non-invasively whilst controlling inspired air condition and breathing pattern. By using relatively recent developments in moisture sensor technology the time consuming and cumbersome techniques of freezing and weighing exhaled breath was avoided allowing significant improvement in measurement time and thereby allowing multiple measurements on subjects and an ease of measurement in patients with in some cases severe lung disease. The aim of this study was to measure non-invasively the respiratory heat and moisture loss in normal subjects and in patients with airways disease. In this clinical setting, we were successful in obtaining measurements in almost all of

asthmatic patients admitted with an acute exacerbation and around 80% of COPD patients. Only a small proportion of COPD patients with severe air-flow limitation were unable to meet the ventilation targets imposed demonstrating the success of this method as a practical measurement technique in a real clinical setting. The results in normals show good agreement with previous studies employing more elaborate techniques. For the first time the effect of ventilatory pattern was quantified and controlled during measurements. It was also found that physical factors such as body surface area (BSA) and forced expiratory volume in one second (FEV1) were negligible compared to the effect of ventilatory pattern and inspired air condition.

It was hypothesized that Respiratory heat and moisture loss (RHML) would be altered in patients with Asthma and Chronic obstructive pulmonary disease (COPD) compared to normal controls due to the effects of airway inflammation and re-modeling. Increased RHML was found in asthmatics over controls as discussed in detail in chapter 5. The difference, although significant, is small (of the order of 10-15%) even for patients with moderately severe exacerbations of their disease (as judged by FEV1 % predicted) and no difference was found between the stable and exacerbation groups. As discussed in chapter 5 this may be due to the influence of many factors such as medications (beta agonist or steroid). Another possible cause for such a small difference between these groups may have been the degree of recruitment of the lower airway in heat exchange. It may be that the efficiency of the upper airway in the conditioning and recovering heat has a significantly greater contribution to overall heat exchange or that variations in upper airway effects between subjects mask the lower airway effects even under the conditions of moderate cooling load employed in this study. Further studies would be best directed towards longitudinal measurements on patients during the stable and exacerbation phases

of disease to help control for these confounders and improve the sensitivity of this technique.

Recent published studies have advocated a temperature washout technique whereby the rate of temperature rise in exhaled breath during a forced expiratory maneuver is measured. In asthmatic patients, studies have reported a faster rise in exhaled breath temperature [84] and higher exhaled plateau temperatures [85] compared to controls whereas in COPD the converse was found [86] suggesting altered heat loss patterns in these airway diseases. The results of the present study and others have demonstrated that heat is consumed in two ways during inspiration; approximately 25% of the energy is used in heating the air (convective) and 75% in evaporating moisture from the mucosal surface to humidify the air stream (evaporative). On expiration the reverse of both processes occurs, namely, convective cooling and condensation of water vapour on the mucosa. This dominance of energy transfer through evaporation and condensation suggests that to characterize the thermodynamic performance of the airways by temperature measurement alone, without accompanying humidity measurements, may be misleading.

Inflammation is classically defined by 'rubor, calor, dolor and tumour'. It is the 'calor' or heat that is the final common pathway in inflammation. It would therefore seem that measurement of this physical property of the airway would offer the most sensitive gauge of inflammation. However as we have seen from this study the process of heat loss from the airways is complex involving not just the dry, convective warming of air but the transfer of heat by evaporation and condensation. This process is dependent on many factors as discussed earlier. Most importantly the relative roles of the bronchial and pulmonary circulations and their contributions as a source of heat and moisture transfer

has yet to be fully quantified particularly in patients with lung diseases. Although this study supports the idea that the differences seen between asthmatics and controls was due to 'upregulation' of the bronchial circulation due to airway inflammation, differences in pulmonary blood flow were not controlled or quantified between subjects. It could be argued that the differences seen were brought about by differences in pulmonary blood flow or cardiac output as a consequence of a hyperdynamic circulation resulting from the systemic inflammatory response. Further work is therefore required to control for these variables.

This technique would lend itself to use in an intensive care setting with ventilated patients. Here the ventilation pattern could be strictly controlled and invasive measurements of pulmonary artery pressure and cardiac output would allow assessment of the influence of these variables. Patients on cardio-pulmonary bypass effectively are on selective bronchial perfusion only. Under these conditions the relative contributions of the bronchial and pulmonary circulations could be evaluated more precisely.

As well as further longitudinal studies (discussed in chapter 5) it would be useful for future studies to look at the effect of beta-2 agonists and inhaled corticosteroids on RHML. Both short-term and longer-term effects in steroid naive patients could easily be carried out to assess the possible vasoconstrictor effects of these drugs. The different phenotypes within the asthmatic group could be further explored by making measurements in patients with exercise induced wheeze to see whether this group has a more pronounced RHML signal.

The pathophysiology of bronchiectasis in cystic fibrosis, which is thought to involve changes in the airway lining fluid and mucous hypersecretion would seem to be good model of altered airway heat and moisture transfer. The future application of the technique described in this thesis to measurements in this group of patients might yield useful insight into the effect of this disease on RHML during stable and exacerbation phases.

The development of a breath test that allows measurement of inflammatory activity in lung diseases such as asthma, COPD and bronchiectasis has obvious attractions. Such a test would allow non-invasive diagnosis and assessment of inflammatory activity. The response to therapy could also be gauged in an easy non-invasive way. The possibility exists of one day having a hand-held device that could even be used by patients at home or in the primary care setting to measure inflammatory activity in advance of it becoming clinically apparent thereby allowing earlier therapeutic intervention, and improved treatment efficacy. Currently, there has been an explosion of interest in techniques looking at the gaseous (nitric oxide, carbon monoxide) and molecular (hydrocarbons, vasoactive amines, lipid peroxidation products and pH) content of breath and its relation to airway inflammation. Such markers derive from the many inflammatory pathways thought to occur in asthma, COPD and cystic fibrosis. The more promising of these are NO and pH. However, as with the present study there is still considerable overlap between disease and control groups confining these methods as research tools for the time being and leaving the discovery of the definitive breath test to gauge airway inflammation as a goal yet to be achieved.

REFERENCES

1. Osler W. The Evolution of Modern Medicine. A series of lectures delivered at Yale University on the Silliman Foundation in April 1913. New Haven: Yale University Press, 1921, pp 196-197.
2. Cudkowicz L. Leonardo da Vinci and the bronchial circulation. Br J Dis Chest 1953; 47:23-5.
3. Chato JC. Reflections on the history of heat and mass transfer in bioengineering. ASME. Trans J Biomech Eng 1981:103:97-101.
4. Pennes HH. Analysis of tissue and arterial blood temperatures in the resting forearm. J Appl Physiol 1948; 1:93-122.
5. Magendie (1829) quoted from Heetderks DR. Observations on reaction of normal nasal mucous membrane. Am J Med Sc 1927; 174: 231.
6. Goodale JL. Experimental study of the respiratory functions of the nose. Boston Medical and surgical Journal 1896. Vol CXXXV, No19; 457-460 and No 20; 487-490.
7. Burch GE. Rate of water and heat loss from the respiratory tract of normal subjects in a sub-tropical climate. Arch Intern Med 1945: 76; 215-327.
8. Webb, P. Air temperatures in respiratory tracts of resting in cold. J Appl Physiol 1951; 4:378-82.
9. McFadden ER Jr, Pichurko BM, Bowman HF, Ingenito E, Burns S, Dowling N, Solway J. Thermal mapping of the airways in humans. J Appl Physiol 1985; 58(2): 564-570.
10. Hanna LM and Scherer PW. Regional control of local airway heat and water vapour losses. J Appl Physiol 1986; 61(2): 624-632.
11. Hanna LM and Scherer PW. A Theoretical model of localized heat and water vapor transport in the human respiratory tract. J Biomech Engin 1986; 108:19-27.

12. Scherer PW. Heat and water transport in the human respiratory system, in: Heat transfer in Biological systems: Analysis and applications, R.C. Eberheart and A Shitzer, eds, Plenum Press, NY, 1985, 287-306.

13. Saidel GM, Kruse KL and Primiano FP. Model simulation of heat and water transport dynamics in an airway. J Biomech Engineer 1983; 105:188-193.

14. Daviskas E, Gonda I and Anderson SD. Mathematical modeling of heat and water transport in human respiratory tract. J Appl Physiol 1990; 69: 362-372.

15. Ingenito EP, Solway J, McFadden ER Jr, Pichurko BM, Cravalho EG, Drazen JM. Finite difference analysis of respiratory heat transfer. J Appl Physiol 1986; 61: 2252-2259.

16. Varene P and Kays C. A graphic analysis of respiratory heat exchange. J Appl Physiol 1987; 63:1374-1380.

17. Tsu ME, Babb AL, Ralph DD, Hlastala MP. Dynamics of heat, water and soluble gas exchange in the human airways: 1. a model study. Annals of Biomedical Engineering 1988; 16:547-571.

18. Tsai CL, Saidel ER, McFadden ER and Fouke JM. Radial heat and water transport across the airway wall. J Appl Physiol 1990; 69: 222-231.

19. Solway J. Airway heat and water fluxes and the tracheobronchial circulation. Eur Respir J 1990; 3: 608s-617s.

20. Solway J, Leff ID, Dreshaj I, Munoz NM, Ingenito EP, Michaels D, Ingram RH Jr, Drazen JM. Circulatory Heat sources for canine respiratory heat exchange. J Clin Invest 1986; 78: 1015-1019.

21. Serikov VB Jerome EH, Fleming NW, Moore PG, Stawitcke FA, Staub NC.. Airway thermal volume in humans and its relation to body size. J Appl Physiol 1997; 83:668-676.

22. Serikov VB and Fleming NW. Pulmonary and bronchial circulations: contributions to heat and water exchange in isolated lungs. J Appl Physiol 2001; 91: 1977-1985.

23. Serikov VB, Rumm MS, Kambara K, Bootomo MI, Osmack AR, Staub NC.. Application of respiratory heat exchange for the measurement of lung water. J Appl Physiol 1992; 72: 944-953.

24. Weibel ER. Morphometry of the human lung. Berlin: Springer Verlag, 1963; p111-123.

25. Tam PY and Verdugo P. Control of mucous hydration as a Donnan equilibrium process. Nature 1989; 292:340-342.

26. Williams PL (ed). Pulmonary microstructure; in Grays Anatomy (37th edition); Chapter 8: p1278. Churchill Livingston 1989.

27. Williams R, Rankin N, Smith T, Galler D, Seakins P BE. Relationship between the humidity and temperature of inspired gas and the function of airway mucosa. Crit Care Med. 1996; 24; 1920-1929.

28. Christie RV and Loomis AL. The pressure of aqueous vapour in the alveolar air. J Physiol 1932; 77: 35-38.

29. Cole, P. Further observations on conditioning of respiratory air. J Laryngol Otol 1953; 67:669-81.

30. Cole. P. Recordings of respiratory air temperature. J Laryngol Otol 1954; 68:295-307.

31. Ingelstedt S. Studies on the conditioning of air in the respiratory tract. Acta Otolaryngol 1956;131 (suppl): 1-80.

32. Anderson S D. Water concentration in the expired air of humans during exercise under arid conditions. Am Rev Respir Dis 1984: 129; A260

33. Hoppe P. Temperatures of expired air under varying climatic conditions. Int J Biometeorol 1981:25; 127-132.

34. Livingstone SD, Nolan RW, Cain JB, Keefe AA. Effect of working in hot environments on respiratory air temperatures. Eur J Physiol 1994; 69:98-101.

35. Madan I, Brigh P and Miller MR. Expired air temperature during a maximal forced expiratory manoeuvre. Eur Respir J 1993; 6:1556-1562.

36. McCutchan JW, Taylor CL. Respiratory heat exchange with varying temperature and humidity of inspired air. J Appl Physiol 1951;4: 121-135.

37. Fanger PO, McNall PE and Nevins RG. Predicted and measured heat losses and thermal comfort conditions for human beings. Symposium on thermal problems in biotechnology. American Society of Mechanical Engineers (ASME) 1968. New York.

38. Welch WR, Tracy CR. Respiratory water loss: a predictive model. J Theor Biol 1977; 65:253-65.

39. Deffebach ME, Charan NB, Lakshminarayan S, Butler J. The Bronchial Circulation; small but a vital attribute of the lung. Am Rev Respir Dis 1987; 135:463-481.

40. Wagner EM, Mitzner WA. Contribution of pulmonary vs. systemic perfusion of airway smooth muscle. J. Appl. Physiol. 1995; 78: 403–409.

41. Bernard SL, Glenny RW, Polisar N, Luchtel D, Lakshminarayan S. Distribution of pulmonary and bronchial blood supply to airways measured by fluorescent microspheres. J. Appl. Physiol. 1996; 80: 430–436.

42. Schmidt-Neilsen K, Schroter RC, Shkonik A. Desaturation of exhaled air in camels. Proc R Soc Lond 1981;211:305-319.

43. Elad D. Biotransport in the human respiratory system. Technology and Health Care 1999; 7:271-284.

44. McFadden ER Jr. Heat and water exchange in human airways. Am Rev Respir Dis 1992; 146:s8-s10.

45. Seeley LE. Study of changes in the temperature and water vapour content of inspired air in the nasal cavity. Am Soc heating Ventilating Eng 1940; 46:259-290.

46. McFadden ER Jr, Pichurko B M. Intra airways thermal profiles during exercise and hyperventilation in normal man. J Clin Invest 1985; 76:1007-10.

47. Varene P, Ferrus L, Manier G, Gire J. Heat and water respiratory exchanges: comparison between mouth and nose breathing in humans. Clin Physiology 1986; 6; 405-414.

48. Ferrus L, Guenard H, Vardon G, Varene P. Respiratory water loss. Resp Physiol 1980: 39; 367-381.

49. Caldwell PR, Gomez DM, Fritts HW Jr. Respiratory heat exchange in normal subjects and in patients with pulmonary disease. J Appl Physiol 1969; 26: 82-88.

50. Cain JB, Livingstone SD, Nolan RW, Keefe AA.. Respiratory heat loss during work at various ambient temperatures. Respir Physiol 1990; 79: 145-150.

51. Piantandosi CA, Thalmann ED. Spaur WH. Metabolic response to respiratory heat loss induced core cooling. J Appl Physiol 1981; 50:829-34.

52. Mitchell JW, Nadell ER, Stolwijk JA. Respiratory weight losses during exercise. J Appl Physiol 1972; 32: 474-476.

53. Tabka Z, Ben Jebria A, Guenard H. Effect of breathing dry warm air on respiratory water loss at rest and during exercise. Repir Physiol 1987; 67: 115-125.

54. Barltrop D. The relation between body temperature and respiration. J Physiol 1954; 125:19-20.

55. Walker JE, Wells CRE and Merrill EW. Heat and water exchange in the respiratory tract. Am J Med 1961; 30: 259-267.

56. Hanson R de G. Respiratory heat loss at increased core temperature. J Appl Physiol 1974; 37:103-7.

57. Baile EM, Dahlby RW, Wiggs BR, Pare PD. Role of tracheal and bronchial circulation in respiratory heat exchange. J Appl Physiol: Respirat Environ Exercise Physiol, 1985; 58: 217-222.

58. Baile EM, Osborne S, Pare PD. Effect of autonomic blockade on tracheobronchial blood flow, J Appl Physiol, 1987; 62: 520-525.

59. Baile EM, Dahlby RW, Wiggs BR, Parsons GH, Pare PD. Effect of cold and warm dry air hyperventilation on canine airway blood flow. J Appl Physiol 1987; 62: 526.

60. Deal EC Jr, McFadden ER Jr, Ingram RH, Breslin FJ, Jaeger JJ. Airway responsiveness to cold air and hyperpnoea in normal subjects and in those with hayfever and asthma. Am Rev Respir Dis 1980; 121:621-628.

61. Anderson SD, Schofield RF, Perry CP, Daviskas E and Kendall M. Sensitivity to heat and water loss at rest and during exercise in asthmatic patients. Eur J Respir Dis 1982; 63:459-471

62. Bundgaard A, Ingemann-Hansen T, Schmidt A, Halkjaer-Kristensen J. Influence of temperature and relative humidity of inhaled gas on exercise induced asthma. Eur J Respir Dis 1982; 63:239-244.

63. Chen WY and Horton DJ. Heat and water loss from the airways and exercise induced asthma. Respiration 1977; 34:305-313.

64. Deal EC Jr, McFadden ER Jr, Ingram RH, Strauss RH, Jaeger JJ. Role of respiratory heat exchange in the production of exercise-induced asthma. J Appl Physiol 1979; 46: 467-475.

65. Gilbert IA, Fouke JM and McFadden ER Jr. Heat and water flux in the intrathoracic airways and exercise induced asthma. J Appl Physiol 1987; 63: 1681-1691.

66. Gilbert IA, Fouke JM and McFadden ER Jr. Intra-airway thermodynamics during exercise and hyperventilation in asthmatics. J Appl Physiol 1988:64: 2167-2174.

67. Anderson SD, Schoeffel JL, Black JL, Daviskas E. Airway cooling as the stimulus to exercise induced asthma – a re-evaluation. Eur J Respir Dis 1985; 67:20-30.

68. Eisenbacher WL and Sheppard D. Respiratory heat loss is not the sole stimulus for bronchoconstriction induced by isocapnoeic hyperpnoea with dry air. Am Rev Respir Dis 1985; 131:894-901.

69. McFadden ER Jr, Nelson JA, Skowronski ME, Lenner KA. Thermally induced asthma and airway drying. Am J Respir Crit Care Med. 1999 Jul; 160: 221-6.

70. Kotaru C, Coreno A, Skowronski M, Ciufo R, McFadden ER Jr.. Exhaled nitric oxide and thermally induced asthma. Am J Respir Crit Care Med 2001; 163: 383-8.

71. Yasuhiro G, Ha shimoto S, Matsumoto K, Na kayama T, Takeshita I and Horie T. Cooling and rewarming-induced IL-8 expression in human bronchial epithelial

cells through p38 MAP kinase-dependent pathway.Biochem Biophys Res Commun 1998; 249: 156-60.

72. Enhorning G, Hohifield J, Krug N, Lema G and Welliver RC. Surfactant function affected by airway inflammation and cooling: possible impact on exercise induced asthma. Eur Respir J 2000; 15: 532-538.

73. Xun L, Wilson JW. Increased vascularity of the bronchial mucosa in mild asthma. Am J Respir Crit Care Med 1997; 156: 229-233.

74. Dunhill MS. The pathology of asthma, with special references to changes in the bronchial mucosa. J Clin Path 1960; 13:27-33.

75. Mitzner W, Wagner E and Brown RH. Is asthma a vascular disorder? Chest 1995 supplement; 107:97S-104S

76. Nakamura T, Katori R, Miyazawa K, Ohtomo S, Watanabe T, Watanabe T, Miura Y, Takizawa T. Bronchial blood flow in patients with chronic pulmonary disease and its influences on respiration and circulation. Dis Chest 1961; 39:193-206.

77. Boushy SF, North LB, Trice JA. The bronchial arteries in chronic obstructive pulmonary disease. Am J Med 1969; 46: 506-15.

78. Cuudkowicz L and Armstrong JB. The bronchial arteries in pulmonary emphysema. Thorax 1953; 8:46-58.

79. Cudkowicz L. Bronchial arterial circulation in man: normal anatomy and responses to disease. In: Moser KM, ed. Pulmonary vascular diseases. New York: Marcel Dekker 1979; 111-232.

80. Nuszkov A, Gulacsy I, Kiss T. Angiography of the bronchial and pulmonary arteries in chronic non-specific lung diseases. Acta Chir Acad Sci Hung 1979; 20:225-34.

81. Liebow AA, Hales MR, Lindskog GE. Enlargement of the bronchial arteries and their anastomoses with the pulmonary arteries in bronchiectasis. Am J Pathol 1949; 25:211-231.

82. Primiano FP Saidel GM, Montague FW Jr, Kruse KL, Green CG, Horowitz JG. Water vapour and temperature dynamics in the upper airways of normal and CF subjects. Eur Respir J 1988; 1:407-414.

83. Rouadi P, Baroody FM, Abbott D, Naureckas E, Solway J, and Naclerio RM. A technique to measure the ability of the human nose to warm and humidify air. J Appl. Physiol 1999. 87: 400-406.

84. Paredi P, Kharitonov SA and Barnes PJ. Faster rise of exhaled breath temperature in Asthma. A novel marker of airway inflammation? Am J Respir Crit Care Med 2002; 165: 181-184.

85. Paredi P, Caramori G, Cramer D, Ward S, Ciaccia A, Papi A, Kharitonov SA and Barnes PJ. Slower rise of exhaled breath temperature in chronic obstructive pulmonary disease. Eur Respir J 2003; 21:439-443.

86. Piacentini GL, Bodini A, Zerman L, Costella s, Zanolia L, Peroni DG, Boner AL. Relationship between exhaled air temperature and exhaled nitric oxide in childhood asthma. Eur Respir J 2002; 20: 108-111.

87. Standards for the diagnosis and care of patients with chronic obstructive pulmonary disease (COPD) and asthma. Official statement of the American Thoracic Society, Adopted by the ATS board of Directors, November 1986. Am Rev Respir Dis 1987; 136:225-244.

88. Pauwels RA, Buist AS, Calverly PM, Jenkins CR and Hurd SS. Global strategy for the diagnosis, management and prevention of chronic obstructive pulmonary disease. NHLBI/WHO Global Initiative for Chronic Obstructive Lung Disease (GOLD) Workshop summary. Am J Respir Crit Care Med 2001; 163: 1256-1276

89. Rogers GFC and Mayhew YR. Properties of mixtures. In Engineering thermodynamics work and heat transfer. 3rd edition. Longman 1980.

90. CIBSE Psychrometric chart for air at atmospheric pressure. CIBSE London 1990.

91. Rogers GFC and Mayhew YR. Thermodynamic and transport properties of fluids – SI Units. 1980. Blackwell.

92. Kim HH, Le Merre C, Demirozu CM, Chediak AD and Wanner AD. Effect of hyperventilation on airway mucosal blood flow in normal subjects. Am J Respir Crit Care Med 1996; 154:1563-1566.

93. Bland JM and Altman DG. Statistics Notes: Measurement error. BMJ 1996; 313: 744 (21 September).

94. Mendes ES, Pereira A, Danta I, Duncan RC and Wanner A. Comparative bronchial constrictive efficacy of inhaled glucocorticosteroids. Eur Respir J 2003; 21: 989-993.

95. Anderson SD, Daviskas E. The airway microvasculature and exercise induced asthma. Thorax 1992:47; 748-752.

96. Bar-Or O, Neuman I and Dotan R. Effects of dry and humid climates on exercise induced asthma in children and pre-adolescents.J Allergy Clin Immun 1977; 60: 163-168.

97. Ben-Dov I, Bar–Yishay E and Godfrey S. Exercise induced asthma without respiratory heat loss. Thorax 1982; 37: 630-631.

98. Boulet, LP and Turcotte, H. Influence of water content of inspired air during and after exercise on induced bronchoconstriction. Eur Respir J. 1991; 4:979-984.

99. Freed AN, Kelly LJ, Menkes HA. Airflow induced bronchospasm. Imbalance between airway cooling and airway drying? Am Rev Respir Dis 1987; 136; 595-9.

100. Gilbert IA, Regnard J, Lenner KA, Nelson JA, McFadden ER Jr. Intrathoracic airstream temperatures during acute expansions of thoracic blood volume. Clinical Sciences 1991; 81:655-661.

101. Hahn A, Anderson SD, Morton AR, Black JL, Fitch KD. A reinterpretation of the effect of temperature and water content on the inspired air in exercise induced asthma. Am Rev Respir Dis 1984:130; 575.

102. Janssen LJ, Lu-Chao, H and Netherton, S. Responsiveness of canine bronchial vasculature to excitatory stimuli and to cooling. Am J Physiol Lung Cell Mol Physiol 2001; 280: L930-937.

103. Kaminsky DA and Lynn M. Pulmonary capillary blood volume in hyperpnea-induced bronchospasm. Am J Respir Crit Care Med 2000:162; 1668-1673.

104. McFadden ER Jr. Exercise and asthma. N Engl J Med. 1987 Aug 20; 317: 502-4.

105. Smith CM, Anderson SD, Walsh S and McElrea M. An investigation of the effects of heat and water exchange in the recovery period after exercise in children with asthma. Am Rev Respir Dis 1989; 140:598-605.

106. Solway J, Pichurko BM, Ingenito EP, McFadden ER Jr, Fanta CH, Ingram RH Jr, Drazen JM. Breathing pattern affects airway wall temperature during cold air hyperpnoea in humans. Am Rev Respir Dis 1985; 132:853-857.

107. Strauss RH, McFadden ER Jr, Ingram RH Jr, Chandler E and Jaeger JJ. Enhancement of exercise induced asthma by cold air. New Engl J Med 1977; 297:743-747.

108. Mihalyka M, Wong J, James AL, Anderson SD, Pare PD. The effect on airway function of inspired air conditions after isocapnic hyperventilation with dry air. J Allergy Clin Immunol 1988; 82:842-8.

109. O'Cain CF, Dowling NB, Slutsky AS, Hensley MJ, Strohl KP, McFadden ER Jr, Ingram RH Jr. Airway effects of respiratory heat loss in normal subjects. J Appl Physiol 1980:49:875.

110. Zawadski DK, Lenner KA and McFadden ER Jr. Comparison of intra-airways temperatures in normal and asthmatic subjects after hyperpnea with hot, cold and ambient air. Am Rev Respir Dis 1988; 138:1553-1558.

111. Anderson SD, Schofield RF, Perry CP, Daviskas E and Kendall M. Sensitivity to heat and water loss at rest and during exercise in asthmatic patients. Eur J Respir Dis 1982; 63:459-471.

APPENDIX 1

INSTRUMENTATION

A1.1 Measurement of temperature

K-type (Chromel-alumel) thermocouples were used for the measurement of air and breath temperatures. They were of miniature welded bead construction offering a 95% response time of 50ms. A compensated reference temperature system was used whereby dedicated temperature indicators terminate each thermocouple at a connection panel inside the chassis and use a compensated network to inject a signal, which compensates for the temperature of the panel before calculating the temperature. The output signal was then amplified and fed into a 16-channel data acquisition system (Fig A2.1). All thermocouples were calibrated whilst connected to their channels and amplifiers. They were calibrated using a water-bath arrangement against a mercury standard to within ± 0.1°C.

Figure A1.1. Choice of thermocouple for measurement of exhaled air temperatures. The thermocouple consists of two dissimilar metals joined, which generate a net thermoelectric voltage between the open pair according to the size of the temperature difference between the ends and the relative thermoelectric properties of the metal wires used.

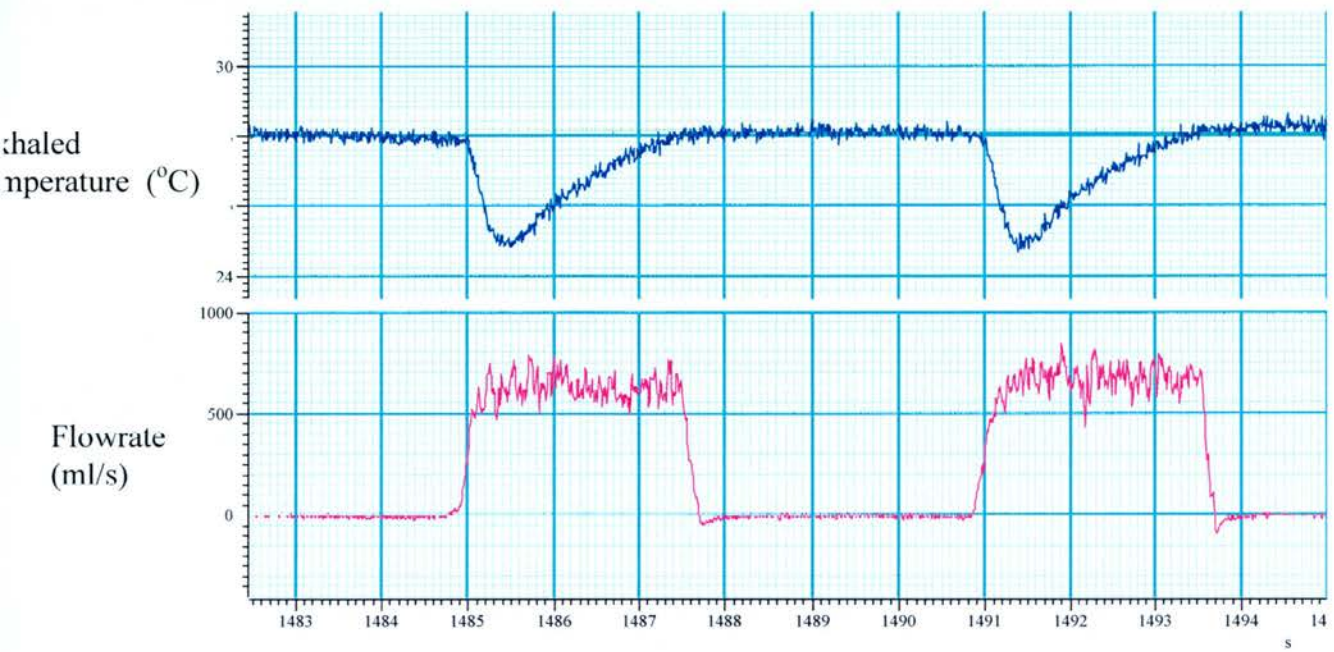

Figure A1.2. Typical thermocouple signal showing exhaled breath temperature in relation to flowrate.

A1.2 Humidity sensors

The sensors are of a 3-layered capacitance construction as shown in Fig A1.2. Water vapour in the active capacitor's dielectric layer equilibrates with the surrounding gas. In so doing the dielectric property is altered in proportion to the absolute concentration of water vapour in the surrounding air. This will be reflected in changes in the output voltage of the device. The porous platinum layer shields the dielectric response from external influences while the protective polymer over layer provides mechanical protection for the platinum layer from contaminants.

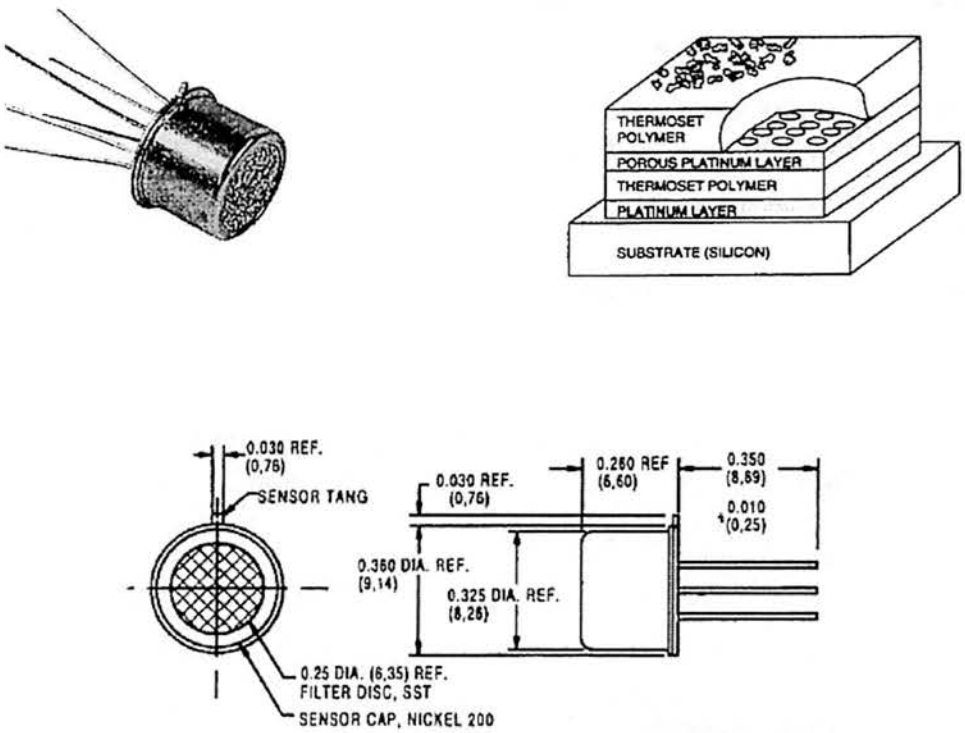

Figure A1.2. Detail of humidity sensor construction. Based on the principle of altered capacitance in proportion to the absolute amount of water vapour that the dielectric layer equilibrates with, the humidity sensor replaces the elaborate freeze and weigh techniques used in the past to measure respiratory moisture loss.

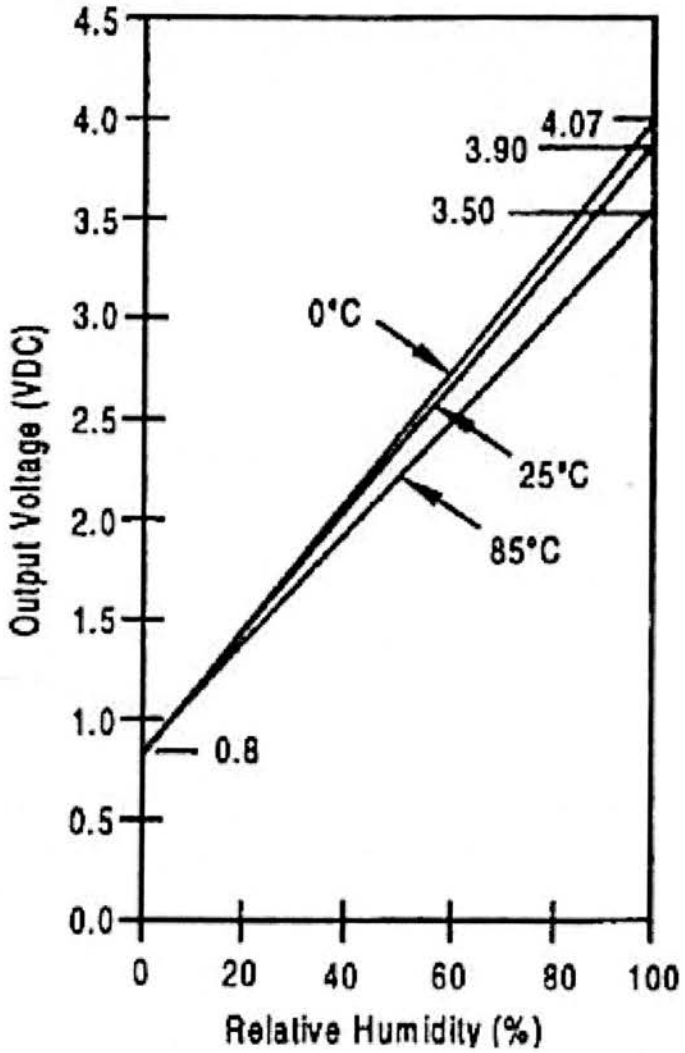

Figure A1.3. Relationship of humidity sensor output voltage to relative humidity. Over the operating range of the sensor (35-40 °C, rh 65-75%) the variation of gain with temperature is ±2%.

A1.3 Phase-shift ultrasonic flowmeter

The flowmeter comprises two ultrasonic transducers which are mounted diagonally across a tube through which subjects breathe. Each transducer can emit and receive sound across the moving airstream. The frequency of the received signal will be altered by the fact that it is being transmitted through a moving stream of air. This alteration is termed the phase shift of the transmitted signal and will depend on the velocity of the airstream, the physical dimensions of the tube, the angle at which the transducer is set and the frequency of the transmitted signal and the speed of sound in air. If the functions of the transducers are reversed a similar relation can be found. The difference between the 2 phase shifts ($\Delta\varphi$) with the ultrasound traveling in each direction can be expressed as a direct linear function of air velocity thus;

$$\Delta\varphi = 4\pi f d \frac{V \cos\theta}{c^2}$$

Where c = *speed of sound in air, f = frequency, d= diameter of tube.*

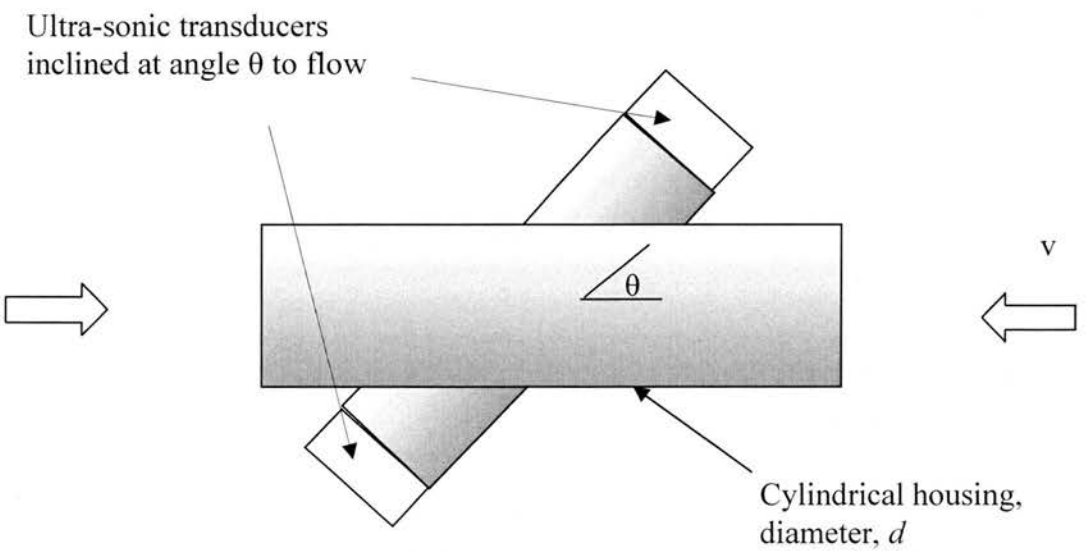

The relationship between the flow velocity and phase shift is inversely proportional to air temperature because of the velocity of sound being proportional to the square root of temperature. Coincidentally the resultant variation in gain of the instrument corrects the volume flowrate for changes in temperature.

This type of flowmeter lends itself to this application in particular as it has low resistance to air flow, minimal dead space, good linearity, stability, robustness and lack of sensitivity to contamination with condensation. The specification of the device is summarized below.

Manufacturer	*Flowmetrics Division* *Birmingham Research and Development Ltd* *Birmingham Research Park* *Vincent Drive* *Birmingham B15 2SQ*
Linearity	< 2% of reading
Baseline stability Inhaled:exhaled Temperature (ambient) <2% fsd / °C	 < 0.2% fsd < 0.2% fsd/°C
Noise, zero flow	< 0.07% fsd, rms (0-60Hz)
Gain stability Ambient:exhalate (20°C) Temperature (25-35°C)	 +0.16% gain change -0.27%/°C
Response time	12ms (100%)
All output impedances	100ohms
Power requirements	9-15V, 250mA. AC or DC
Flow range Dead space	+/- 20 l/s 30ml

APPENDIX 2

DATA ACQUISITION

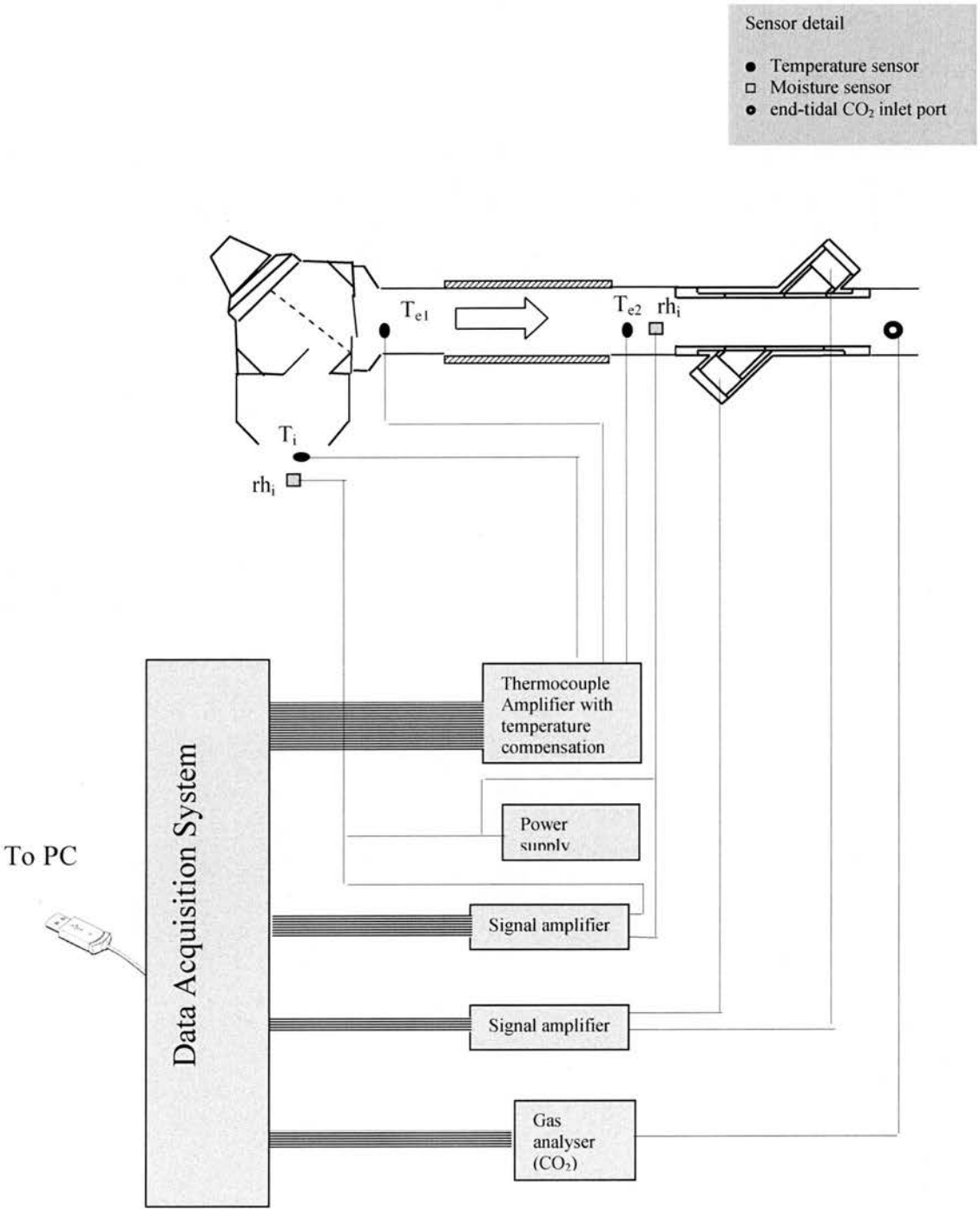

Figure A2.1. Schematic of instrumentation in breathing circuit. Thermocouple and humidity sensor output was conditioned by purpose built multichannel amplifiers. All signals were sampled at 100 Hz and captured on a 16-channel computerized data acquisition system (model 14011, CED, Cambridge, UK), which interfaced with software (spike 2, CED, Cambridge, UK) to allow real time display of signals and storage of data to disk.

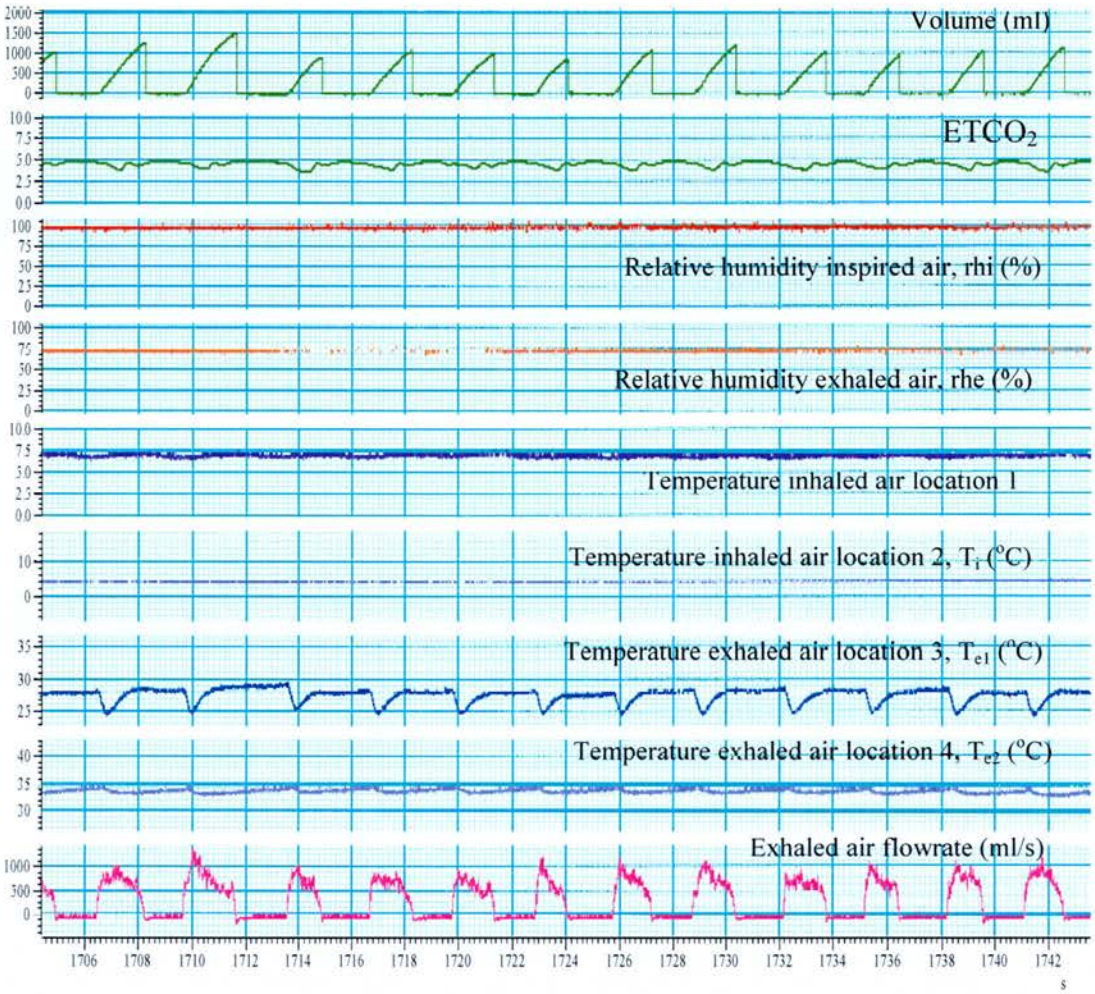

Figure A2.2. Real-time display of expired volume, end-tidal CO_2, inspired and exhaled relative humidity, inhaled and exhaled temperature and flowrate. Signals taken from subjects breathing at a target ventilation pattern. The real-time signals allow steady state conditions to be established and hence measurement of respiratory heat and moisture loss.

APPENDIX 3

Experimental Error

Calculation of Hans Rudolf valve dead-space effect – 'wash-in and washout' effect.

'Wash-in' Effect

The inhaled and exhaled air mixes with the small amount of dead-space air within the Hans-Rudolf valve. During inspiration this dead-space air will be warmer and more saturated than the colder dryer inspirate whereas during expiration it will be cooler and dryer than the exhaled air. There will therefore be a small gain in enthalpy across the valve during inspiration and a loss during expiration. The following quantifies this effect as a source of error in the overall measurement of respiratory heat and moisture loss (RHML).

Assuming adiabatic mixing between inspired air and valve dead space air i.e. no net gain or loss of energy in mixing process, an energy balance is expressed as;

$$m_i h_i + m_d h_d = (m_i + m_d)\, h_i'$$

$$\textit{therefore, } h_i' = \frac{m_i h_i + m_d h_d}{m_i + m_d}$$

where m_i = *mass flowrate of inspired air (kg/s),* m_d = *mass flowrate of dead-space air (kg/s),* h_i=*enthalpy of inspired air (kJ/kg),* h_d=*enthalpy of dead-space air (kJ/kg),* h_i' =*enthalpy of mixed inhaled air (kJ/kg)*

Assuming the inspired air to be at 7°C and with an absolute humidity of 5.8 g/kg, a minute ventilation (V) of 15litres/min, a tidal volume of 1500ml and the valve dead-space volume to be 30ml at a temperature of 27.7°C with absolute humidity 28.5 g/kg.

$m = \rho_a V$, *where* ρ_a = *density of air kg/m*^{3}

Then, $m_i = 1.129 \times \frac{15}{60} \times 10^{-3} = 3.125 \times 10^{-4}\ kg/s$

$m_d = 1.25 \times \frac{0.3}{60} \times 10^{-3} = 5.64 \times 10^{-6}\ kg/s$

From Psychrometric chart [90]*, for* $T_i = 7^oC$, $w_i = 5.8\ g/kg$ *then* $h_i = 21.6\ kJ/kg$. *Similarly* $h_d = 88.1\ kJ/kg$

Therefore,

$$h_i' = \frac{m_i h_i + m_d h_d}{m_i + m_d} = 22.8\ kJ/kg$$

The small enthalpy gain across the valve during inspiration is therefore h_i' - h_i = *1.2 kJ/kg* which accounts for 1.7% of the total enthalpy change across the system.

'Wash-out' Effect

Using the same assumption as above, there will be a small enthalpy loss across the valve due to the mixing of exhaled air with the colder valve dead-space air.

$$h_e' = \frac{m_e h_e + m_d h_d}{m_e + m_d}$$

where m_i = *mass flowrate of inspired air (kg/s),* h_e*=enthalpy of exhaled air (kJ/kg),* h_d*=enthalpy of dead-space air (kJ/kg),* h_e' *=enthalpy of mixed exhaled air (kJ/kg). This leads to;*

$h_e' = 86.5\ kJ/kg$

The small enthalpy loss across the valve during inspiration is therefore h_e' - h_e = *1.5 kJ/kg*, representing 2.2% of the total enthalpy difference.

The 'wash-in' and 'wash-out' effects can therefore be considered small (≈2%) compared to the magnitude of overall energy exchange and can be ignored for the purpose of measurement of individual RHML.

Humidity Sensor Response time error

The response time for the humidity sensor (5s) is such that for the breathing patterns used in this study, inter-breath variations in relative humidity were not detected. The position of the humidity sensor distal to the mouth and at the end of the heated tube section means that the sensor will 'see' a damped signal as a result of more efficient mixing between exhaled dead-space gas. Measurements were taken over a prolonged period to allow steady state conditions to be achieved. Potential error may arise due to the sensor not detecting inter-breath variation in relative humidity. If we consider a bi-compartmental model of expired air whereby the initial portion of exhaled air is unsaturated and the second compartment comprises fully condition gas. Then the ideal RH signal from a sensor placed next to the mouth will rise exponentially to 100%RH from an initial value determined largely by inspired air condition. In order to estimate the magnitude of this error we can consider the 'worst case scenario' (Figure A3) where the sensor placed at the mouth fails to detect the extreme inter-breath variation in RH due to the first-compartment effect. We know from the studies of Ferrus et al [48] using mass spectrometry (Figure 1.4) that the first compartment is approximately 10% of the tidal volume. Considering Figure A3, the *ideal* moisture sensor detects the change in moisture (w_e-w_i) over the first compartment whereas the sensor with the slow response time detects the steady state plateau value. Assuming a linear rise in sensor signal, the moisture loss per breath (m_i) from the *ideal* sensor is given by;

$$m_i = (w_e - w_i)V - \frac{1}{2}\Lambda V(w_e - w_i)$$

Whereas the moisture loss per breath from the *damped* sensor is given by;

$$m_i' = (w_e - w_i)V$$

The % difference between *ideal* and *damped* measurements is therefore;

$$\frac{m_i' - m_i}{m_i'} = \frac{\Delta V}{2V}$$

If for a tidal breath of 1500ml we assume the first compartment comprises 150ml then the % difference between the sensors would be of the order $\frac{150}{2 \times 1500} = 5$ %. This represents a maximum theoretical error assuming the sensor is positioned in close proximity to the mouth where it will be exposed to extreme variation in moisture levels. As described earlier in the present study the sensor was positioned distal to the mouth at the end of a heated tube section. At this location due to improved dead space mixing the sensor is exposed to much less variation in humidity levels breath to breath and therefore this error is likely to be much less than 5%.

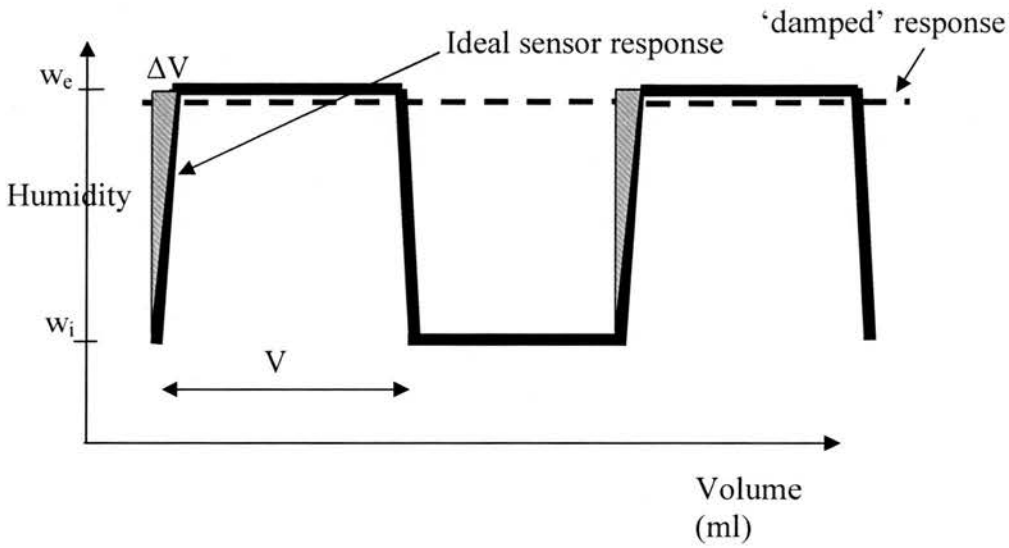

Comparison of measured water loss against 'freeze and weigh' standard

To test the accuracy of the moisture sensors measurements were made on 10 normal controls over a range of minute ventilations and compared with the data obtained by the 'freeze and weigh' technique (*Ferrus et al* [48]) under similar conditions. The results are shown in Figure A4. As can be seen from the data there is excellent agreement between sensor measurements and 'freeze and weigh' measurements under matched conditions (agreement to within < 2%). The error due to the sensor response time is considered negligible.

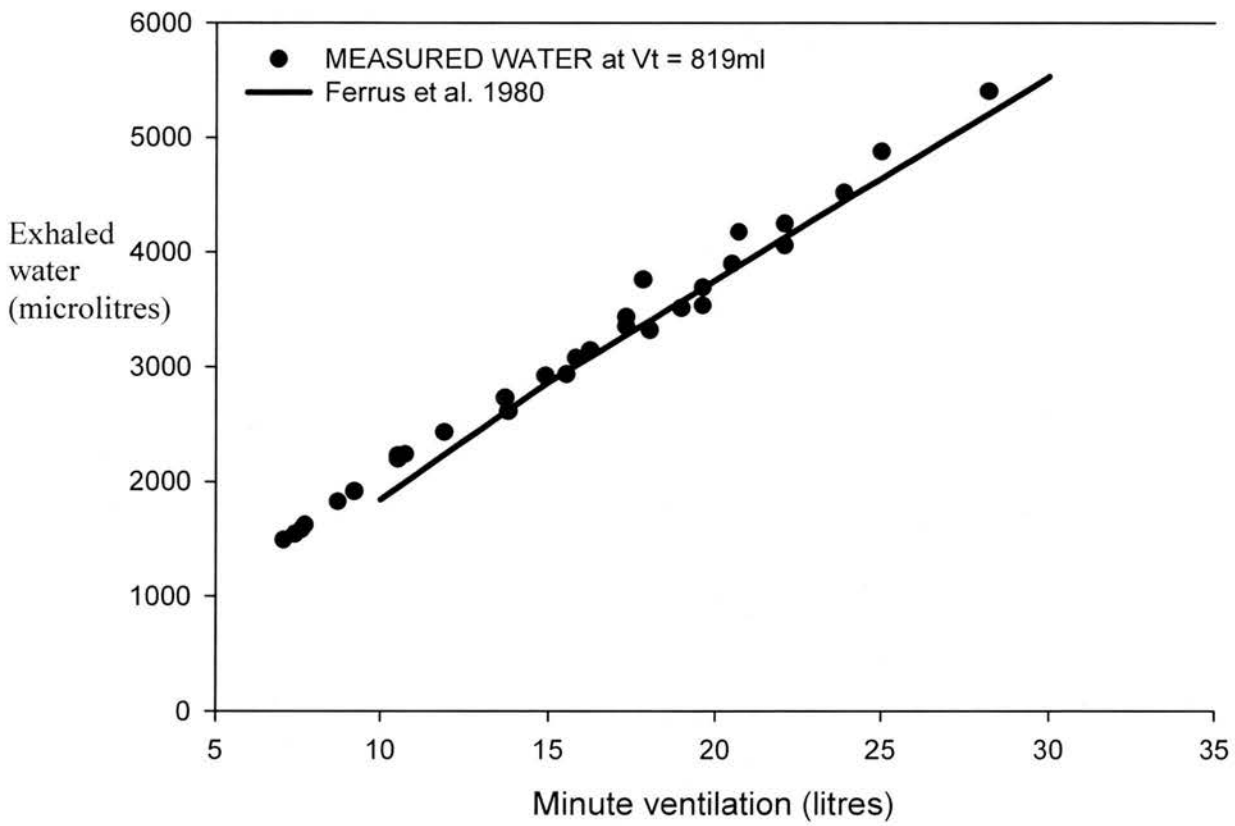

Cumulative error in calculated respiratory heat and moisture loss (RHML)

Referring to section 3.3.2 outlining the calculation of the overall RHML; this worked example forms the basis for the following evaluation of the cumulative error in the calculation of this quantity.

From the example section (3.3.2),

RHML (Q) = m Δh =m (h_e-h_i)

As described in section (3.3.1), enthalpy (h) is a linear function of the 2 independent variable w and T. In this example;

w_e =24.4 g/kg ± 2%, T_e = 28.5 ± 0.1°C , h_e =96.5 kJ/kg

The associated error in the calculation of h_e is therefore given by;

$$\frac{\Lambda h_e}{h_e} = \sqrt{\left(\frac{\Lambda w_e}{w_e}\right)^2 + \left(\frac{\Lambda T_e}{T_e}\right)^2} = \sqrt{(0.02)^2 + \left(\frac{0.1}{28.5}\right)^2} = 0.02$$

Therefore h_e =96.5 ± 1.95 kJ/kg

Similarly for w_i =5.6 g/kg ± 2%, T_i = 6.5 ± 0.1°C, h_i =20.6 kJ/kg

$$\frac{\Lambda h_i}{h_i} == \sqrt{(0.02)^2 + \left(\frac{0.1}{6.5}\right)^2} = 0.025$$

Therefore h_e =20.6 ± 0.52 kJ/kg

$$\frac{\Lambda(h_e - hi)}{h_e - h_i} = \sqrt{(0.02)^2 + (0.025)^2} = 0.03$$

h_e - h_i = 96.5- 20.6 =73.4 ± 2.34 kJ/kg

$m = \rho V$, V=349.7 ± 3.5 ml/s

$$\frac{\Lambda Q}{Q} == \sqrt{(0.01)^2 + (0.03)^2} = 0.032$$

Q = 29.3 ± 0.92 Watts

APPENDIX 4

VENTILATORY FLOW TARGETING SOFTWARE

Software was written in *QuickBasic* in order to generate on screen a visual and auditory target for expiratory flowrate and breath frequency respectively for subjects to follow. The software takes as input the signal from an ultrasonic flowmeter (described in Appendix 1.2) which is conditioned via an Amplicon pc26ad Card. The subject's breathing pattern is displayed in real time and in addition the expiratory flowrate is displayed against a target flowrate set by the user (FigA3.2). The user can also set the subject's breathing rate by means of an auditory cue (beeps). A 2-tone system cues inspiration and expiration. The duration of inspiration and expiration is set equal. Flowrate targeting was chosen over volume targeting to avoid the tendency of subjects to dynamically hyperinflate. If subjects are instructed to adhere to a square wave expiratory pattern then effectively minute volume and tidal volume target patterns can be set. The operator is offered a succession of screens, which prompt for the ventilation target pattern as shown in Figure A3.1.

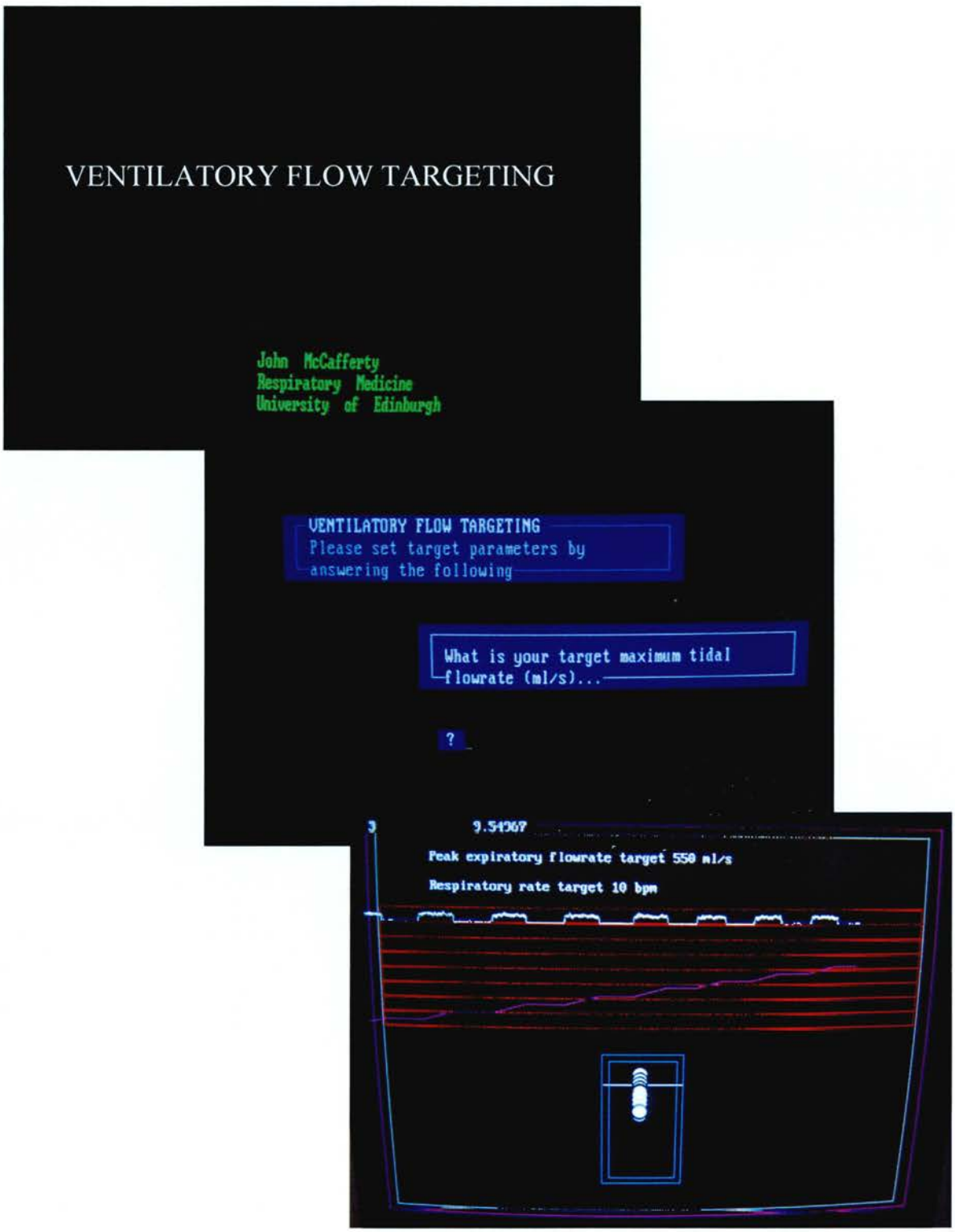

Figure A3.1. Ventilation targeting software screen displays. These prompt the user for ventilation target parameters such as expiratory flowrate and breaths per minute.

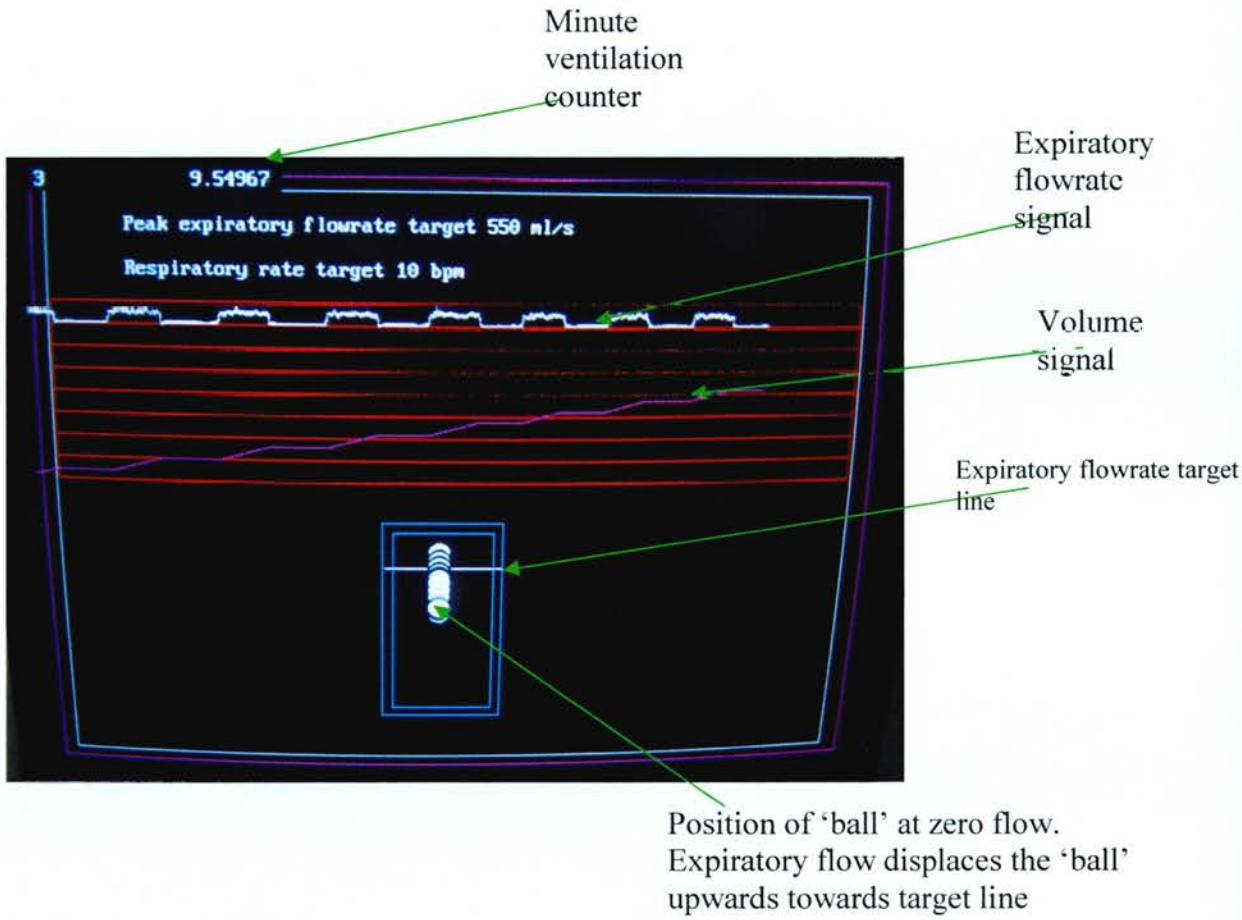

Figure A3.2. Ventilation targeting system. The subject's breathing pattern is displayed in real time and the expiratory flowrate is displayed against a target flowrate set by the user. The user can also set the subject's breathing rate by means of a an auditary cue (beeps). The system allows standardization of breathing pattern for measurement of respiratory heat and moisture loss (RHML).

```
DECLARE SUB targetdraw ()
DECLARE SUB targetfreq10 ()
DECLARE SUB targetfreq15 ()
DECLARE SUB targetfreq20 ()
DECLARE SUB targetfreq25 ()
DECLARE SUB targetfreq30 ()
DECLARE SUB targetfreq35 ()
DECLARE SUB targetfreq40 ()
DECLARE SUB SCRDRAW ()
DECLARE SUB CLEARSCREEN (MAXX, MAXY, SIZ, DL)
DECLARE SUB DRWBOX1 ()
DECLARE SUB fprint (Text$, textx%, texty%, colour%, file%)
DECLARE SUB CLEARSCREEN (MAXX, MAXY, SIZ, DL)
DECLARE SUB fopen (file$, file%)
DECLARE SUB Delay (A AS SINGLE)
DECLARE SUB DisplayBox (X AS INTEGER, Y AS INTEGER, FrameColourA AS INTEGER, FrameColourB AS INTEGER,
TextColourA AS INTEGER, TextColourB AS INTEGER, FrameColour AS INTEGER, FrameLabel AS STRING, Text AS
STRING, Size AS INTEGER, Speed AS SINGLE, _
WaitKey AS INTEGER)
DECLARE SUB CloseBox (X AS INTEGER, Y AS INTEGER, Size AS INTEGER, Lines AS INTEGER, Speed AS SINGLE)

DIM SHARED OnScreen(25, 80) AS INTEGER
DIM SHARED OnColour(25, 80) AS INTEGER
DIM SHARED Lines AS INTEGER


Start:
'$INCLUDE: 'c:\qb45\pc26at.bi'
'INTRO GRAPHICS
SCREEN 12
PAINT (1, 1), 10
CLEARSCREEN 640, 480, 3, 0
SLEEP 1
CLS

' SIGNATURE SCREEN
A$ = "C:\JOHN\QBWINFNT\"
fopen A$ + "IMPACT.qbf", 1
fopen A$ + "roman.qbf", 2
fopen A$ + "terminal.qbf", 3
fprint "VENTILATORY FLOW TARGETING", 100, 150, 7, 1
fprint "John McCafferty", 250, 350, 2, 3
fprint "Respiratory Medicine", 250, 375, 2, 3
fprint "University of Edinburgh", 250, 400, 2, 3
CLOSE
DO UNTIL INKEY$ <> ""
LOOP
flag1:

WINDOW (0, -150)-(4000, 500)

DIM newaddr AS INTEGER
DIM numchans AS INTEGER
DIM NumScans AS INTEGER
DIM result AS INTEGER
DIM VOLTS(16, 3) AS SINGLE
DIM SHARED target(2000)
DIM F AS SINGLE
CONST PI = 3.141593
DIM SHARED tvol AS INTEGER
DIM SHARED tfreq AS INTEGER

v% = 1
pg% = 1

CLS
```

```
'INPUT TARGET DATA
SCREEN 0
COLOR 7, 0
' Display Header
CALL DisplayBox(5, 10, 9, 1, 7, 1, 15, "VENTILATORY FLOW TARGETING ", "Please set target parameters by answering the following", 40, .05, 0)
' Display Text
CALL DisplayBox(10, 25, 7, 1, 15, 1, 0, "", "What is your target maximum tidal flowrate (ml/s)...", 40, .05, 0)
LOCATE 15, 27
INPUT " "; tvol
CALL CloseBox(10, 25, 40, Lines, .05)
CALL DisplayBox(10, 25, 7, 1, 15, 1, 0, "", "What is your target ventilatory rate (bpm)", 40, .05, 0)
LOCATE 16, 27
INPUT " "; tfreq
CALL CloseBox(10, 25, 40, Lines, .05)

'initialise ADC
chanNo = 1
newaddr = &H300
CALL InitAddr(newaddr)

'set channels to be read
FOR chan = 0 TO (chanNo - 1)
chans(chan) = chan
NEXT chan
numchans = chanNo
CALL SetAdChans(chans(), numchans)

'zeroing of the flowmeter
zero: CALL DisplayBox(10, 25, 7, 1, 15, 1, 0, "", "Do you want to zero the flowmeter ?", 40, .05, 0)
LOCATE 17, 27
INPUT " "; zero$
IF zero$ = "y" THEN
CLS
GOTO getdat
END IF
IF zero$ = "n" THEN GOTO store
IF zero$ <> "n" AND zero$ <> "y" THEN GOTO zero

CALL CloseBox(10, 25, 40, Lines, .05)
getdat: CALL SoftScanAd(ConvData(), 1)
result = (ConvData(chans(0), 0))
IF result < 2048 THEN
zero = 2 * (result / 2047)
ELSE
zero = -2 * (4096 - result) / 2048
END IF
'convert to L/sec
F = zero / .2
LOCATE 22, 5
PRINT INT(F * 100) / 100
CALL DisplayBox(10, 25, 7, 1, 15, 1, 0, "", "press z when zero is steady", 40, .05, 0)
IF INKEY$ = "z" THEN GOTO store
GOTO getdat

CALL CloseBox(10, 25, 40, Lines, .05)
'open file on d: for output

store: CALL DisplayBox(10, 25, 7, 1, 15, 1, 0, "", "filename for storing data", 40, .05, 0)
LOCATE 18, 27
INPUT ""; file$
CALL CloseBox(10, 25, 40, Lines, .05)
file$ = "c:\temp\" + file$ + ".asc"
OPEN file$ FOR OUTPUT AS #1

'pause prior to data sampling
pause: CALL DisplayBox(10, 25, 7, 1, 15, 1, 0, "", "press s to proceed and e to stop", 40, .05, 1)
'
DO
LOOP UNTIL INKEY$ = "s"
'restore screen mode
SCREEN 12
w = 1
```

```
v% = 1

' set clock controlled sampling
control = newaddr + 7
counter0 = newaddr + 4
counter1 = newaddr + 5
counter2 = newaddr + 6

OUT control, 52
OUT control, 116
OUT control, 180

OUT counter0, &H10
OUT counter0, &H27
OUT counter1, &HFF
OUT counter1, &HFF
OUT counter2, &HFF
OUT counter2, &HFF



'draw target lines
CLS
CALL SCRDRAW
CALL targetdraw


'call breath frequency auditory target sounds
scue:
IF tfreq = 10 THEN
CALL targetfreq10
ELSEIF tfreq = 15 THEN CALL targetfreq15
ELSEIF tfreq = 20 THEN CALL targetfreq20
ELSEIF tfreq = 25 THEN CALL targetfreq25
ELSEIF tfreq = 30 THEN CALL targetfreq30
ELSEIF tfreq = 35 THEN CALL targetfreq35
ELSEIF tfreq = 40 THEN CALL targetfreq40
END IF
'Data acquisition loop
DO UNTIL INKEY$ = "e"
gettime:
oldtim = tim
gettim2:
OUT control, 68
tim = INP(counter1): hi = INP(counter1)
IF tim = oldtim GOTO gettim2

' sample flow at 100Hz, plot FV loop and vol/time, put flow readings into
' array
getdat2:
CALL SoftScanAd(ConvData(), 1)
'Convert all data to volts and save in array Volts(channel no,sample number)
FOR chan = 0 TO (numchans - 1)
p% = ConvData(chan, 0)

IF p% < 2048 THEN
VOLTS(chan, 0) = 2 * (p% / 2047)
ELSE
VOLTS(chan, 0) = -2 * (4096 - p%) / 2048
END IF
NEXT chan

'print flow data and target display on screen
IF INKEY$ = "c" THEN
GOTO scue
END IF

FOR chan = 0 TO (numchans - 1)
PSET (v%, (VOLTS(chan, 0) * 100) + 300), 15

CIRCLE (1850, (VOLTS(chan, 0) * 400) + 50), 50, 5
PAINT (1850, (VOLTS(chan, 0) * 400) + 50), 50, 5
CIRCLE (1850, (VOLTS(chan, 0) * 400) + 50), 50, 0
```

```
PAINT (1850, (VOLTS(chan, 0) * 400) + 50), 50, 0


'save data to file
PRINT #1, v%; "          "; VOLTS(chan, 0)
NEXT chan
'reset screen display
v% = v% + 1
IF v% > 4000 THEN
CLS
v% = 1
pg% = pg% + 1
CALL targetdraw
CALL SCRDRAW
LOCATE 1, 1: PRINT pg%

END IF

'end data acquisition loop
LOOP

repeat: LOCATE 30, 15: INPUT "Press r to repeat, x to exit"; repeat$
IF repeat$ = "r" THEN
CLEAR
GOTO flag1
ELSEIF repeat$ = "x" THEN
END
ELSE
LOCATE 28, 2: PRINT "Invalid key enter again"
GOTO repeat
END IF

END

'SUBROUTINES.....

SUB CLEARSCREEN (MAXX, MAXY, SIZ, DL)
IF SIZ > 100 THEN SIZ = 100
FOR S = 0 TO 500 / (SIZ * 2)
Y = 0 + (S * SIZ)
FOR X = 0 + S TO MAXX - S STEP SIZ
LINE (X, Y)-(X + SIZ, Y + SIZ), 0, BF
FOR I = 1 TO DL: NEXT I
NEXT X
X = MAXX - (S * SIZ)
FOR Y = 0 + S TO MAXY - S STEP SIZ
LINE (X, Y)-(X + SIZ, Y + SIZ), 0, BF
FOR I = 1 TO DL: NEXT I
NEXT Y
Y = MAXY - (S * SIZ)
FOR X = MAXX - S TO 0 + S STEP -SIZ
LINE (X, Y)-(X + SIZ, Y + SIZ), 0, BF
FOR I = 1 TO DL: NEXT I
NEXT X
X = 0 + (S * SIZ)
FOR Y = MAXY - S TO 0 + S STEP -SIZ
LINE (X, Y)-(X + SIZ, Y + SIZ), 0, BF
FOR I = 1 TO DL: NEXT I
NEXT Y
NEXT S
CLS
END SUB

SUB CloseBox (X AS INTEGER, Y AS INTEGER, Size AS INTEGER, Lines AS INTEGER, Speed AS SINGLE) STATIC

Size = Size + 10
IF Speed > 0 THEN
' Descending Soud
FOR I = 1500 TO 500 STEP -(35 - (Lines * 5))
SOUND I, I / 20000
NEXT
END IF
FOR A = (Lines + X) TO (X - 1) STEP -1
```

```
' Delay between line draws
CALL Delay(Speed)
LOCATE A + 2, Y
FOR E = Y TO (Y + Size - 4)
COLOR 8, 0
IF A = X - 1 THEN
Foreground = OnColour(A + 2, E) AND 15
Background = OnColour(A + 2, E) \ 16
COLOR Foreground, Background
PRINT CHR$(OnScreen(A + 2, E));
ELSE
COLOR 8, 0
LOCATE ((A - 1) + Lines), E
PRINT CHR$(OnScreen(((A - 1) + Lines), E));
' Fix first two Y co-ordinates after dimming
LOCATE (A - 1 + Lines), Y
FOR F = Y TO Y + 1
Foreground = OnColour(A + 1, F) AND 15
Background = OnColour(A + 1, F) \ 16
COLOR Foreground, Background
PRINT CHR$(OnScreen(A + 1, F));
NEXT F
' Draw Full Coloured Pulled Line
LOCATE A + 2, E
Foreground = OnColour(A + 2, E) AND 15
Background = OnColour(A + 2, E) \ 16
COLOR Foreground, Background
PRINT CHR$(OnScreen(A + 2, E));
END IF
NEXT E
NEXT A

LOCATE X, Y
FOR F = Y TO (Y + Size - 4)
' Draw Full Coloured Pulled Line
Foreground = OnColour(X, F) AND 15
Background = OnColour(X, F) \ 16
COLOR Foreground, Background
PRINT CHR$(OnScreen(X, F));
NEXT F
ERASE OnColour
ERASE OnScreen
Lines = 0

END SUB
SUB Delay (A AS SINGLE) STATIC
Start! = TIMER
DO
LOOP UNTIL TIMER - Start! >= A


END SUB

SUB DisplayBox (X AS INTEGER, Y AS INTEGER, FrameColourA AS INTEGER, FrameColourB AS INTEGER, TextColourA
AS INTEGER, TextColourB AS INTEGER, FrameColour AS INTEGER, FrameLabel AS STRING, Text AS STRING, Size AS
INTEGER, Speed AS SINGLE, WaitKey AS _
INTEGER) STATIC


DisplayBox(X,Y,FrameColourA,FrameColourB,TextColourA,TextColourB,FrameColour, "FrameLabel","Text",Max Columns,
Speed of Roll, Pause Toggle)

' Initialize all variables
CharProg = 1
OrgX = X
NewX = X
Lines = LEN(Text) / Size
Lines = INT(Lines + .5)

' Determine if Sound is on... if so: Ascending Sound
IF WaitKey = 1 OR Speed > 0 THEN
FOR I = 500 TO 1500 STEP (35 - Lines * 5)
SOUND I, I / 20000
```

```
NEXT
END IF
' Capture Text to be Over-Written by Box and Shadow
FOR A = Y TO (Y + Size + 6)
FOR B = X TO (X + Lines + 2)
OnScreen(B, A) = SCREEN(B, A)
OnColour(B, A) = SCREEN(B, A, 1)
NEXT B
NEXT A
' Draw Box
LOCATE NewX, Y: COLOR FrameColourA, FrameColourB: PRINT " ÚÄ";

' Display Frame Header
IF LEN(FrameLabel) < Size THEN
COLOR FrameColour
PRINT FrameLabel;
COLOR FrameColourA, FrameColourB
FOR A = 1 TO (Size - LEN(FrameLabel) - 1)
PRINT "Ä";
NEXT A
ELSE
' Draw Top Text Border
FOR A = 1 TO Size - 1
PRINT "Ä";
NEXT A
END IF
PRINT "Ä¿ "
FOR A = 1 TO Lines
NewX = NewX + 1
COLOR FrameColourA, FrameColourB
LOCATE NewX, Y
PRINT " ÀÄ";
FOR C = 1 TO Size - 1
PRINT "Ä";
NEXT C
PRINT "ÄÙ "
COLOR 8, 0
' Draw dimmed bottom
FOR B = Y TO (Y + Size + 6)
LOCATE ((NewX - 1) + Lines), B
PRINT CHR$(OnScreen(((NewX - 1) + Lines), B));
NEXT B
CALL Delay(Speed / 2)
COLOR FrameColourA, FrameColourB
LOCATE NewX, Y
PRINT " ³ ";
COLOR TextColourA, TextColourB
PRINT SPACE$(Size - 1);
COLOR FrameColourA, FrameColourB
PRINT " ³ ";

' Draw dimmed edges
COLOR 8, 0:
FOR B = (Y + Size + 5) TO (Y + Size + 6)
PRINT CHR$(OnScreen(NewX, B));
NEXT B
NEXT A
NewX = NewX + 1
COLOR FrameColourA, FrameColourB
LOCATE NewX, Y
PRINT " ÀÄ";
FOR C = 1 TO Size - 1
PRINT "Ä";
NEXT C
PRINT "ÄÙ ";
' Draw final dimmed edge
COLOR 8, 0
FOR B = (Y + Size + 5) TO (Y + Size + 6)
PRINT CHR$(OnScreen(NewX, B));
NEXT B
' Draw dimmed bottom
FOR B = Y + 2 TO (Y + Size + 6)
LOCATE (X + Lines + 2), B
```

```
PRINT CHR$(OnScreen((X + Lines + 2), B));
NEXT B
' Display Text
FOR D = 1 TO Lines
COLOR TextColourA, TextColourB
DO
Temp$ = MID$(Text, CharProg, Size)
IF LEN(Text) - CharProg <= Size THEN
X = X + 1
LOCATE X, Y + 3
PRINT MID$(Text, CharProg, Size)
CharProg = CharProg + LEN(Temp$)
ELSE
X = X + 1
LOCATE X, Y + 3
FOR Ccnt = LEN(Temp$) TO 1 STEP -1
IF MID$(Temp$, Ccnt, 1) = " " THEN EXIT FOR
NEXT Ccnt
PRINT LEFT$(Temp$, Ccnt)
CharProg = CharProg + Ccnt
END IF
LOOP UNTIL CharProg >= LEN(Text)
NEXT D
IF WaitKey = 1 THEN
DO WHILE INKEY$ = ""
LOOP
END IF

END SUB
SUB DRWBOX1
'draws box around text
square5$ = "S15 BM110,50 R100 D15 L100 U15"
DRAW "C5 X" + VARPTR$(square5$)

END SUB
SUB fopen (file$, file%)
OPEN file$ FOR RANDOM AS file% LEN = 2

END SUB
SUB fprint (Text$, textx%, texty%, colour%, file%)
'lpi: lines per integer
'fws: font word spacing
'fls: font letter spacing
'p% : pointer
GET file%, 1, lpi%
GET file%, 2, fws%
GET file%, 3, fls%
FOR count% = 1 TO LEN(Text$)
m% = ASC(MID$(Text$, count%, 1)) - 29
IF m% > 3 THEN
GET file%, m%, a1%
GET file%, m% + 1, a2%
FOR N% = a1% TO a2% - 1 STEP lpi%
FOR z% = 0 TO lpi% - 1
GET file%, N% + z%, l%
LINE (p% + textx%, (16 * z%) + texty%)-(p% + textx%, (16 * z%) + 15 + texty%), colour%, , l%
NEXT z%
p% = p% + 1
NEXT N%
p% = p% + fls%
ELSE
p% = p% + fws%
END IF
NEXT count%
END SUB

SUB SCRDRAW
'draws flowrate trace box
square1$ = "S17 BM315,95 R70 D32 L140 U32 R70"
DRAW "C4 X" + VARPTR$(square1$)
scale1$ = "BL70 BD4 R140 BD4 L140 BD4 R140 BD4 L140 BD4 R140 BD4 L140 BD4 R140"
DRAW "C4 X" + VARPTR$(scale1$)
'draws target box
```

```
square2$ = "S15 BM300,420 R10 U40 L20 D40 R10"
DRAW "C3 X" + VARPTR$(square2$)
square3$ = "BD2 R12 U44 L24 D44 R12"
DRAW "C3 X" + VARPTR$(square3$)
'draws screen border
square4$ = "S25 BM5,5 R100 D75 L100 U75"
DRAW "C5 X" + VARPTR$(square4$)
square6$ = "S24 BM15,15 R100 D75 L100 U75"
DRAW "C7 X" + VARPTR$(square6$)

END SUB
SUB targetdraw
LOCATE 3, 10: PRINT "Peak expiratory flowrate target"; tvol; "ml/s"
LOCATE 5, 10: PRINT "Respiratory rate target"; tfreq; "bpm"
WINDOW (0, -150)-(4000, 500)
LINE (1600, 50 + (tvol * .08))-(2150, 50 + (tvol * .08))
LINE (1600, 50 - (tvol * .08))-(2150, 50 - (tvol * .08))
END SUB
SUB targetfreq10
PLAY "MBMST80L1O2CACACACACACACACACACA"
END SUB
SUB targetfreq15
PLAY "MBMST60L2O2CACACACACACACACACACA"
END SUB
SUB targetfreq20
PLAY "MBMST80L2O2CACACACACACACACACACA"
END SUB
SUB targetfreq25
PLAY "MBMST100L2O2CACACACACACACACACACA"
END SUB
SUB targetfreq30
PLAY "MBMST60L4O2CACACACACACACACACACA"
END SUB

SUB targetfreq35
PLAY "MBMST140L2O2CACACACACACACACACACA"
END SUB

SUB targetfreq40
BR$ = "CACACACACACACACACACA"
PLAY "MBMST80L4O2 X" + VARPTR$(BR$)
END
```

APPENDIX 4

ABSTRACTS AND PUBLICATIONS

This study resulted in a number of abstracts and publications listed below.

1. McCafferty J, Kew PA, Haston A, and Innes JA. A novel device for the precise measurement of respiratory heat and moisture loss. *Thorax 2002; 57: Siii (32).*

2. Tate S, McCafferty J, Innes JA and Greening AP. Effect of varying respiratory pattern on exhaled breath condensate collection. *Thorax 2002; 57: Siii* (33).

3. McCafferty JB and Innes JA. Quantifying airway heat and moisture loss in health and lung disease. Am J Respir Crit Care Med 2003; 167(7):A975.

4. McCafferty JB, Bradshaw T, Tate S, Greening AP and Innes JA. Effect of ventilatory pattern and inspired air condition on exhaled breath condensate collection. Eur Respiratory Journal 2003;

5. McCafferty J.B.; Innes J.A.; Paredi P.; Kharitonov S.A.; Barnes P.J. Exhaled breath temperature in airways disease. European Respiratory Journal 2003; 22 (2): 393-395.

6. McCafferty JB, Bradshaw T, Tate S, Greening AP and Innes JA Effects of breathing pattern and inspired air conditions on breath condensate volume, pH, nitrite, and protein concentrations. *Thorax 2004; 59:694-698.*

7. McCafferty JB and Innes JA. Respiratory heat and moisture loss (RHML) in health, asthma and COPD. *Respiratory Research. In submission.*

RESPIRATORY PHYSIOLOGY

Effects of breathing pattern and inspired air conditions on breath condensate volume, pH, nitrite, and protein concentrations

J B McCafferty, T A Bradshaw, S Tate, A P Greening, J A Innes

Thorax 2004;**59**:694–698. doi: 10.1136/thx.2003.016949

See end of article for authors' affiliations

Correspondence to: Dr J McCafferty, Respiratory Unit, Western General Hospital, Crewe Road, Edinburgh EH2 4XU, UK; john.mccafferty@ed.ac.uk

Received 5 October 2003
Accepted 14 April 2004

Background: The effects of breathing pattern and inspired air conditions on the volume and content of exhaled breath condensate (EBC) were investigated.
Methods: Total exhaled water (TEW), EBC volume, pH, nitrite and protein concentrations were measured in three groups of 10 healthy subjects breathing into a condenser at different target minute ventilations (Vm), tidal volumes (Vt), and inspired air conditions.
Results: The volumes of both TEW and EBC increased significantly with Vm. For Vm 7.5, 15 and 22.5 l/min, mean (SD) EBC was 627 (258) µl, 1019 (313) µl, and 1358 (364) µl, respectively ($p<0.001$) and TEW was 1879 (378) µl, 2986 (496) µl, and 4679 (700) µl, respectively ($p<0.001$). TEW was significantly higher than EBC, reflecting a condenser efficiency of 40% at a target Vm of 7.5 l/min which reduced to 29% at Vm 22.5 l/min. Lower Vt gave less TEW than higher Vt (26.6 *v* 30.7 µl/l, mean difference 4.1 (95% CI 2.6 to 5.6), $p<0.001$) and a smaller EBC volume (4.3 *v* 7.6 µl/l, mean difference 3.4 (95% CI 2.3 to 4.5), $p<0.001$). Cooler and drier inspired air yielded less water vapour and less breath condensate than standard conditions ($p<0.05$). Changes in the breathing pattern had no effect on EBC protein and nitrite concentrations and pH.
Conclusion: These results show that condensate volume can be increased by using high Vt and increased Vm without compromising the dilution of the sample.

Exhaled breath condensate (EBC) has been proposed as a non-invasive means of measuring airway inflammation. Unlike traditional methods of sampling secretions from the lower respiratory tract such as bronchoalveolar lavage, EBC analysis has the advantage of being simple to perform, may be repeated frequently, and can be applied to patients during both the stable and exacerbation phase of disease. The condensate derives from expired water vapour and volatile gases, but the presence of non-volatile solutes suggests that droplets of airway lining fluid have also been collected due to aerosolisation during turbulent airflow. Analysis of these solutes may potentially provide insights into the pathophysiology of lung diseases such as asthma,[1 3] cystic fibrosis,[4 5] and chronic obstructive pulmonary disease.[6 7]

While EBC shows promise as a source for biomarkers in pulmonary diseases, large variability has been reported in the concentration of solutes in EBC samples with considerable overlap between normal subjects and disease groups.[4 7] In the absence of supporting data, much of this has been attributed to variations in the proportion of water vapour diluting the airway lining fluid or variations in flow affecting the amount of aerosolised solute. The dilution effect was recently studied by Effros *et al*[8] who sought to quantify this by measuring ion concentrations in EBC. By assuming the airway lining fluid to be isosmolar to plasma, they estimated that variations in dilution may affect analyte concentrations by a factor of up to 100 or more. Previous studies of respiratory pattern and breath condensate have been inconclusive. Schleiss *et al*[9] found that the concentration of the volatile solute hydrogen peroxide was dependent on flow rate, whereas Montuschi *et al*[10] found 8-isoprostane levels to be independent of flow rate. They also found a high degree of variability in repeated samples even under controlled conditions, suggesting a mechanism other than dilution as a cause.

Although the major determinant of exhaled water vapour volume is minute ventilation (Vm) and duration of collection,[11] the effect of differences in ventilatory pattern (such as tidal volume (Vt)) has not been quantified. It is also well established that cooler and drier inspired air produces a lower concentration of water vapour in the exhaled breath,[12] yet this has not been quantitatively assessed in the context of EBC collection.

The aim of this study was therefore to determine the effect of ventilatory pattern (Vm and Vt) and inspired air conditions on the volume of condensate collected and the concentration of certain non-volatile solutes (nitrite and protein) and pH in EBC.

METHODS

Collection of EBC

EBC was collected on a commercial breath condenser (EcoScreen, Jaeger, Germany). Samples were collected in interchangeable sampling tubes (one per sample) with subjects breathing (with nose clip) through a non-rebreathing two way valve. All sampling tubes were disinfected for 30 minutes using 1% potassium monopersulphate solution (Virkon, Antec International Ltd, UK), rinsed for 2 hours by flushing with tap water, then rinsed with ultrapure water (ELGA Labwater, UK) and air dried prior to use. Samples were centrifuged (2000 rpm, 2 minutes) before measurement of volume, immediately frozen, and stored refrigerated at −80°C.

pH of EBC

The pH of the EBC was measured immediately after collection (without deaeration) using a calibrated pH meter

Abbreviations: EBC, exhaled breath condensate; TEW, total exhaled water; Vm, minute ventilation; Vt, tidal volume

incorporating an ISFET sensor with temperature compensation (model KS723, Camlab, Cambridge, UK) with an accuracy of ±0.1 pH.

EBC nitrite concentration

The nitrite concentration was determined by a colorimetric assay based on the Griess reaction[13] in which triplicates of 100 µl EBC were reacted with 25 µl Griess reagent and measured at absorbance of 570 nm with a microplate reader (MR 710, Dynatec). Assay sensitivity was 0.5 µmol/l. Samples were stored in polypropylene containers and analysed within 4 weeks to minimise contamination and problems of instability.

EBC protein concentration

The protein concentration was measured based on the bicinchoninic acid method using a commercially available protein assay reagent kit (Micro BCA Protein Assay, Pierce, Rockford, IL, USA). Assay sensitivity was 0.5 µg/ml.

Measurement of flow, temperature, and humidity

To control and test for the effects of inspired air temperature and humidity the breath condenser was attached to a custom built device housing temperature, humidity, and flow sensors as shown in fig 1. Subjects breathed through a two way valve with temperature and humidity sensors located on the inspiratory and expiratory sides allowing measurement of the condition of the air inspired and the moisture content of the exhaled breath. Inspired air was supplied in a flow-past configuration from an air conditioning unit providing control over the air temperature and moisture content. Temperature sensors were K-type thermocouples (accuracy ±0.1°C). Humidity sensors were of thermoset polymer capacitance construction (accuracy of ±2%, Model HIH-3602-A, Honeywell, USA). Expiratory flow was measured using an ultrasonic phase shift flow meter (Model FR-413, BRDL, Birmingham, UK). The linearity of the sensor was <2% and the residual error due to temperature variation <1% in the temperature range 0–40°C. Together these measurements make possible calculation of the total quantity of exhaled water (TEW, see below).

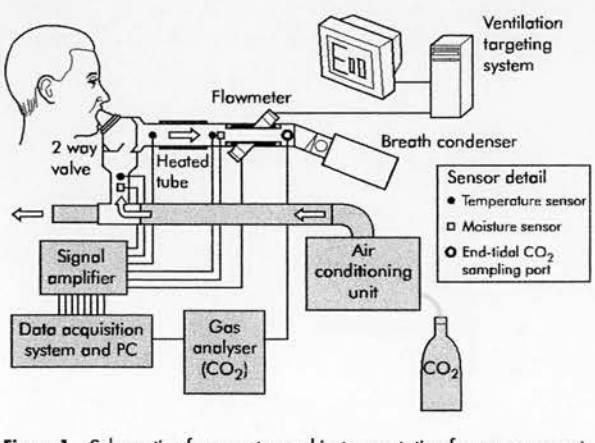

Figure 1 Schematic of apparatus and instrumentation for measurement of total exhaled water and collection of exhaled breath condensate. Subjects breathe through a non-rebreathing two way valve at a pattern set by the ventilation targeting system which generates an audiovisual feedback signal setting ventilatory rate and expiratory flow, respectively. An air conditioning unit controls the temperature and moisture content of the inspired air. Temperature and humidity sensors are located as shown.

Ventilation pattern targeting

Ventilatory patterns were set by feeding the expiratory flow signal into a PC with purpose built breath targeting software which generated a visual and auditory target for expiratory flow rate and respiratory rate, respectively. Inspiratory to expiratory ratio was set at unity. Eucapnia was maintained at the higher minute ventilations by measuring end tidal CO_2 and adding CO_2 in the inspirate as necessary.

Thermocouple and humidity sensor output was conditioned by purpose built multichannel amplifiers. All signals were captured on a 16-channel computerised data acquisition system (Model 1401, CED, Cambridge, UK) which interfaced with software (Spike 2, CED, Cambridge, UK) to allow real time signal display and storage of data to disk.

Effect of additional circuit and instrumentation on EBC collection

To assess any effects from the added dead space associated with the flow meter and other instrumentation, EBC collections were taken at equivalent ventilatory patterns with 10 subjects breathing directly through the standard two way non-rebreathing valve attached to the breath condenser alone and flow measured at the expiratory port of the condenser.

Effects of breathing pattern on EBC collection

To test the effect of Vm, EBC was collected from 10 healthy non-smoking subjects over timed 6 minute intervals at three target Vm values (table 1, protocol 1), each at high and lower target Vt. The conditions of the inspired air were measured and maintained at 22°C.

To test the effects of Vt, EBC was collected from 10 healthy non-smoking subjects over timed 6 minute intervals for a fixed target Vm at high and low target Vt patterns at an inspired temperature of 7°C.

Effect of inspirate temperature and humidity

At a fixed ventilatory pattern (Vt 1500 ml, 10 breaths/min), 6 minute collections of EBC were taken with 10 subjects breathing warm room air (20°C) and colder, drier air (9°C) (table 1, protocol 3).

Analysis of data

Total exhaled water (µl) for each 6 minute collection period was calculated as:

$$TEW = \frac{\rho_a}{\rho_w} V_T w$$

where w = absolute humidity of exhaled air (g/kg), V_T = total respired volume (litres ATPS from integrated flow meter signal), ρ_a = air density (20°C), and ρ_w = water density (20°C). The absolute humidity of expired air was derived from the mean temperature and moisture sensor signal (measuring relative humidity) which were referred to the physical properties of moist air at atmospheric pressure.

Statistical analysis was performed using SigmaPlot 2001 for Windows version 8.0 and Sigmastat 2001 for Windows (SPSS Science Inc, USA). Paired *t* tests were used to compare the EBC data and a value of $p<0.05$ was considered significant. Two way ANOVA was used for the analysis of Vm data and Friedman's two way analysis of variance for data which were not normally distributed (Minitab release 14, Statistical Software, Minitab Inc, USA) was used for the relationship between ventilation and EBC protein, nitrite, and pH.

Study approval for tests on human subjects was granted by the Lothian regional ethics committee and consent was obtained from all participating subjects.

Table 1 Protocol designs showing ventilatory patterns and inspired air conditions

Protocol no	No of subjects	Mean FEV_1 (l)	Target ventilation pattern		Inspired air conditions	
			Vt (ml)	Vm (l)	Temperature (°C)	Moisture content (mg/g)
1	10	3.9	1500	7.5, 15, 22.5	22 (1.2)	6 (0.3)
			750	7.5, 15, 22.5		
2	10	3.9	1500	15	7 (0.5)	5.6 (0.2)
			500	15		
3	10	3.6	1500	15	20 (1.8)	9 (1.1)
					9 (1.8)	5 (0.5)

Vt = tidal volume; Vm = minute ventilation; FEV_1 = forced expiratory volume in 1 second.

RESULTS

Effect of additional circuit and instrumentation on EBC collection

No difference was found in the volume of EBC or the pH, nitrite and protein concentrations when subjects breathed with or without the instrumented tubing section joined to the condenser based on paired *t* tests where a p value of >0.05 was not considered statistically significant (EBC: 1155 µl with and 1029 µl without, mean difference 136 µl (95% CI −14 to 286); pH: 6.3 *v* 6.4, mean difference 0.1 (95% CI −0.15 to 0.35); nitrite: 4.1 *v* 4.0, mean difference 0.1 (95% CI −0.72 to 0.92); protein: 8.1 *v* 5.1, mean difference 3.5 (95% CI −0.3 to 7.3)).

Effect of Vm on TEW

For target Vm values of 7.5, 15 and 22.5 l (all at Vt 1.5 l), subjects achieved mean (SD) values of 8.6 (1.95), 15.1 (2.55), and 22.8 (3.27) l/min, respectively. The effect of Vm on TEW and EBC volumes is shown in fig 2. These data were analysed using two way analysis of variance with repeated measures and Tukey's method for multiple comparisons. For all values of Vm the volume of TEW was significantly greater than the EBC volume ($p<0.001$). For both TEW and EBC there was a significant increase in volume with increased Vm ($p<0.05$). The volume of TEW rose significantly more with Vm than did the volume of EBC ($p<0.001$).

For Vm values of 7.5, 15 and 22.5 l/min the mean (SD) volume of EBC was 627 (258) µl, 1019 (313) µl, and 1358 (364) µl, respectively ($p<0.001$) and the volume of TEW was 1879 (378) µl, 2986 (496) µl, and 4679 (700) µl, respectively ($p<0.001$). Water vapour availability (TEW) was significantly higher than EBC, giving a condenser efficiency of 40% at Vm 7.5 l/min which decreased to 29% at Vm 22.5 l/min.

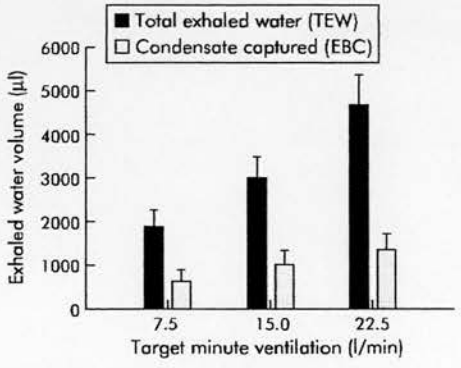

Figure 2 Volumes of total exhaled water (TEW) and exhaled breath condensate (EBC) collected from 10 subjects breathing at three minute ventilation (Vm) targets. Using two way analysis of variance with repeated measures and Tukey's method for multiple comparisons, the volume of TEW was significantly greater than the EBC volume at all values of Vm ($p<0.001$). For both TEW and EBC there was a significant increase in volume with increasing Vm ($p<0.05$). The volume of TEW rose significantly more with increased Vm than did the volume of EBC ($p<0.001$). Limits denote standard error of the mean.

Effect of Vt at fixed Vm

For target Vt values of 500 ml and 1500 ml, subjects achieved actual target volumes of 578 (98) ml and 1540 (232) ml. The effect of Vt is shown in fig 3 where lower Vt patterns gave significantly less TEW (per litre respired) than higher Vt (26.6 *v* 30.7 µl/l, mean difference 4.1 (95% CI 2.6 to 5.6), $p<0.001$). This was also reflected in the volume of EBC collected (4.3 *v* 7.6 µl/l, mean difference 3.4 (95% CI 2.3 to 4.5), $p<0.001$).

Effect of inspired air conditions

Subjects breathing at equivalent ventilatory patterns but with cooler, drier inspirate were found to yield less water vapour (TEW 33.4 *v* 35.6 µl /l, mean difference 2.2 µl /l (95% CI 0.2 to 4.2), $p<0.05$) and less breath condensate (EBC 8.6 *v* 10.1 µl/l, mean difference 1.5 µl /l (95% CI 0.3 to 2.7), $p<0.05$).

Effect of ventilatory pattern on exhaled pH, nitrite and protein

Despite the effects of Vm and Vt on condensate volume (figs 2 and 3), the ventilatory pattern had no significant effect on condensate pH, nitrite and protein concentrations using Freidman's two way analysis of variance (since data were not normally distributed). Overall mean (SD) concentrations of protein and nitrite in the EBC were 6.0 (3.4) µg/ml and 3.9 (2.2) µM, respectively, and pH was 6.3 (0.3); fig 4.

DISCUSSION

The volumes of both TEW and EBC increased significantly with Vm. The volume of EBC varied between 627 µl and

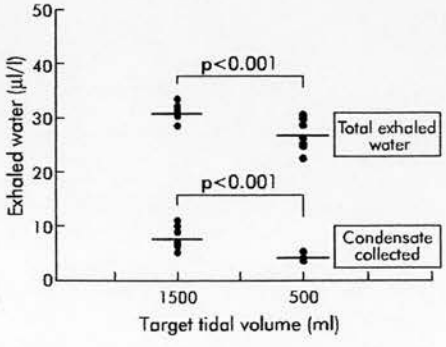

Figure 3 Effect of tidal volume (Vt) on measured volumes of exhaled water and breath condensate. At lower Vt subjects yielded less exhaled water and breath condensate per litre respired for the same minute ventilation; p values denote the level of significance based on paired *t* tests. Limits denote standard error of the mean.

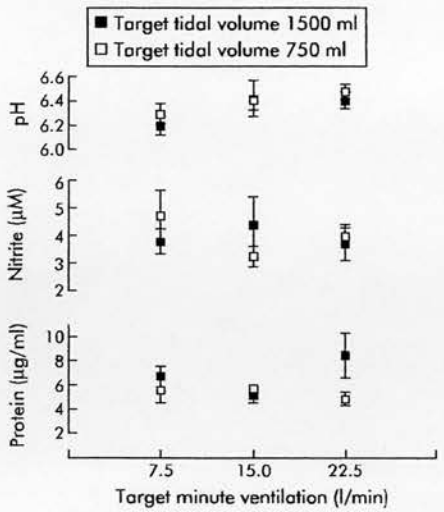

Figure 4 Mean EBC protein and nitrite concentrations and pH for each target minute ventilation (Vm) and tidal volume (Vt). Despite the effects of Vm and Vt on condensate volume (figs 2 and 3), Friedman's analysis of variance showed that Vm and Vt had no effect on EBC concentrations of protein, nitrite, or pH (all $p>0.05$).

1358 μl for a 6 minute collection in the Vm range 7.5–22.5 l/min. This indicates that, for this collection device with subjects breathing at a typical resting Vm of 10 l/min, a 6 minute collection would generate a sample of approximately 900 μl. The volume of TEW was significantly higher than the volume of EBC throughout the Vm range studied. This indicates that the condenser efficiency is far from 100% (range 40–29%). It would be reasonable to suppose that this inefficiency also applies to the trapping of aerosolised droplets and that a device with improved efficiency would yield an increased quantity of solutes, thereby enhancing the sensitivity of this technique. A mean reduction of 962 ml in Vt was associated with a 15% reduction in TEW for the same Vm; however, no corresponding effect was seen on solute dilution. This would imply that, at lower Vt, proportionally less solute is aerosolised for a given Vm and therefore the concentrations of solutes are maintained constant.

Inspired air conditions were found to have a small but significant effect on volumes of TEW and EBC. A fall in the inspired air temperature and humidity was associated with a reduction of up to 6% in TEW and EBC, implying a similar degree of reduction in the dilution of solutes under cooler, drier conditions. However, this was not seen in the concentrations of nitrite and protein measured, probably because the effect—although significant—was small relative to the measurement error associated with assays of very small quantities of solutes. It is therefore unlikely that variations in inspired air conditions commonly encountered in the laboratory would account for significant measurement error.

The absence of an effect of ventilatory pattern on the protein concentration suggests that non-volatile solute concentrations are independent of breathing pattern. This is supported by the findings of Montuschi *et al*[10] for 8-isoprostane. pH is influenced by volatile solutes yet still showed no variance with breathing pattern, which suggests that breathing pattern is not an important determinant of either volatile or non-volatile solute concentrations in EBC. However, this finding is in contrast to the results of Schleiss *et al*[9] for hydrogen peroxide in EBC. They proposed a bi-compartmental model which argues that, if solute concentration is not flow dependent, then this would imply that solutes were arising from the more distal airway and alveolar region. An alternative explanation is that the aerosolisation is flow dependent, occurring in the proximal airway during inspiration and expiration with the net expiratory flux contributing to EBC. This process occurs in parallel with evaporation and condensation of water from the airway lining fluid, thereby maintaining constant the ratio of analyte to water vapour dilution.

For the purpose of comparison, the inspiratory to expiratory (IE) ratio in this study was set at 1:1 with subjects also being required to reproduce a square wave expiratory waveform. It is recognised that the ventilatory pattern is not solely defined by Vm and Vt, but that factors such as IE ratio and the shape of the inspiratory/expiratory flow rate signals may also be important in the context of airway water transport. Mathematical models of this complex process[14] would suggest that a low IE ratio pattern would result in a lower expiratory water vapour concentration than a high IE pattern for the same Vt and Vm. It is also likely that the IE ratio will have an effect on the net flux of aerosolised droplets. Further studies are required to assess the significance of this effect on water vapour and analyte concentrations in EBC collections.

This study has shown that the effect of ventilatory pattern and inspired air conditions on exhaled water vapour and EBC volume to be significant but insufficient to explain the high degree of variability in solute concentrations seen in the studies by Effros *et al*[8] and others.[4 7 9] Likely sources of this variability include variation in aerosolisation, capture of droplets, and assay variability rather than water vapour dilution. Future attention must therefore be directed towards minimising these sources of variability in order to improve the overall sensitivity of this technique.

In conclusion, these results suggest that condensate yield can be significantly augmented by targeting the ventilatory pattern to higher tidal volumes (>1000 ml)) and minute ventilations over 15 l/min. Such augmentation will not significantly affect analyte concentrations.

ACKNOWLEDGEMENTS

The authors acknowledge the contribution of Dr PA Kew and Mr A Haston, Department of Mechanical Engineering, Heriot-Watt University, Edinburgh for technical assistance with instrumentation, and Ms M Imric, Respiratory Unit, Western General Hospital for assistance with nitrite and protein assays.

Authors' affiliations
J B McCafferty, T A Bradshaw, S Tate, A P Greening, J A Innes, Respiratory Unit, Western General Hospital and University of Edinburgh, Edinburgh, UK

Funded by Chest, Heart and Stroke Scotland, UK

REFERENCES

1 **Hunt JF**, Fang K, Mlik R, *et al*. Endogenous airways acidification. Implication for asthma pathophysiology. *Am J Respir Crit Care Med* 2000;**161**:694–9.
2 **Hunt JF**, Byrns RE, Ignarro LJ, *et al*. Condensed expirate nitrite as a home marker for acute asthma. *Lancet* 1995;**346**:1235–6.
3 **Corradi M**, Folesani G, Andreoli R, *et al*. Aldehydes and glutathione in exhaled breath condensate of children with asthma exacerbation. *Am J Respir Crit Care Med* 2003;**167**:395–9.
4 **Ho LP**, Faccenda I, Innes JA, *et al*. Expired hydrogen peroxide in breath condensate of cystic fibrosis patients. *Eur Respir J* 2000;**16**:95–100.
5 **Ho LP**, Innes JA, Greening AP. Nitrite level in breath condensate of patients with cystic fibrosis is elevated in contrast to exhaled nitric oxide. *Thorax* 1998;**53**:680–4.
6 **Dekhuijzen PN**, Abben KK, Dekker I, *et al*. Increased exhalation of hydrogen peroxide in patients with stable and unstable chronic obstructive pulmonary disease. *Am J Respir Crit Care Med* 1996;**154**:813–6.
7 **Montuschi P**, Collins JV, Ciabattoni G, *et al*. Exhaled 8-isoprostane as an in-vivo biomarker of lung oxidative stress in patients with COPD and healthy smokers. *Am J Respir Crit Care Med* 2000;**162**:1175–7.

8 **Effros RM**, Hoagland KW, Bosbous M, *et al*. Dilution of respiratory solutes in exhaled condensates. *Am J Respir Crit Care Med* 2002;**165**:663–9.
9 **Schleiss MB**, Holz O, Behnke M, *et al*. The concentration of hydrogen peroxide in exhaled air depends on expiratory flow rate. *Eur Respir J* 2000;**16**:1115–8.
10 **Montuschi P**, Kharitonov SA, Ciabattoni G, *et al*. Exhaled 8-isoprostane as a new non-invasive biomarker of oxidative stress in cystic fibrosis. *Thorax* 2000;**55**:205–9.
11 **Gessner C**, Kuhn H, Seyfarth HJ, *et al*. Factors influencing breath condensate collection. *Pneumonologie* 2001;**55**:414–9.
12 **Ferrus L**, Guenard H, Vardon G, *et al*. Respiratory water loss. *Respir Physiol* 1980;**39**:367–81.
13 **Green LC**, Wagner DA, Glogowski J, *et al*. Analysis of nitrate, nitrite and [^{15}N] in biological fluids. *Anal Biochem* 1982;**126**:131–8.
14 **Ignito EP**, Solway J, McFadden ER Jr, *et al*. Finite difference analysis of respiratory heat transfer. *J Appl Physiol* 1986;**61**:2252–9.

LUNG ALERT

The "hygiene hypothesis" revisited

▲ Benn CS, Melbye M, Wohlfahrt J, *et al*. Cohort study of sibling effect, infectious diseases, and risk of atopic dermatitis during first 18 months of life. *BMJ* 2004;**328**:1223–7

▲ Tulic MK, Fiset P-O, Manoukian JJ, *et al*. Role of toll-like receptor 4 in protection by bacterial lipopolysaccharide in the nasal mucosa of atopic children but not adults. *Lancet* 2004;**363**:1689–97

The "hygiene hypothesis" suggests that decreasing exposure to micro-organisms during infancy is responsible for the increasing prevalence of atopy. However, while a decreased risk of atopic disease is associated with various surrogate markers of microbial exposure including early attendance at day care, a greater number of siblings and living on a farm, specific associations between clinical episodes of infection and atopy remain ill defined and the possible mechanisms obscure.

Two recent papers have sought to characterise further the links between infection and atopy. At a population level, Benn and colleagues used a series of four interviews to study 24 341 mother-child pairs from 12 weeks gestation until the child was 18 months old. Relationships between atopic dermatitis and the incidence of clinically apparent infections were investigated. By 6 months of age 54% of children had experienced at least one infectious episode (most commonly a cold) and at the age of 18 months 11% of the children had atopic dermatitis. While inverse correlations between the presence of atopic dermatitis and a greater number of siblings, living on a farm, pet keeping, and early day care were confirmed, the occurrence of a clinically apparent infection did not result in a decreased risk of atopy. Indeed, the risk was slightly increased. Perhaps exposure to environmental organisms in the absence of clinically apparent disease is a more important phenomenon?

At a molecular level, Tulic and co-workers report the results of a study investigating the response of ex vivo nasal mucosal samples to stimulation with allergen in the presence and absence of lipopolysaccharide (LPS). The subjects comprised 22 children and 17 adults, both with and without atopy. LPS, a major component of gram negative bacterial cell walls, interacts with host tissue via the toll-like receptor TLR-4. This provides an important link between the innate and acquired immune responses and may be one way in which exposure to micro-organisms could modulate the subsequent risk of atopy. In the presence of LPS, allergen stimulation of the nasal mucosa from atopic children (but not adults) resulted in a Th1 type response rather than the Th2 phenotype observed with allergen alone. This effect was shown to be mediated via TLR-4, with upregulation of the immunoregulatory cytokine interleukin-10. Since atopy is classically associated with a Th2 type response, the results suggest a mechanism by which exposure to microbial products might protect from atopic disease.

Debate surrounding the "hygiene hypothesis" continues. These two papers, rigorously conducted and using very different approaches, provide interesting insights into the possible underlying mechanisms.

J R Hurst
Lung Alert Editor, *Thorax*; jrhurst@lineone.net